Development and Characterization of Polysiloxane Polymer Films for Use in Optical Sensor Technology

By

Krista Lynn Plett

A thesis submitted to the Department of Chemistry

in conformity to the requirements for the degree of

Doctor of Philosophy

Queen's University

Kingston, Ontario, Canada

September 2008

Abstract

A novel sensor using a polymer coated long-period grating (LPG) has been proposed for monitoring levels of organic contaminants in air or water systems. The sensor operates by detecting refractive index changes in the polymer coating as analytes partition in. Polymer coatings used must be able to reversibly and reproducibly absorb contaminants of interest from the sample and have a refractive index just below that of the fiber cladding.

The synthesis and characterization of several chemically selective polysiloxanes is described. Pre-polymer materials are made through the catalyzed condensation of silane monomers. Different functional groups are incorporated either through polymerizing functionalized monomers, or by post-functionalizing the polymer through a platinum-catalyzed hydrosilylation reaction. The pre-polymer materials are crosslinked into elastomeric films using titanium(IV) tetraisopropoxide. The polymer refractive index is controlled through altering the ratios of functional groups within the polymer or changing the loading levels of titanium. Four polymers were made, having different functional groups and optimized refractive indices for use on the proposed sensor.

The partition coefficients for the polymers with a variety of solvents are calculated and compared. Each polymer was found to have a slightly different chemical selectivity pattern, demonstrating that a set of polymers could be used to generate a sensor array. Partition coefficient data was calculated from the gas phase by considering the change in polymer refractive index as the solvents

partitioned into the polymer. The Lorentz-Lorenz equation was used to model the relationship between the change in refractive index and the solvent concentration within the polymer.

Finally, polymers were applied to LPGs and used to successfully detect various solvents from the gas phase. This was accomplished by monitoring the entire LPG spectrum, and also by considering loss at a single wavelength using fiber-loop ring-down spectroscopy.

Acknowledgements

I would like to thank my supervisor, Dr. Stephen Brown, for his guidance throughout my project, his wisdom and his encouragement. I also extend my thanks to the members of my supervisory committee, Dr. Hans-Peter Loock and Dr. Richard Oleschuk, as well as the other faculty members that have helped me along the way.

Thanks to Dr. Jack Barnes for his technical expertise and friendship, Dr. Ray Bowers and the various other members, past and present, of the Brown and Loock labs.

Thanks to the many summer students and fourth year project students that contributed towards the results of this thesis: Louise de la Durantaye, Crystal Maitland, Karin Ho, Alykhan Sumar, Wayne Gow, Marian Dreher, Gabriela Rappell, Ivy Lam and Gillian Mackey.

I would also like to thank the Natural Sciences and Engineering Council of Canada, Precarn Inc., and Queen's University for financial support.

Finally, I would like to acknowledge my husband, Jonathan, for being fabulous in every way and for keeping me sane over the last couple years, my family for their love and support, and God for giving me the mind and will to accomplish all of this.

Statement of originality

The present study, to the best of the author's knowledge, comprises the following original work.

1. The development of customized polysiloxane polymers that exhibit both differential chemical selectivity and adjustable refractive indices.

2. The calculation of film/air partition coefficients for four polysiloxanes with various solvents.

3. The demonstration of the use of a polymer coating on a long-period grating (LPG) for detecting gas phase analytes

Table of Contents

List of Tables

List of Figures and Illustrations

List of Abbreviations

^{1}H-NMR – Proton nuclear magnetic resonance

APTES – 3-aminopropyl triethoxy silane

ATR-IR – Attenuated total reflectance infrared

CCD – Charge coupled device

$CDCl_3$ – Deuterated chloroform

DDPS – Diethoxy diphenyl silane

DMSO – Dimethyl sulfoxide

FLRDS – Fiber-loop ring-down spectroscopy

IR - Infrared

K_{fa} – Partition coefficient: film/air

K_{fs} – Partition coefficient: film/solution

K_{oa} – Partition coefficient: octanol/air

K_{ow} – Partition coefficient: octanol/water

LPG – Long-period grating

MALDI-TOF-MS – Matrix assisted laser desorption ionization time of flight mass spectrometry

MIP – Molecularly imprinted polymer

M_n – Number average molecular weight

M_w – Weight average molecular weight

NIR – Near infrared

OSA – Optical Spectrum Analyzer

PAH – Polycyclic aromatic hydrocarbon

PCHMS – Poly (3-cyclohexylpropyl) methyl siloxane

PCMS – Poly (3-cyanopropyl) methyl siloxane

PDMS – Poly dimethyl siloxane

PDPS – Poly diphenyl siloxane

PFMS – Poly (3,3,3-trifluoropropyl) methyl siloxane

PMMA – Poly (methyl methacrylate)

PMOS – Poly methyl octyl siloxane

SAW – Surface Acoustic Wave

SPME – Solid-phase microextraction

SPR – Surface Plasmon resonance

TCE – Trichloroethylene

THF – Tetrahydrofuran

VOC – Volatile organic compound

Chapter 1

Introduction

1.1 General Introduction

Stricter environmental controls and demands are being placed on industries and governments, creating an increased need for rapid and reliable assessment and monitoring of contaminant levels in the environment.[1,2] At present, the vast majority of solutions available necessitate the constant collection of samples from the field and transport back to a lab for analysis. This not only is time consuming and expensive, but it introduces a delay of possibly many days between a contamination event occurring and being detected. Continuous monitoring is necessary to provide a complete picture of the dynamic situation at a site.

The development of instruments which are portable and designed for use in the field would address some of these issues. While these instruments avoid the necessity of transporting samples back to a lab and possible contamination from the journey, they still require trained personnel to sample the site, and continuous monitoring is not achieved.

There is a need, then, for a self-contained device that can continuously monitor its environment for the presence of contaminants. One solution for this need is sensors technology. Sensors are growing in application and can be used

in not only environmental monitoring, but in the medical field, molecular biotechnology and industry.[3]

Herein, a sensor system which targets gas phase organic compounds, such as volatile organic compounds (VOCs) or chlorinated solvents, is described. The Canadian Environmental Protection Act (CEPA, 1999) identifies both VOCs and chlorinated solvents, such as trichloroethylene, as toxic substances.[4] VOCs are of great environmental concern, having been identified as a major contributor to smog among other things.[5] Trichloroethylene is used as a degreaser or solvent in many industrial applications and VOCs are found in many consumer products. The prevalence of these compounds and their impact on human health makes it of vital importance to monitor them and limit their exposure to the environment. Ontario workplace standards state the maximum allowable concentration of benzene to be 1 ppm in air.[6] The Ontario Ministry of the Environment restricts the concentrations of xylenes and toluene to 0.2 ppm[7] and 0.5 ppm[8] respectively. Ideally, sensors for these compounds should therefore have detection limits in the low ppm or ppb range.

The system proposed operates by utilizing an optical fiber modified by a long-period grating (LPG).[9] This grating is sensitive to the refractive index of the environment immediately surrounding it and when that environment is altered, such as when a contaminant is present, its transmission spectrum shifts. The key to the success of this instrument lies in a polymer coating that surrounds the grating. This polymer coating can selectively absorb compounds of different chemical natures from the environment, causing a change in its refractive index,

and a subsequent change in the LPG transmission spectrum (see figure 1.1). The polymer coating allows only compounds of interest to be absorbed and produce a signal, excluding matrix effects. It also concentrates the compound, allowing for increased sensitivity.

Most polymers are not selective for a single compound, but rather a range of chemically similar compounds.[10] One coated LPG is therefore not sufficient for species determination. Combining several coated gratings together into an array imparts selectivity into the system. Each grating would have a different polymer coating with selectivity for a different class of compounds. A given compound would produce a characteristic fingerprint response across the array. By combining this basic system with multivariate and pattern recognition data

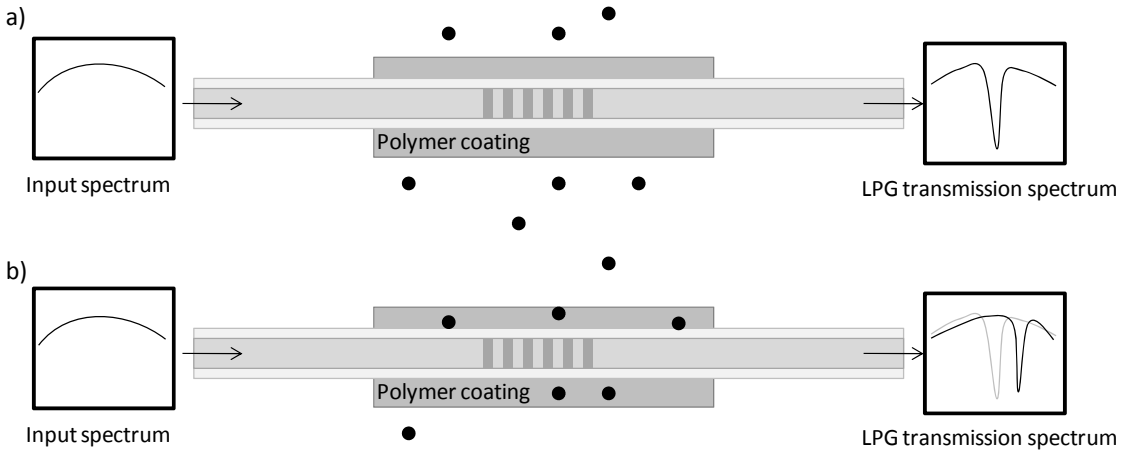

Figure 1.1 The transmission spectrum of an LPG coated with a polymer (a) shifts as analytes partition into the polymer and change its refractive index (b).

processing, an intelligent sensor array can be created.[11] This sensor would in principle be able to differentiate between different chemical species and determine their concentrations.

1.2 Optical Fibers

1.2.1 Refractive Index

Refractive index is a material property of any dielectric material, approximately equal to the square root of the real portion of the dielectric constant[12]. Materials which are more polarizable will have a higher value for the refractive index. The refractive index of a material is wavelength dependent. In the literature, most values are reported at 589 nm, the D-line in the emission spectrum of sodium vapour. The operating wavelength of the proposed sensor is 1550 nm, so here, refractive index is frequently reported at that wavelength.

In practical terms, the refractive index determines the speed at which light travels through a material and also governs refraction and reflection at an interface between two dielectrics. Refraction and reflection is quantified by Snell's Law:

$$n_1 \sin\theta_1 = n_2 \sin\theta_2 \qquad (1)$$

where n_1 and n_2 are the refractive indices of the two materials, θ_1 is the angles of incidence and θ_2 is the angle of refraction (see figure 1.2).

A critical angle, θ_c, can be calculated for a given interface between two materials. The critical angle is the incident angle which results in $\theta_2=90^o$ and is equal to:

$$\theta_c = \sin^{-1}(n_2/n_1). \quad (2)$$

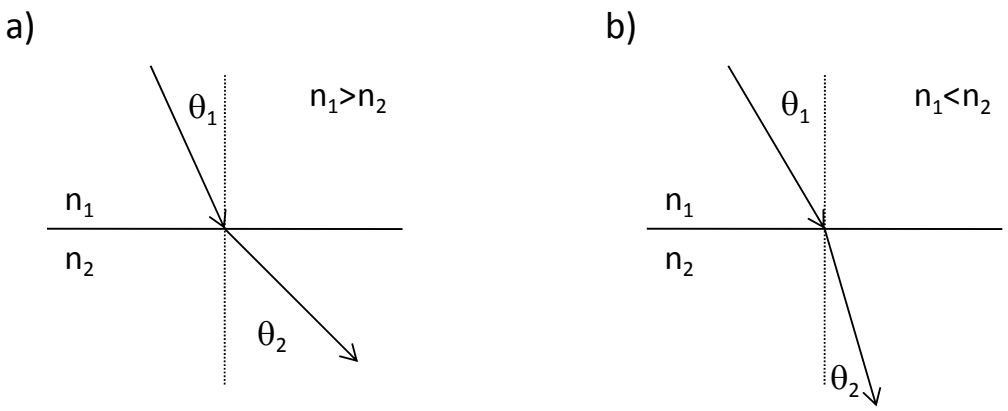

Figure 1.2 Light bending at an interface of two dielectrics according to Snell's Law as it travels into a lower refractive index material (a) or a higher refractive index material (b).

Angles of incidence lower than the critical angle result in refraction of the light into the second material, whereas angles of incidence greater than the critical angle result in total internal reflection of the light (see figure 1.3).

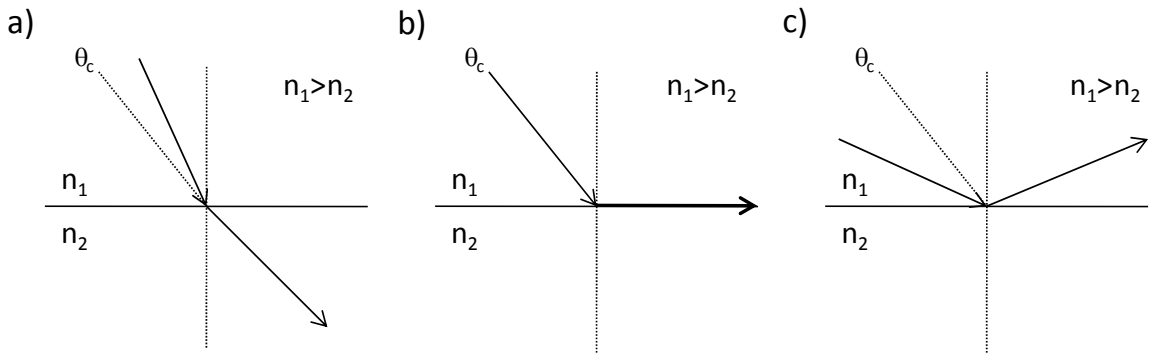

Figure 1.3 The behavior of incident light at angles less than the critical angle (a), at the critical angle (b) and at angles greater than the critical angle (c).

This principle is used in fiber optics, where light travels in the core of the fiber through total internal reflection. The refractive index of the cladding material is less than that of the core, and the light travels at an angle which is greater than the critical angle, ensuring that the light is reflected and propagated down the core (see figure 1.4). It is the interaction of the incident and reflected light that creates the evanescent wave penetrating into the cladding.

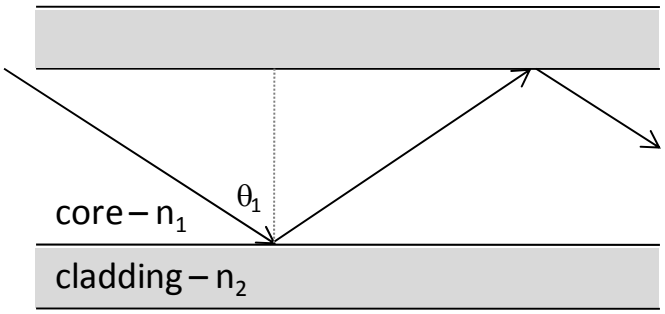

Figure 1.4 Light traveling in a multimode optical fiber by total internal reflection where $n_1>n_2$ and $\theta_1>\theta_c$

Optical fibers can be classified as either multimode fibers or single mode fibers. As the name suggests, in a multimode fiber, multiple modes of light are propagated in the core. The principle of total internal reflection described above applies well to light travelling in a multimode fiber.

In a single mode optical fiber, such as the one used in our sensor platform, the core has a very narrow diameter (about 8-10 μm) as compared to a multimode fiber. The core can only support one propagating mode. Light can be better visualized as a wave propagating through the fiber as in Figure 1.5. For a fiber with a long period grating, coupling to the cladding occurs when there is a phase match between the core propagating mode and a cladding mode. The evanescent wave would be the portion of the waveform travelling outside of the cladding.

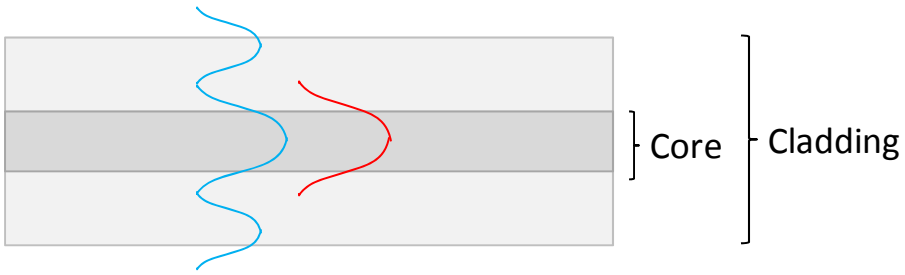

Figure 1.5 Core propagating mode (red) and a cladding mode (blue) travelling through a single mode optical fiber. The curves for each mode represent the variation in light intensity across the fiber.

1.2.2 Sensors based on Optical Fibers

There are many examples of optical sensor systems using optical fibers described in the literature.[3] Optical fibers are advantageous because they are able to convey light with minimal loss, expense and physical size. Fiber optic

sensors can be categorized as either extrinsic or intrinsic sensors.[13] In extrinsic sensors, sensing occurs at the terminal end of the optical fiber, with the fiber primarily providing a means to transfer light to and from the sensor element. Alternatively, for intrinsic sensors, sensing occurs along the length of the fiber. Here the optical fiber is used to transfer light from one point to another, but it also becomes part of the sensor element itself. It is this latter conformation that we are considering.

Sensors based on evanescent wave sensing, where light penetrates out from the optical fiber into the surrounding environment for a short distance, constitute an active area of research.[3] In this way it is possible for the light transmitted by the fiber to interact with the environment exterior to the fiber. Fiber optic evanescent wave sensors work on the same principles as the better established attenuated total reflectance infrared (ATR-IR) spectroscopy.[13] The evanescent wave is caused by the interaction of the incident and reflected light as light is transmitted through a waveguide by total internal reflection. It decays exponentially with increasing distance from the waveguide. One can define a penetration depth (d_p) of the evanescent field, which is the distance required for the evanescent field to reach 1/e of its original intensity. It is dependent on the wavelength of the light (λ), incident angle (θ) and the refractive indices of both waveguide (n_1) and environment (n_2) (see figure 1.6).

$$d_p = \frac{\lambda}{2\pi\sqrt{n_1^2 sin^2\theta - n_2^2}} \qquad (3)$$

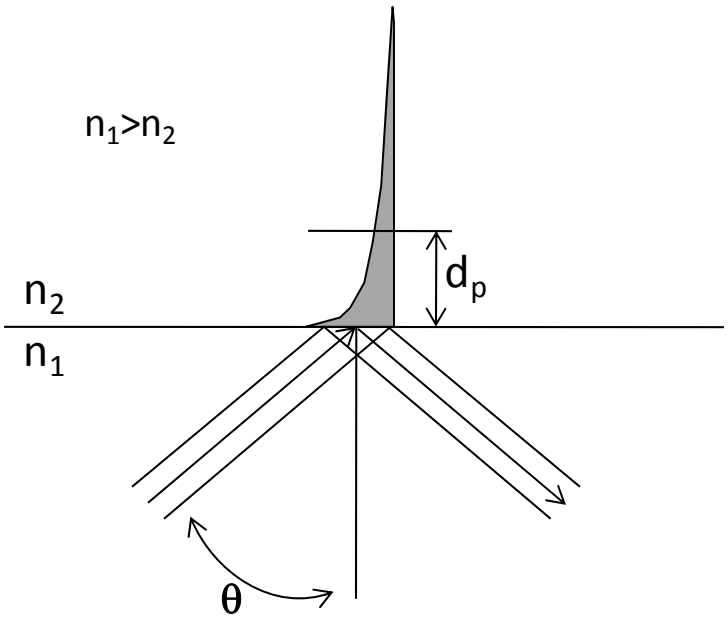

Figure 1.6 Evanescent wave with penetration depth d_p, created by light traveling with incident angle θ in a medium of refractive index n_1 with an external refractive index of n_2.

For sensing applications, a high penetration depth allows for a greater interaction with the environment and thus greater sensitivity.[14,15] As seen in equation 3, a greater penetration depth can be achieved at a given wavelength of light through altering the incident angle, or by having an environmental refractive index that is similar to the waveguide refractive index. Krska *et al.*[16] did work with evanescent wave sensors, varying the angle at which laser light was directed into a multimode optical fiber. They showed that increasing the angle between the laser and the fiber axis caused an increase in sensitivity. This is due to both an increase in the penetration depth of the evanescent field and an increase in the number of reflections occurring over the sensing region. A few years later, Tobis'ka *et al.*[17] used bent fibers to increase the sensitivity of evanescent wave

measurements. Bending optical fibers increases the intensity of the evanescent field and thus the sensitivity to analytes.

Sensors used for evanescent field sensing often use a selective polymer coating as a cladding material.[14-18] The purpose of this layer is two fold. If the polymer thickness is greater than the penetration depth of the evanescent field, it will exclude effects from the sample matrix. In addition, the sensing layer can be designed to selectively absorb the analyte of interest and concentrate it from the sample solution.

The analyte is detected as it partitions into the polymer and absorbs light from the evanescent field, reducing transmission through the fiber. Some selectivity is imparted into the sensor based on which wavelength of light is absorbed.

A number of groups have worked on evanescent wave sensors operating in the mid-infrared (3-25 μm).[14,16,17] This wavelength range works well for the detection of chlorinated hydrocarbons, which have strong absorption bands in this area. The research groups used polyethylene, polypropylene, or polyisobutylene and their combinations as sensitive coatings on multimode silver halide optical waveguides to absorb the chlorinated hydrocarbons from water. Detection limits were in the part per billion range.

The near IR can also yield useful information for detecting hydrocarbons and aromatics, as the C-H overtones are in this region. Sensfelder *et al.*[20] demonstrated the detection of low part per million levels of crude oil and gasoline

in water by considering absorption of NIR radiation (1600-1850 nm) in an evanescent field sensor.

One main difficulty with working in the IR range is the need to develop both optical fibers and polymer coatings that do not absorb the IR light significantly. Zimmermann *et al*.[15] did work in the near IR range. They used poly(dimethyl siloxane) and poly(methyl phenyl) siloxane polymers. Some absorption bands from the polymer overlapped that of the analyte of interest. To eliminate this interference, they synthesized deuterated analogs of the polymers.

Another way to avoid interferences from the fiber or coating is to work in another part of the spectrum. Schwotzer *et al*.[21] did work with evanescent wave sensing in the ultraviolet. The polysiloxane and Teflon coatings used did not absorb significantly in this wavelength range. They sensed aromatic and polycyclic aromatic compounds, which absorb well in the ultraviolet. Detection limits of about 20 ppm for toluene in water were obtained. Compounds which do not absorb significantly in the ultraviolet would not be able to be detected by this system.

Transmission losses in these evanescent sensors included two sources. Some loss was due to absorption of light by analytes, however, as analytes partitioned into the polymer coating, a change in coating refractive index (n_2) was also produced. This refractive index change altered the numerical aperture of the fiber and, as a result, the fiber transmission. The numerical aperture is defined as:

$$NA = \sqrt{n_1^2 - n_2^2} \qquad (4)$$

A larger numerical aperture will result in higher transmission through the fiber. The change in refractive index also altered the depth of the evanescent wave, allowing for more interaction and absorption by the analyte. Thus evanescent wave sensing does not necessarily follow a straightforward Beer's law pattern when monitoring absorption.

An alternative to using evanescent wave absorption to detect analytes is to monitor changes in the transmission spectrum due to refractive index changes in the polymer coating. This eliminates the need for expensive fibers and coatings that do not absorb in the spectral region of interest. In addition, virtually any compound which will partition into the polymer can be detected, as refractive index is a universal property. The ability to discriminate between compounds based on their absorption wavelength is lost however.

Chomat *et al*.[18] used an optical fiber with an inverted graded index, making it more sensitive to environmental refractive index changes, to detect toluene in water. Their fiber was coated with PDMS and used light at 850 nm, a non-absorbing wavelength. Changes in refractive index caused changes in the transmission of the fiber, which was detected. They reported detection limits in the low part per million range. Other similar work has been done using regular coated multimode fibers[17,21]

1.3 Long Period Gratings

Long-period gratings (LPGs) were first reported in the mid 1990s, and have been used since in sensor applications for monitoring temperature, strain or refractive index.[9,22-24] Similar in form to Bragg gratings, they are periodic modulations of refractive index within the core of a single mode optical fiber. They act to couple light from the core propagating mode into the cladding modes. Due to the high loss in the cladding modes, the light is quickly dissipated. Only certain wavelengths are coupled, and this depends on the grating period and the effective refractive index of both core and cladding, according to the formula:

$$\lambda_{max} = \Lambda(n_{eff,core} - n^{i}_{eff,clad}) \qquad (5)$$

Where λ_{max} is the wavelength of the attenuation maximum, Λ is the grating period, $n_{eff,core}$ is the effective refractive index of the core, a function of both the refractive index of the core and cladding material, and $n^{i}_{eff,clad}$ is the effective refractive index of the i^{th} cladding mode, a function of both the refractive index of the cladding material and the external environment. For long period gratings, the grating period is typically 100 μm to 1 mm, whereas for Bragg gratings the period is much smaller, usually less than 1 μm. Changes in either the grating period (strain) or the effective refractive indices will cause a peak shift in the attenuation spectrum of the grating, which can be detected.

The above equation (5) generally only holds for the situation in which $n_{core}>n_{clad}>n_{eff,external}$. In this scenario, certain modes of light propagate through both core and cladding by total internal reflection. In the case where an external coating is thicker than the penetration depth of the evanescent field (a few micrometers), the condition $n_{clad}>n_{external}$ must hold as $n_{eff,external} = n_{external}$.. For situations where $n_{clad}<n_{external}$, the cladding no longer operates as an effective waveguide and all light is lost. Any high refractive index coatings applied to the grating must be very thin and uniform with a lower refractive index surrounding so that $n_{eff,external}$ is lower than n_{clad}. It is possible to do chemical sensing using high refractive index coatings, though the thickness requirements make it more challenging for some coating materials.[25] For this work, only coatings having refractive indices below that of the cladding are considered and their thickness is greater than that of the penetration depth of the evanescent field.

The dependence of the attenuated wavelength on the refractive index of the environment opens up the possibility of using LPGs as refractive index sensors.[26] The change in attenuated wavelength with refractive index is non-linear, with the greatest wavelength change occurring when the coating refractive index is near to that of the cladding (see figure 1.7). There are a few examples of using LPGs as chemical sensors in the literature. Some use the fiber LPG without a polymer coating and rely on changes of the bulk refractive index of the solution.[27-31] Depending on the properties of the particular grating used, changes in refractive index in the fifth decimal place can be detected. Despite this

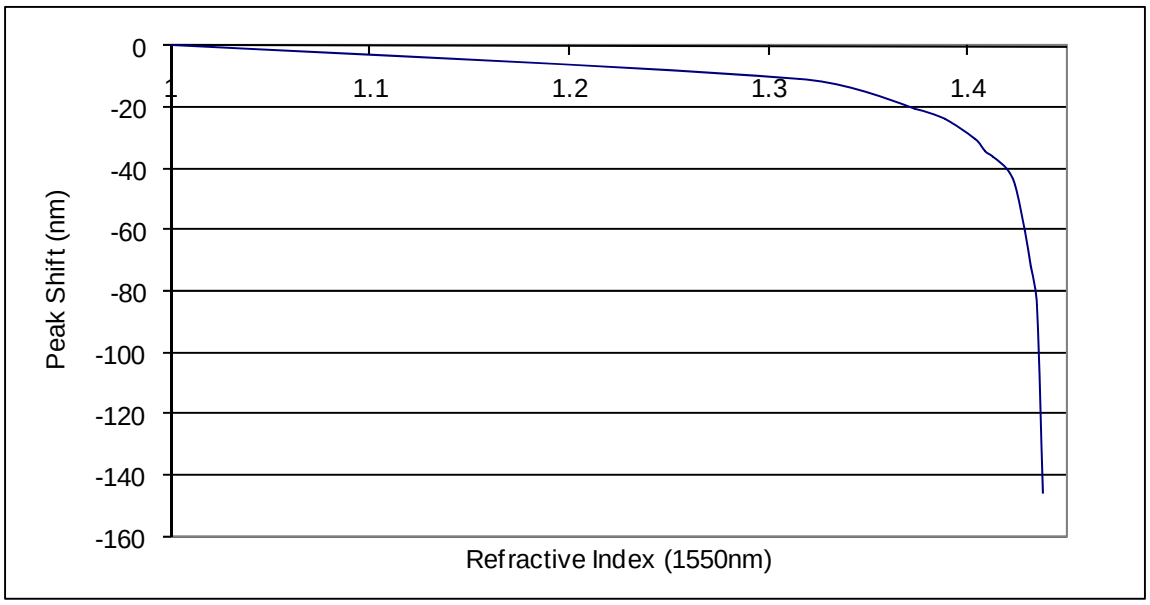

Figure 1.7 Graph showing the peak shift of the LPG attenuation maximum with changing external refractive index.

apparent sensitivity, significant amounts of an analyte must be present to cause this change in refractive index. For example, Allsop *et al.*[27] used an uncoated LPG sensor to detect xylene in paraffin. A concentration of 400 ppm xylene was necessary to produce the minimum detectable change in refractive index of 6 x 10^{-5}. The sensor was also completely non specific.

It is possible to coat an LPG to enhance its sensitivity. Coating an LPG with a polymer, analogous to the evanescent wave sensors described earlier, is not common in the literature. Other non polymer coatings, however, have been applied to LPGs to enhance analyte detection.

DeLisa *et al*.[32] use a selective thin coating of antibodies on a single mode LPG to detect an antigen, Human IgG. They achieved detection limits in the low part per million range with this sensor. Due to their method of signal processing

this detection limit cannot be compared to a change in refractive index or peak shift. An LPG coated with a thin antibody modified hydrogel was used by Pennington *et al*.[33] to detect the HIV protein p24, as well as atrazine in the low ppm range. In this range, peak shifts of less than 1 nm were obtained. Keith *et al.*[34] coated an LPG with a thin copper sensitive coating containing Cibracron Blue. Using this set up they were able to quantify copper(II) ions down to a detection limit of 1.3 mg/L (ppm). This corresponds to a peak shift of about 0.15 nm. Another approach used by Tang *et al.*[35] was to combine LPG technology with surface plasmon resonance (SPR). They coated an LPG with a thin coating of colloidal gold particles, modified with a dinitrophenol compound. The detection limit for the anti-dinitrophenol antibody was reported as 9.5×10^{-10} M, or 0.14 ppm. They detect the compound by considering changes in LPG spectrum transmission intensity.

Finally, Ishap *et al.*[36] coated an LPG with a thin film. This film had a thickness of less than 100 nm and was not added to specifically detect a given compound, but to alter the refractive index sensitivity of the LPG. The thin high refractive index coating altered the ability of the cladding to act as a waveguide and, subsequently, the fiber's refractive index sensitivity. This allowed for greater sensitivity in solution refractive index measurements, particularly for refractive indices greater than that of the silica cladding material.

In addition to being used as refractive index sensors there are several applications of LPGs as sensors for temperature[37], strain[38-39] or as liquid level sensors.[40] An LPG has also been used as an evanescent wave absorption

sensor.[41] The addition of the grating into the fiber enhanced the sensitivity of the system compared with a regular unaltered fiber by coupling a greater portion of waveguided light into the cladding than would occur in a conventional evanescent configuration.

1.4 Polymer Coatings for Fiber Optic Sensors

1.4.1 Synthesis of Polymers

The word polymer comes from the Greek and simply means “many units”. Polymers are composed of repeating monomer units, chemically bonded together into long chains. The synthesis of a polymer from monomeric building blocks usually falls under one of two basic reaction types: chain or step polymerization.[42]

In the chain process, there is an initiation step where a reactive species, often a free radical, is created. In propagation steps, the reactive species reacts with monomers, each time adding length to the polymer chain. In this way, high molecular weight species are quickly built up. The chain growth is stopped by a termination step, which, depending on the reaction and conditions, can take a variety of forms. Combination and chain transfer are common methods of termination (see figure 1.8). Common polymers such as polystyrene, polymethyl methacrylate and polyethylene are formed in this way.

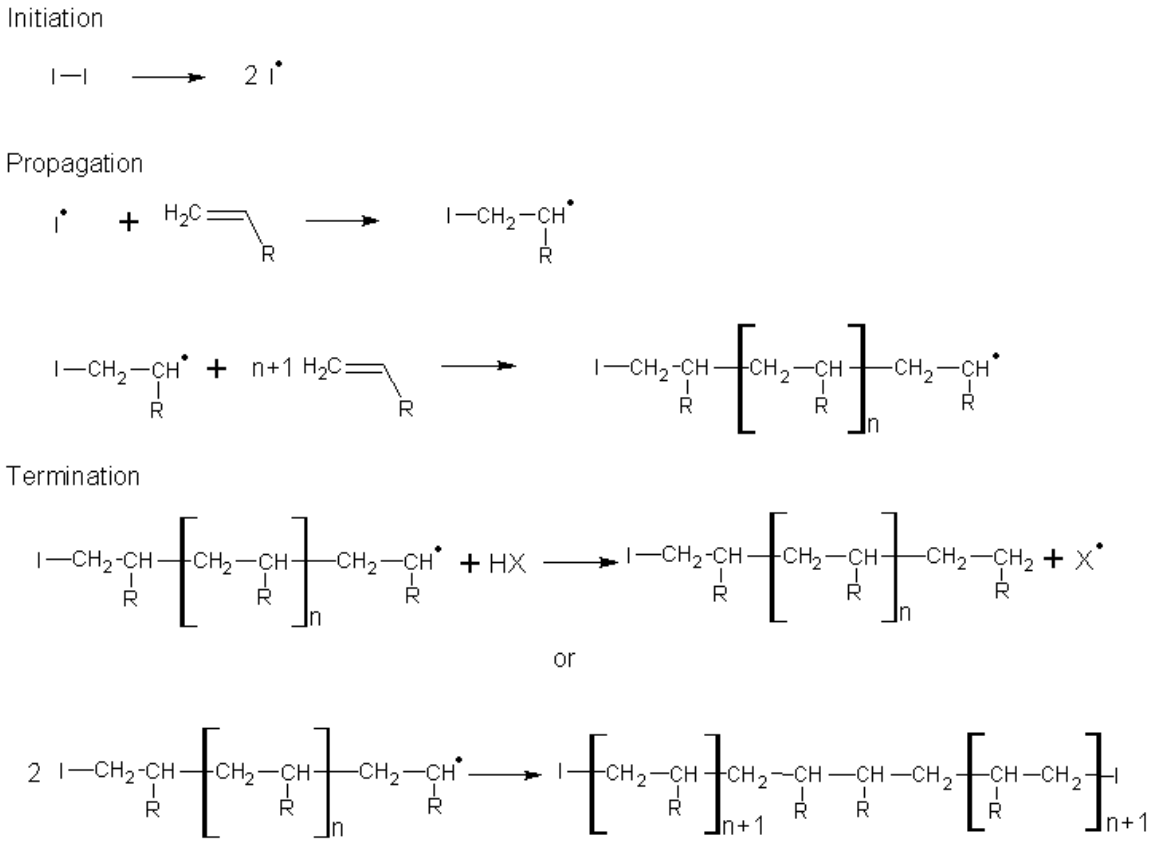

Figure 1.8 General reaction scheme for a typical chain polymerization where I is an initiator and X can be another polymer chain or species in solution.

In the step process, difunctional monomers react together to form bonds and build a polymer chain (see figure 1.9). Any two species can react, thus the average molecular weight of a step growth polymer tends to grow more slowly than that of a chain growth polymer. The polysiloxanes studied here are formed by a step process, as are other commercially important polymers such as polyesters, polyurethanes and polyamides (e.g. nylon).

Polymers can be composed of linear chains, or the addition of a small amount of trifunctional groups or special crosslinking materials can combine the

linear chains into a branched network. This increases the structural integrity of the formed polymer.

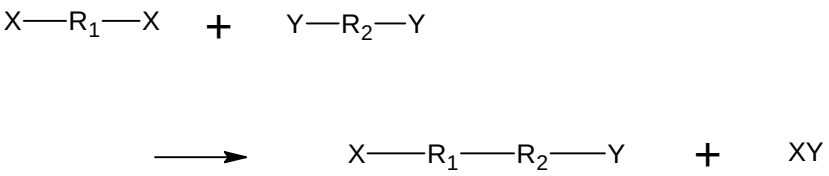

Figure 1.9 General reaction scheme for a step polymerization, where R_1 and R_2 are difunctional hydrocarbons and X and Y are the segments of the functional groups lost in the condensation reaction.

1.4.2 Chemical Requirements

Polymers used as selective coatings for optical sensor applications should have a high affinity for the analyte of interest. This can be quantified by calculating the film-solution partition coefficient, K_{fs}. Similar to the octanol-water partition coefficient, K_{ow}, K_{fs} is equal to the ratio of the concentration of the analyte in the film coating to the concentration in the sample solution at equilibrium.

$$K_{fs} = \frac{[analyte]_{film}}{[analyte]_{solution}} \quad (6)$$

K_{fa} can also be calculated, which considers the partitioning between the film and air for gas-phase samples. High values for the partition coefficient indicate a high affinity for the analyte. Polymer coatings for sensors should not only have a high partition coefficient for a given analyte, but they should be able to absorb the analyte reversibly and reproducibly to be used for continuous monitoring.

Common polymers used in the literature for evanescent wave sensing include poly(dimethyl siloxane) and its derivatives[15,17-18,20-22], acrylosiloxanes [21-22], or poly(ethylene) and related compounds[14,16,19]. These polymers will all absorb organic compounds, however, they are not species specific. They will absorb a great number of organic compounds, including ones that may not be of interest or may cause interference. For many applications this is acceptable, however for monitoring samples of mixed composition other approaches must be taken.

Multiple polymers, all with different affinities for a suite of compounds, can be combined into an array to produce quantitative, chemically specific information. Each compound would have a fingerprint response across the array, allowing it to be identified even in a mixture through methods such as principal components analysis.[43-45]

Kannan *et al*.[46] demonstrated that a combination of PDMS and carbowax can be used in an array format to distinguish between different nitroaromatic isomers. This was not possible for any one of the polymers individually. Penza *et al.*[43] used a set of four polymer films and principal components analysis to

analyze mixtures of methanol and 2-propanol with a surface acoustic wave (SAW) sensor. Bourgeois *et al.*[45] used an array of eight conducting polymers to monitor the headspace from wastewater by detecting changes in sensor resistance.

As an alternative to developing many polymers having broad preferences for one class over another, coatings that are far more specific can be developed. This can be done by using antibody coatings[32-33] or incorporating specific chelating groups into the coating[34,47]. These tend to be more expensive routes. The development of molecularly imprinted polymers (MIPs) allows for making more selective polymers, while still retaining the advantages of being inexpensive and relatively easy to synthesize[48]. In molecular imprinting, a tightly cross-linked polymer is formed in the presence of a template molecule. The polymer forms around the template, which is later removed, creating binding sites of the correct shape to accommodate that template molecule[49]. These polymers tend to be very selective, and have been compared to antibodies for their molecular recognition capabilities.[50]

MIPs have been used as selective solid phase extraction phases[51] or as coatings for sensors. Matsuguchi *et al.*[52] coated poly(methyl methacrylate) imprinted with either toluene or p-xylene on a quartz crystal microbalance sensor. The polymers showed greater affinity for whichever molecule they were imprinted with. Dickert *et al*.[50] coated a quartz crystal microbalance sensor with a molecularly imprinted polymer. They used polyurethane imprinted with either fresh or used motor oil for sensing mixtures of PAHs in water. MIPs have also

been used in biological applications, and are able to distinguish between different enantiomers, such as L-Lysine and D-Lysine.[53]

While MIPs find effective use in single compound detection, for the more general use sensor proposed here, they are less useful. In addition MIPs do not normally have the required physical and optical properties for use in an LPG-based sensor.

1.4.3 Physical and Optical Requirements

In addition to having desirable chemical properties, a polymer coating for optical sensors should also have certain physical properties. Depending on the application, a coating should be uniform, flexible, robust, optically transparent, and inexpensive. The refractive index of the polymer is also important as it greatly affects sensitivity in both evanescent wave and long-period grating sensors. The penetration depth of the evanescent field is dependent on the refractive index of the coating in comparison with the fiber core. Thus a coating that has a refractive index similar to that of the core will afford greater interaction with the evanescent field. This is also important for LPG based sensors, where the change in attenuation maximum with change in coating refractive index is dramatically greater for polymer coatings with refractive indices close to that of the fiber cladding.

1.4.3.1 Refractive Index of Mixtures

The refractive index of multiple materials in a homogenous mixture can be roughly approximated as a weighted average of the refractive index of the various components of the mixture. There are several mathematical models that serve to better approximate the refractive index of mixtures. Perhaps the most well known is the Lorentz-Lorenz relationship[54]. Generalized to m components it is:

$$\frac{n_{1\to m}^2 - 1}{n_{1\to m}^2 + 2} = \sum_{i=1}^{m} \Phi_i \frac{n_i^2 - 1}{n_i^2 + 2} \tag{7}$$

Where Φ_i is the volume fraction, n_i is the refractive index of pure component i and $n_{1\to m}$ is the refractive index of the mixture of components 1 through m. The Lorentz-Lorenz equation assumes isotropic samples, such as liquid samples or liquid-like samples, where the mixture has a volume equal to the sum of the volumes of the individual components.

1.4.3.2 Polymer Refractive Indices

The refractive index values of polymeric materials cover a wide range. Table 1.1 lists a number of common polymer materials and their respective refractive indices. The requirements of the finished sensor are for a polymer coating that, at the usual sodium D-line (589 nm), has a refractive index of just below 1.46, the refractive index of the cladding. Poly dimethyl siloxane (PDMS) has a refractive index of about 1.40, which puts it within reach of this range only

Polymer	**Refractive Index (589 nm)**
Poly (hexafluoropropylene oxide)	1.3010
Poly (tetrafluoroethylene)	1.3500
Poly (dimethyl siloxane)	1.4035
Poly (methyl octyl siloxane)	1.4450
Poly (propylene oxide)	1.4570
Poly (ethylene glycol)	1.4590
Poly (methyl methacrylate)	1.4893
Poly (vinyl alcohol)	1.5000
Polyethylene, low density	1.5100
Poly (methyl phenyl siloxane)	1.5330
Poly (vinyl chloride)	1.5390
Polyethylene, high density	1.5400
Polycarbonate resin	1.5860
Polystyrene	1.5894

Table 1.1 Refractive Indices of common polymer materials at 589 nm and 25 ^{o}C[55]

after some modification. Other polymers have refractive indices within the correct range but lack the other desirable material properties of PDMS.

1.4.3.3 Refractive Index Modification in Polymers

The refractive index of polymers can be adjusted by controlling the composition of the polymer. Many examples in the literature explore modification of polysiloxane refractive indices, primarily for purposes of optical coupling or building optical devices with the polymers[56-58].

Control of refractive index is important when mixing substances together for optical components or optical coupling. Mixing two immiscible materials together that have different refractive indices can result in haziness and light scattering. Similarly, using a material for optical coupling that has a refractive index significantly different than the components it is coupling together can result in optical losses. Some recent research on SPR looks at using a thin polymer layer to couple SPR components together[59-60]. Previous work used gels or index matching fluids, which, while effective, tended to be messy and contamination from the fluids was an issue. PDMS performed well but due to its different refractive index, there were significant optical losses. This is a situation where the advantages of being able to control polymer refractive index are apparent.

One common way to alter the refractive index of a PDMS based polymer is to mix in varying amounts of diphenyl siloxane, or methyl phenyl siloxane. Gu *et al*.[56] report that increasing the mole percent of poly diphenyl siloxane in PDMS resulted in a linear increase in the refractive index. Increasing the amount of

diphenyl siloxane from 6.1 mole percent to 27.8 resulted in an increase in refractive index from 1.4268 to 1.5028.

Kohjiha *et al.*[57] demonstrated that other functional groups incorporated into the PDMS are capable of changing the refractive index. They used phenyl, napthyl, anthryl and n-perfluorooctyl side groups to linearly alter the polymer refractive index in the range from 1.35 to 1.70. Colomines *et al*.[61] showed a linear relationship between refractive index and the weight percent of fluorine within a polysiloxane polymer. Matejec *et al.*[62] synthesized a variety of UV curable organically modified siloxane via the sol gel method for use in optical sensors. They demonstrated that changing the composition of the polymer and the included functional group altered the refractive index of the resulting polymer.

The refractive index of PDMS can also be altered by adding metals such as titanium. Nakade *et al*.[58] showed that adding titanium into PDMS caused a linear increase in refractive index. Titanium has a comparatively high refractive index, and even small amounts of the compound can increase the polymer refractive index substantially. Compounds such as titanium(IV) tetraisopropoxide have the additional advantage of simultaneously crosslinking the polymer.

Mixing diverse polymer types together can also be used to control refractive index. Okamoto[63] showed that the refractive index of polycarbonate can be lowered by mixing it with PDMS or PMMA. The relationship between percent PDMS in the polycarbonate and refractive index was also linear.

1.5 Polysiloxanes

With these demands in mind, the polymer chosen for initial testing in our proposed sensor system was poly(dimethylsiloxane) (PDMS).

PDMS has a long history of being used in solid phase microextraction (SPME) experiments.[64-65] The polymer is robust, hydrophobic and transparent. In addition, PDMS can reversibly absorb most non polar organic contaminants from aqueous or gaseous samples. It tends to absorb organics from water in correlation with the compound's octanol-water coefficient.[66-67] The refractive index of PDMS, without modification, is in the region of 1.39-1.41 at 589 nm.

PDMS has been used in conjunction with fiber optic sensors to extract and detect a variety of organic compounds, including aromatics[18,21], hydrocarbons[17] and chlorinated compounds.[15] As PDMS is not selective in the non polar organic compounds it absorbs, other functional groups, such as diphenyl siloxane can be incorporated to favour different compounds. The addition of the phenyl functionality is quite common.[15,21-22] It has the advantage of increasing the polymer's affinity to aromatics, as well as increasing the polymer refractive index, which in many cases results in an increase in sensitivity. The phenyl group is not limited to improving absorption of aromatics. Zimmermann *et al.*[15] evaluated PDMS and poly methyl phenyl siloxane for absorbing contaminants. They found that the addition of the phenyl group improved absorption of trichloroethylene (TCE).

Other functional groups can also be used. Matejec *et al.*[62] incorporate a thiol functionality into PDMS to make the polymer coating sensitive to CO_2 and SO_2 gases. Abdelghani *et al*.[68] investigated the performance of fluorosiloxane polymers coated on an SPR fiber sensor. They found that the fluorosiloxane mixed in a 50:50 ratio with PDMS was best at absorbing various chlorinated and aromatic solvents. Haug *et al.*[69] coated cyano, methyl and chlorooctadecyl polysiloxanes onto sensors to evaluate their response to various VOCs. They found that there was a different response among the films used. Finally, Ronot *et al*.[70] showed that the chemical selectivity of polysiloxanes to water, ethanol, acetone, dichloromethane and toluene could be adjusted through the addition of amino, vinyl or glycidoxypropyl groups.

In this work, in addition to poly(dimethyl siloxane), we synthesized poly(diphenyl siloxane), poly(methyl octyl siloxane), poly (3-cyanopropyl methyl siloxane) and poly (3,3,3-trifluoropropyl methyl siloxane) as test polymers for our system. These functional groups are well known and readily available because of their usage in capillary gas liquid chromatography where they serve as stationary phases in specialized columns. The performance of these modified siloxane films in LPG sensors is described, in terms of chemical selectivity and refractive index range. The test polymers were evaluated with a number of VOCs and a chlorinated compound of environmental interest. The compounds were chosen to cover a range of polarities and functional groups to explore the effectiveness of the sensor with compounds of different chemical classes.

1.6 References:

1. B. Adhikari, S. Majumdar, Polymers in sensor applications, Prog. Polym. Sci., 29, (2004) 699-766.
2. S. M. Klainer, J. R. Thomas, J. C. Francis, Fiber-optic chemical sensors offer a realistic solution to environmental monitoring needs, Sens. Actuators, B, 11, (1993) 81-86.
3. O. Wolfbeis, Fiber-optic chemical sensors and biosensors, Anal. Chem., 78, (2006) 3859-3874.
4. Environment Canada, CEPA environmental registry – toxic substances list – schedule 1, (2008) <http://www.ec.gc.ca/CEPARegistry/subs_list/Toxicupdate.cfm>, accessed Sept. 2008.
5. Environment Canada, News Releases, (2008) <http://www.ec.gc.ca/default.asp?lang=En&n=714D9AAE-1&news=88B8311A-FB2E-4E5A-AA81-BC24118113D9>, accessed Sept. 2008.
6. Ontario Ministry of Labour, Government commits to regularly update occupational exposure limits, (2004) <http://www.labour.gov.on.ca/english/news/2004/04-52b.html>, accessed Sept. 2008.
7. Ontario Ministry of the Environment, (2005) <http://www.ene.gov.on.ca/envision/env_reg/er/documents/2005/airstandards/PA04E0035.pdf>, accessed Sept. 2008.

8. Ontario Ministry of the Environment, (2008) <http://www.ene.gov.on.ca/publications/6569e-chem.pdf>, accessed Sept. 2008.
9. V. Bhatia, A. M. Vengsarkar, Optical fiber long-period grating sensors, Optics Lett., 21, (1996) 692-694.
10. R. A. Potyrailo, Polymeric sensor materials: Toward an alliance of combinatorial and rational design tools? Angew. Chem. Int. Ed., 45, (2006) 702-723.
11. K. J. Albert, N. S. Lewis, C. L. Schauer, G. A. Sotzing, S. E. Stitzel, T. P. Vaid, D. R. Walt, Cross-reactive chemical sensor arrays, Chem. Rev., 100, (2000) 2595-2626.
12. M. Born, E. Wolf, Principles of Optics, 4th Ed., Pergamon Press, Oxford, 1970, p. 36-38.
13. M. E. Bosch, A. J. R. Sanchez, F. S. Rojas, C. B. Ojeda, Recent developments in optical fiber biosensors, Sensors, 7, (2007) 797-859.
14. B. Mizaikoff, Mid-infrared evanescent wave sensors – a novel approach for subsea monitoring, Meas. Sci. Technol., 10 (1999) 1185-1194.
15. B. Zimmermann, J. Burck, H.-J. Ache, Studies on siloxane polymers for NIR-evanescent wave absorbance sensors, Sens. Actuators, B, 41 (1997) 45-54.
16. R. Krska, R. Kellner, U. Schiessl, M. Tacke, A. Katzir, Fiber optic sensor for chlorinated hydrocarbons in water based on infrared fibers and tunable diode lasers, Appl. Phys. Lett., 63 (1993) 1868-1870.

17. P. Tobiska, M. Chomat, V. Matejec, D. Berkova, I. Huttel, Investigation of fiber-optic evanescent-wave sensors for detection of liquid hydrocarbons, Sens. Actuators, B, 51, (1998) 152-158.
18. M. Chomat, D. Berkova, V. Matejec, I. Kasik, G. Kuncova, M. Hayer, Optical detection of toluene in water using an IGI optical fiber with a short sensing region, Sens. Actuators, B, 87 (2002) 258-267.
19. R. Howley, B. D. MacCraith, K. O'Dwyer, P. Kirwan, P. McLoughlin, A study of the factors affecting the diffusion of chlorinated hydrocarbons into polyisobutylene and polyethylene-co-propylene for evanescent wave sensing, Vib. Spectrosc., 31, (2003) 271-278.
20. E. Sensfelder, J. Burck, H.-J. Ache, Determination of hydrocarbons in water by evanescent wave absorption spectroscopy in the near-infrared region, Fresenius J. Anal. Chem., 354, (1996) 848-851.
21. G. Schwotzer, I. Latka, H. Lehmann, R. Willsch, Optical sensing of hydrocarbons in air or in water using UV absorption in the evanescent field of fibers, Sens. Actuators, B, 38-39 (1997) 150-153.
22. V. Matejec, M. Chomat, D. Berkova, J. Mrazek, R. Ardeleanu, V. Harabagiu, M. Pinteala, B. C. Simionescu, Detection of toluene dissolved in water by using PCS fibers excited by an inclined collimated beam, Sens. Actuators, B, 90 (2003) 204-210.
23. S. W. James, R. P. Tatam, Optical fiber long-period grating sensors: characteristics and application, Meas. Sci. Technol., 14, (2003), R49-R61.

24. V. Bhatia, Application of long-period gratings to single and multi-parameter sensing, Opt. Express, 4, (1999) 457-466.
25. R. Hou, Z. Ghassemlooy, A. Hassan, C. Lu, K. P. Dowker, Modelling of long-period fibre grating response to refractive index higher than that of cladding, Meas. Sci. Technol., 12, (2001) 1709-1713.
26. H. J. Patrick, A. D. Kersey, F. Bucholtz, Analysis of the response of long period fiber gratings to external index of refraction, J. Lightwave Technol., 16, (1998) 1606-1612.
27. T. Allsop, L. Zhang, I. Bennion, Detection of organic aromatic compounds in paraffin by a long-period fiber grating optical sensor with optimized sensitivity, Opt. Commun., 191, (2001) 181-190.
28. X. Shu, D. Huang, Highly sensitive chemical sensor based on the measurement of the separation of dual resonant peaks in a 100-μm-period fiber grating, Opt. Commun., 171, (1999) 65-69.
29. J. H. Chong, P. Shum, H. Haryono, A. Yohana, M. K. Rao, C. Lu, Y. Zhu, Measurements of refractive index sensitivity using long-period grating refractometer, Opt. Commun., 229, (2004) 65-69.
30. R. Falate, R. C. Kamikawachi, M. Muller, H. J. Kalinowski, J.L. Fabris, Fiber optic sensors for hydrocarbon detection, Sens. Actuators, B, 105, (2005) 430-436.
31. R. Falciai, A. G. Mignani, A. Vannini, Long period gratings as solution concentration sensors, Sens. Actuators, B, 74, (2001) 74-77.

32. M. P. DeLisa, Z. Zhang, M. Shiloach, S. Pilevar, C. C. Davis, J. S. Sirkis, W. E. Bentley, Evanescent wave long-period fiber bragg grating as an immobilized antibody sensor, Anal. Chem. 71, (2000) 2895-2900.
33. C. Pennington, M. Jones, M. Evans, R. VanTassell, J. Averett, Fiber optic based biosensors utilizing long period grating (LPG) technology, Proceedings of SPIE, 4255, (2001) 53-63.
34. J. Keith, L. C. Hess, W. U. Spendel, J. A. Cox, G. E. Pacey, The investigation of the behavior of a long period grating sensor with a copper sensitive coating fabricated by layer-by-layer electrostatic adsorption, Talanta, 70, (2006) 818-822.
35. J.-L. Tang, S.-F. Cheng, W.-T. Hsu, T.-Y. Chiang, L.-K. Chau, Fiber-optic biochemical sensing with a colloidal gold-modified long period fiber grating, Sens. Actuators, B, 119, (2006) 105-109.
36. I. M. Ishap, A. Quintela, S. W. James, G. J. Ashwell, J. M. Lopez-Higuera, R. P. Tatam, Modification of the refractive index response of long period grating using thin film overlays, Sens. Actuators, B, 107, (2005) 738-741.
37. S. Khaliq, S. W. James, R. P. Tatam, Enhanced sensitivity fiber optic long period grating temperature sensor, Meas. Sci. Technol., 13, (2002) 792-795.
38. L. A. Wang, C. Y. Lin, G. W. Chern, A torsion sensor made of a corrugated long period fiber grating, Meas. Sci. Technol., 12, (2001) 793-799.

39. C.-Y. Lin, L. A. Wang, G.-W. Chern, Corrugated Long-Period fiber gratings as strain, torsion, and bending sensors, J. Lightwave Technol., 19 (2001) 1159-1168.
40. S. Khaliq, S. W. James, R. P. Tatam, Fiber-optic liquid-level sensor using a long-period grating, Opt. Lett., 26, (2001) 1224-1226.
41. S. T. Lee, R. D. Kumar, P. S. Kumar, P. Radhakrishnan, C. P. G. Vallabhan, V. P. N. Nampoori, Long period gratings in multimode optical fibers: application in chemical sensing, Opt. Commun., 224, (2003) 237-241.
42. C. E. Carraher, Polymer Chemistry, 7th Ed., CRC Press Inc. Boca Raton, 2008, p. 83-88, 597.
43. M. Penza, G. Cassano, Application of principal component analysis and artificial neural networks to recognize the individual VOCs of methanol/2-propanol in a binary mixture by SAW multi-sensor array, Sens. Actuators, B, 89 (2003) 269-284.
44. A. Hierlemann, U. Weimar, G. Kraus, M. Scheizer-Berberich, W. Gopel, Polymer-based sensor arrays and multicomponent analysis for the detection of hazardous organic vapours in the environment, Sens. Actuators, B, 26-27, (1995) 126-134.
45. Bourgeois, W., R. M. Stuetz, Use of a chemical sensor array for detecting pollutants in domestic wastewater, Water Research, 36, (2002) 4505-4512.

46. G. K. Kannan, J. C. Kappor, Adsorption studies of carbowax and poly dimethyl siloxane to use as chemical array for nitro aromatic vapour sensing, Sens. Actuators, B, 110, (2005) 312-320.
47. N. Moriguchi, T. Tsugaru, S Amiya, Molecular design of the polymer forming the complex with metal. [II]: poly (dimethyl siloxane) with pyridine ring, J. Mol. Struct., 477 (1999) 181-189.
48. K. Haupt, K. Mosbach, Molecularly imprinted polymers and their use in biomimetic sensors, Chem. Rev., 100, (2000) 2495-2504.
49. P. A. G. Cormack, A. Z. Elorza, Molecularly Imprinted Polymers: synthesis and characterization, J. Chromatogr. B, 804, (2004) 173-182.
50. F. L. Dickert, P. Lieberzeit, M. Tortschanoff, Molecular imprints as artificial antibodies – a new generation of chemical sensors, Sens. Actuators, B, 65, (2000) 186-189.
51. E. Caro, R. M. Marce, P. A. G. Cormack, D. C. Sherrington, F. Borrull, On-line solid-phase extraction with molecularly imprinted polymers to selectively extract substituted 4-chlorophenols and 4-nitrophenol from water, J. Chromatogr. A, 995, (2003) 233-238.
52. M. Matsuguchi, T. Uno, Molecular imprinting strategy for solvent molecules and its application for QCM-based VOC vapor sensing, Sens. Actuators, B, 113, (2006) 94-99.
53. R. Panahi, E. Vasheghani-Farahani, S. A. Shojaosadati, Separation of L-lysine from dilute aqueous solution using molecular imprinting technique, Biochem. Eng. J., 35 (2007) 352-356.

54. R. Mehra, Application of refractive index mixing rules in binary systems of hexadecane and heptadecane with n-alkanols at different temperatures, Proc. Indian Acad. Sci. (Chem. Sci.), 115, (2003) 147-152.
55. Parker-Texloc, Refractive index of polymers/haze value, (2006) <www.texloc.com/closet/cl_refractiveindex.html>, accessed June 2008.
56. Q. G. Gu, Q. L. Zhou, Preparation of high strength and optically transparent silicone rubber, Eur. Polym. J., 34 (1998) 1727-1733.
57. S. Kohjiha, K. Maeda, S. Yamashita, Chemical modification of silicone elastomers for optics, J. Mater. Sci., 25 (1990) 3365-3374.
58. M. Nakade, K. Kameyama, M. Ogawa, Synthesis and Properties of titanium dioxide/polydimethylsiloxane hybrid particles, J. Mater. Sci., 39 (2004) 4131-4137.
59. S. Owega, D. Poitras, K. Faid, Solid-state optical coupling for surface Plasmon resonance sensors, Sens. Actuators, B, 114, (2006) 212-217.
60. T. Masadome, Y. Asano, T. Imato, S. Ohkubo, T. Tobita, H. Tabei, Y. Iwasaki, O. Niwa, Y. Fushinuki, Preparation of refractive index matching polymer film alternative to oil for use in portable surface-plasmon resonance phenomenom-based chemical sensor method, Anal. Bioanal. Chem., 373, (2002) 222-226.
61. G. Colomines, S. Andre, X. Andrieu, A. Rousseau, B. Boutivin, Synthesis and Characterization of ultraviolet-curable fluorinated polydimethylsiloxanes as ultraviolet-transparent coatings for optical fiber gratings, J. Appl. Polym. Sci., 90 (2003) 2021-2026.

62. V. Matejec, K. Rose, M. Hayer, M. Pospisilova, M. Chomat, Development of organically modified polysiloxanes for coating optical fibers and their sensitivity to gases and solvents, Sens. Actuators, B, 38-39, (1997) 438-442.
63. M. Okamoto, Relationship between the composition of polycarbonate copolymers and the refractive index, J. Appl. Polym. Sci., 84, (2002) 514-521.
64. C. Dietz, J. Sanz, C. Camara, Recent developments in solid-phase microextraction coatings and related techniques, J. Chromatogr., A, 1103, (2006) 183-192.
65. J. A. Koziel, I. Novak, Sampling and sample preparation strategies based on solid-phase microextraction for analysis of indoor air, Trends in analytical chemistry, 21, (2002) 840-850.
66. P. Mayer, W. H. J. Vaes, J. L. M. Hermens, Absorption of hydrophobic compounds into the poly(dimethylsiloxane) coating of solid-phase microextraction fibers: High partition coefficients and fluorescence microscopy images, Anal. Chem., 72 (2000) 459-464.
67. R. S. Brown, P. Akhtar, J. Akerman, L. Hampel, I. S. Kozin, L. A. Villerius, H. J. C. Klamer, Partition controlled delivery of hydrophobic substances in toxicity tests using poly(dimethylsiloxane) (PDMS) films, Environ. Sci. Technol., 35, (2001) 4097-4102.
68. A. Abdelghani, N. Jaffrezic-Renault, SPR fiber sensor sensitised by fluorosiloxane polymers, Sens. Actuators, B, 74, (2001) 117-123.

69. M. Haug, K. D. Schierbaum, G. Gauglitz, W. Gopel, Chemical sensors based on polysiloxanes: comparison between optical, quartz microbalance, calorimetric and capacitance sensors, Sens. Actuators, B, 11 (1993) 383-391.
70. C. Ronot, M. Archenault, H. Gagnaire, J. P. Goure, N. Jaffrezic-Renault, T. Pichery, Detection of chemical vapours with a specifically coated optical-fiber sensor, Sens. Actuators, B, 11, (1993) 375-381.

Chapter 2

Synthesis of Polysiloxanes

2.1 Introduction

2.1.1 Polysiloxane Synthesis

Poly(dimethyl siloxane) (PDMS) (figure 2.1a) is a well known polymer material which finds many applications, from lubricants, to technical equipment parts, to solid-phase microextraction (SPME) materials, to bathtub sealants. It was first synthesized in the early 1940s by Eugene Rochow and William Gilliam[1]. Since then it has undergone much work and refinement and is commercially available in a variety of forms.

PDMS has a number of properties that make it desirable for use as a sensitive coating in sensor applications. Most importantly, it is a hydrophobic polymer and as such, absorbs a great number of hydrophobic compounds. It is well known as an SPME material and tends to absorb compounds in close correlation with their hydrophobicity[2-5]. It is also capable of absorbing these compounds in a completely reversible manner, making the coating reusable over a long period of time. The polymer is relatively inexpensive, durable, biocompatible and resistant to fouling[6]. For these reasons, the polymer was an excellent starting place for exploring polymer coatings for our proposed sensor platform.

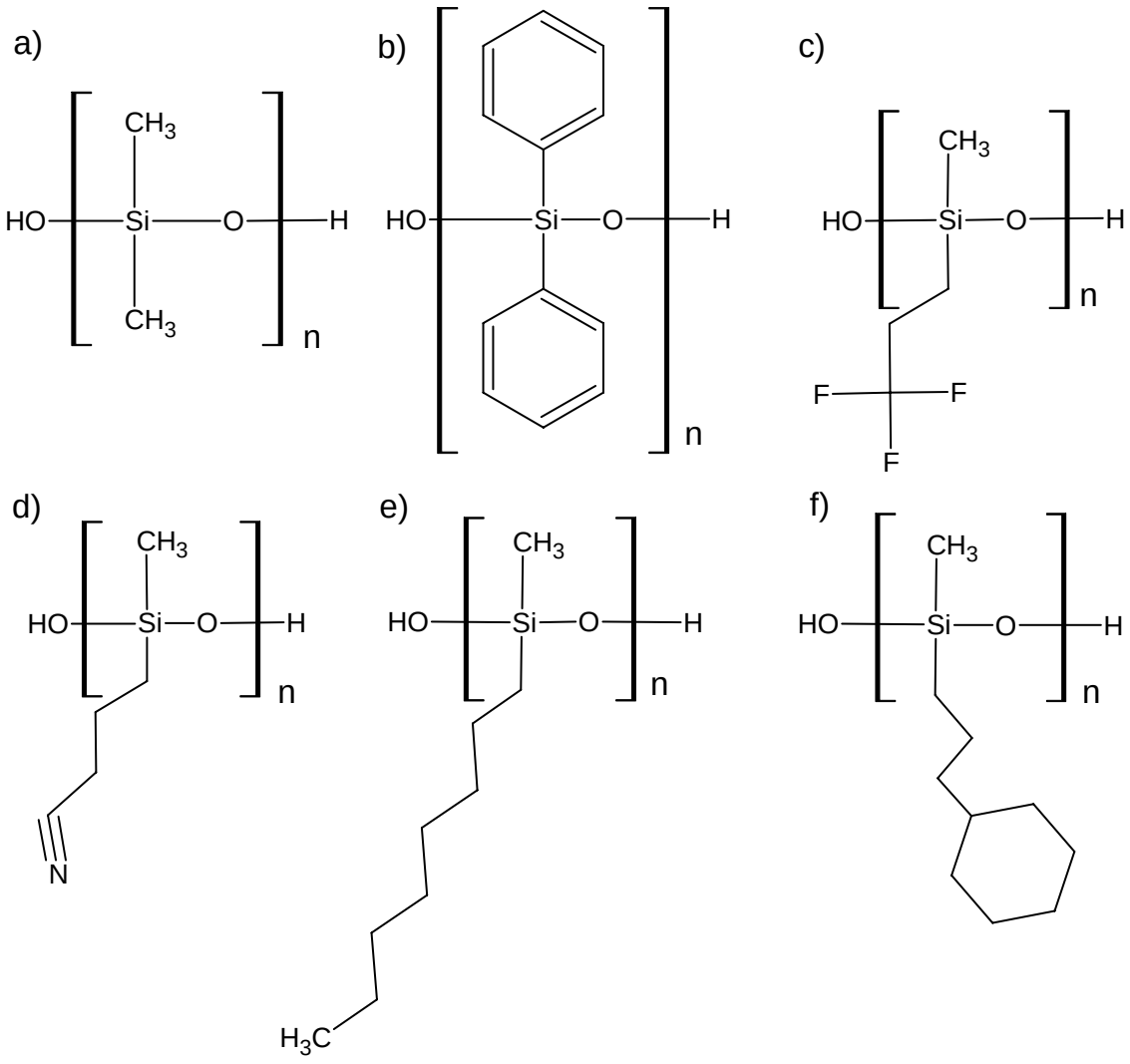

Figure 2.1 Structures of polymers – a) poly dimethyl siloxane; b) poly diphenyl siloxane; c) poly (3,3,3-trifluoropropyl)methyl siloxane; d) poly (3-cyanopropyl)methyl siloxane; e) poly methyloctyl siloxane; f) poly (2-cyclohexylethyl)methyl siloxane

Many research groups working with fiber optic based sensors use PDMS or one of its derivatives as a sensitive coating. Of these, some will use a commercially available material to coat their fibers[7], or use optical fibers that come premade with a silicone polymer cladding[8-10]. Commercially available options are attractive as the polymer is consistent between experiments, gives excellent film quality and is less time consuming than synthesizing a polymer from monomers. However, altering the chemical selectivity or refractive index of the polymer through chemical modification is not as easy with a commercial polymer as with a custom synthesized polymer.

Synthesizing polysiloxanes from monomers greatly increases the practical range in polymer composition. Polysiloxanes can be synthesized through a two-step synthetic scheme. In the first step, monomers are condensed to form a pre-polymer, consisting of straight chain oligomers with approximately 8-30 repeat units. In the second step, the pre-polymer material is crosslinked to form an elastomer.

Pre-polymer materials can be easily synthesized using dichloro or dialkoxy substituted silane monomers. Either an acid or base catalyzed synthesis method can potentially be extended to a number of different silane monomers to create distinct polysiloxanes. Average molecular weights over 1000 amu and a low percentage of cyclic material are desirable for creating polymers that can later be crosslinked into elastomeric products. A glacial acetic acid catalyzed method was demonstrated in a previous report[11] to give these desired properties. Highly concentrated bases are also known to produce high molecular weight siloxanes

with limited cyclic material[12]. Crosslinking of the pre-polymer materials can be accomplished through the addition of small amounts of tri or tetrachloro monomers, or with the addition of a crosslinking compound such as titanium(IV) tetraisopropoxide[13,14].

This synthetic approach allows for the incorporation of a wide variety of functional groups in place of the standard methyl group. Polysiloxanes created this way include poly methyl octyl siloxane (PMOS), poly diphenyl siloxane (PDPS), poly (3,3,3-trifluoropropyl)methyl siloxane (PFMS) and poly (3-cyanopropyl)methyl siloxane (PCMS) (see figure 2.1). These functionalized polymers are fairly well known in gas chromatography where these substituted polysiloxanes make up many of the specialized liquid phases for coating GC capillary columns. All of the monomers for these compounds are relatively inexpensive and simple to obtain.

To expand beyond these well known functional groups is more difficult. Many functional groups that may be desirable to explore are simply not available as a dichloro or dialkoxy substituted silane. Thus, to further extend the number of siloxanes, other synthetic methods must be considered. One promising method is the use of platinum catalysts to catalyze the hydrosilylation of vinyl terminated molecules to a hydrosiloxane. Conceivably, any vinyl terminated compound can be incorporated into the siloxane backbone using this method. This method was first explored by Speier[15] in the late 1950s. He used hexachloroplatinic acid, now frequently referred to as Speier's catalyst, to couple simple alkenes to hydrosilanes. The addition of other functional groups to

hydrosilanes is somewhat more complicated as competing side reactions reduce the yield of product. This is particularly evident when trying to add a chlorinated alkene to a hydrosilane[16], as the chlorine can be exchanged for a hydrogen, or react with the hydrosilane in place of the vinyl group. Other platinum catalysts have been developed which are active even in the presence of other functional groups. For example, bis(dialkylsulfido) platinum(II) salts have been shown to work well for the addition of acetate and amide containing alkenes[17].

In this thesis, the preparation of polysiloxanes with cyclohexyl, chloro and amino substitutions was attempted using a hexachloro platinic acid catalyzed hydrosilylation reaction.

2.1.2 Characterization of Polymer Materials

When polymers have very high molecular weight, conventional methods of analysis are not necessarily effective for determining chemical structure or molecular weight. A polymer sample does not have a single molecular weight but a distribution of molecular weights depending on the number of monomeric units combined, or the degree of polymerization. Many analytical methods for polymers focus on determining the average molecular weight and polydispersity of the polymer.

Average molecular weight is usually calculated in one of two ways, the weight average M_w, or the number average M_n:

$$M_w = \frac{\sum_i m_i^2 N_i}{\sum_i m_i N_i} \quad (1)$$

$$M_n = \frac{\sum_i m_i N_i}{\sum_i N_i} \quad (2)$$

where m_i is the mass and N_i is the number of polymer molecules having that mass.

The weight average molecular weight will always be equal to or higher than the number average molecular weight. The polydispersity of a polymer sample, defined as the ratio of the weight average to the number average molecular weight, will therefore range in value from one and up. Samples with a large distribution of chain lengths will have a larger polydispersity.

Classical methods like osmometry or end group titrations can be used to determine number average molecular weights. Other methods such as light scattering or sedimentation can be used to calculate the weight average molecular weight. More modern methods of polymer analysis include size exclusion chromatography or NMR spectroscopy.

Mass spectrometry can give an actual molecular mass value for compounds, making it a perfect candidate for determining the average molecular weights of polymers. In particular, the advent of matrix assisted laser desorption ionization time of flight (MALDI-TOF) mass spectrometry has opened up the possibility of analyzing large molecules, like polymers, without fragmentation. MALDI-TOF-MS is an excellent method for roughly characterizing the distribution of molecular weights in the polymer and for structure confirmation, based on the molecular weight of the repeat group[18]. It is not as effective at obtaining an accurate value for the average molecular weight of the polymer. This is because

mass bias creates a molecular weight which is artificially low as it is more difficult to ionize high molecular weight polymer chains[18]. Careful control of instrument conditions can minimize this to some extent.

2.1.3 Refractive Index modification in polymers for optical applications

The refractive index of polymer materials can be fine-tuned by controlling the composition of the polymer during synthesis, as described in section 1.4.3.3. This allows the polymer coatings to be used in optical applications where refractive index must be controlled, such as in sensor applications, where having a specific refractive index enhances sensitivity. The technology also has potential application in building siloxane based optical devices, such as gratings.

For eventual use on an LPG based sensor, polymers having a refractive index just below that of the fiber cladding, about 1.425 at 1550nm, were synthesized.

2.2 Experimental

2.2.1 Synthesis

All of the polysiloxanes used were synthesized from their individual monomers in a two-step process. The first step was condensation of the monomers, through either an acid or base catalyzed condensation reaction, to produce a “pre-polymer” liquid consisting of linear polymer chains ranging from

about 8 to 20 or more repeat units. Some cyclic oligomers may have been produced as an impurity. The second step was cross-linking the pre-polymer material using a tetra-functional crosslinker to produce a siloxane elastomer. Monomers used were dichlorodimethyl silane (Aldrich, Milwaukee, WI), diethoxydiphenyl silane (Aldrich), (3-cyanopropyl)methyldichloro silane (Alfa Aesar, Ward Hill, MA), (3,3,3-trifluoropropyl)methyldichloro silane (Alfa Aesar) and dichloromethyloctyl silane (Aldrich).

Poly (dimethyl siloxane) prepolymer

In the first polymerization step, poly(dimethyl siloxane) (PDMS) was formed using both acid and base catalysis. In the acid catalyzed method, adapted from Zimmermann *et al.*[11] 9.63 mL of dichlorodimethyl silane (80 mmol) was dripped into a solution containing 3.80 mL of methanol and 4.58 mL (80 mmol) of glacial acetic acid over about 10 minutes. The solution was stirred for an hour under reflux (60^{o}C), and then heated to drive off volatile impurities. In the base catalyzed method, 5 g of dichlorodimethyl silane (38.7 mmol) was stirred at 0^{o}C while 1 mL of 14 M NaOH was added dropwise over an hour. After an additional hour of stirring, 3 mL of methylene chloride and 8 mL of water were added. The organic layer was washed several times with dilute base and water until a neutral pH was reached. Solvent from the organic layer was evaporated to leave behind the PDMS material.

MALDI TOF MS Analysis: Polymer repeat unit = 74 m/z (-Si(CH$_3$)$_2$O-)

Poly (diphenyl siloxane) prepolymer

Poly(diphenyl siloxane) (PDPS) was created in either a 1:9 or 1:4 mole ratio with PDMS. Synthesis of the PDPS was also done using both acid and base catalysis using similar procedures to the PDMS polymerization.

^{1}H NMR Analysis: 0.05 ppm (Si-C$\underline{H}_3$); 7.20 and 7.50ppm (Si-C$_6\underline{H}_5$)

Poly (methyloctyl siloxane) prepolymer

Poly (methyloctyl siloxane) (PMOS) was made with the base catalyzed method only. Acid catalysis did not result in sufficiently high molecular weight material.

MALDI TOF MS Analysis: Polymer repeat unit = 172 m/z (-Si(CH_3)(C_8H_{17})O-)

Poly (3,3,3-trifluoropropyl) methyl siloxane prepolymer

Poly ((3,3,3-trifluoropropyl)methyl siloxane) (PFMS) was made both as a pure polymer and in a 1:4 mole ratio with PMOS. Base catalysis was used as high molecular weights were not obtained with the acid method.

MALDI TOF MS Analysis: Polymer repeat unit = 156 m/z

(-Si(CH_3)($CH_2CH_2CF_3$)O-)

Poly ((3-cyanopropyl) methyl siloxane) prepolymer

Poly ((3-cyanopropyl) methyl siloxane) (PCMS) was made with a modified acid catalyzed procedure. Initial attempts to polymerize the monomer in acid resulted in side reactions that either crosslinked the pre-polymer, or reacted

away the nitrile group to produce other functional groups (according to MALDI-TOF-MS analysis after polymerization). Due to the apparent reactivity of the nitrile group, more gentle reaction conditions were necessary. 1.58 mL (10 mmol) of (3-cyanopropyl)methyldichloro silane was slowly added over 10 minutes into 0.48 mL of methanol, 0.19 mL (5 mmol) of formic acid and 1.00 mL of methylene chloride. The reaction was kept at 0 ^{o}C. As soon as the monomer addition was complete, the reaction mixture was bubbled with nitrogen. 1 mL aliquots of methylene chloride were added periodically to keep the reaction mixture viscosity low while the remaining acids and impurities were driven off.

MALDI TOF MS Analysis: Polymer repeat unit = 127m/z (-Si(CH_3)(C_3H_6CN)O-)

Poly ((3-cyclohexylpropyl)methyl siloxane) prepolymer

Poly ((3-cyclohexylpropyl)methyl siloxane) (PCHMS) was formed using two steps. In the first step, poly (methyl siloxane)-co-poly (dimethyl siloxane) (50/50 mole %) was synthesized using acid catalysis.

^{1}H NMR Analysis: 0.05 ppm (Si-C$\underline{H}_3$); 4.6 ppm (Si-$\underline{H}$)

In the second step, allyl cyclohexane was added to the co-polymer via hydrosilylation with hexachloroplatinic acid. For the hydrosilylation procedure, 0.60 g (0.0045 mol) of the product polymer from the first step was combined with 0.772 g allylcyclohexane (10% mole excess), 7.2 mL chloroform and 0.3 mg of hexachloroplatinic acid. The flask was equipped with a condenser and stir bar and placed in a water bath set to 80 ^{o}C. The reaction was left at 80 ^{o}C for three

hours, then left to cool. The resulting product was washed with water to remove impurities and remaining catalyst and dried under nitrogen to remove the solvent. *^{1}H NMR Analysis: 0.05 ppm (Si-C$\underline{H}_3$); 0.4 ppm (Si-C$\underline{H}_2CH_2$-); 0.8 ppm (Si-$CH_2C\underline{H}_2CH_2$-); 1.25 ppm (Si-$CH_2CH_2C\underline{H}_2C_6H_{11}$); 1.1 and 1.6 ppm (Si-$CH_2CH_2CH_2C_6\underline{H}_{11}$)*

2.2.2 Characterization

The structures of the pre-polymer materials were confirmed by either MALDI-TOF-MS or ^{1}H NMR. MALDI-TOF-MS spectra were collected on a Voyager DE STR instrument. Samples were mixed with a 2,5-dihydroxybenzoic acid matrix. ^{1}H NMR spectra were collected on a 400 MHz Avance-400 NMR, in $CDCl_3$ solvent.

In the second polymerization step, the siloxane pre-polymers were mixed in various combinations to obtain the desired ratios of functional groups. They were then diluted in a 1:20 volume ratio with hexanes, or methylene chloride for the PCMS, and Titanium (IV) tetraisopropoxide (Aldrich) was added in various amounts to crosslink the polymer. The titanium(IV) tetraisopropoxide was added as a 10% (v/v) solution in hexanes, as it is reactive in air and in consideration of the small volumes required. Small borosilicate glass slides (~1”x 0.5”) (Fisher, Ottawa, ON) were made by breaking clean microscope slides into six portions. These were set in a 1M solution of KOH to etch for ten minutes, rinsed with deionized water, followed by rinsing in ethanol and then left to air dry. 100 μL

aliquots of the polymer solution were deposited onto the upper surface of the slides, and the polymers were left to cure for 24 hours.

Refractive indices of the various polymer films were measured on a custom-built refractometer as described in section 3.2.

2.3 Results and Discussion

The goal of this work was to be able to make several chemically distinct polymer films that have different affinities for various proposed analytes. Other constraints placed on the polymer include the need for it to be optically transparent, uniform, physically coated onto an optical fiber, and most importantly, have a refractive index close to 1.455 (or 1.425 at 1550nm). PDMS was chosen as an ideal starting material, as it satisfies almost all of the material properties except refractive index, which is around 1.40 but can be modified by a changing the polymer composition.

2.3.1 Modifying commercially available PDMS materials

The ideal system, in terms of simplicity, would be to use commercially available PDMS as a base and add various functional groups which would be incorporated into the polymer network during curing. We considered two commercial candidates.

Dow Corning Aquarium Grade PDMS Sealant cures in approximately 24 hours upon exposure to air using a condensation reaction. Acetate end groups

are hydrolyzed by water in the air to produce acetic acid and a silanol group. The silanol can condense with another acetate end group, with loss of acetic acid, or with another silanol end group, with loss of water. Tri- and tetra-functional crosslinkers are also included. In this way the polymer cures into a tough elastomer. The polymer can be dissolved in organic solvents prior to curing and cast in thin layers. We attempted to add diphenyl siloxane groups to this polymer by adding in diethoxy diphenyl silane (DDPS) prior to curing. We never obtained incorporation of the functional group throughout the polymer. The finished rubber tended to be greasy on the outside, suggesting that the unincorporated diphenyl silane slowly separated out. Addition of 3-aminopropyl triethoxy silane (APTES) was somewhat more successful, but the cured rubber became opaque and sticky.

A second commercially available polymer, Sylgard 184, also available from Dow Corning, was tested. This polymer cures differently and is supplied as a two component preparation. Hydrosilanes are coupled with vinyl substituted silanes via a platinum catalyst, making ethylene bridges which crosslink the polymer. Addition of either APTES or DDPS resulted in the polymer not curing. Since the mechanism of curing in the Sylgard 184 polymer is significantly different from that of the Aquarium Sealant, an allyl amine additive was tried. Having its own vinyl group, allyl amine could take advantage of the hydrosilylation mechanism of curing, adding itself directly onto the polymer backbone. This also did not meet with success. The catalyst of the Sylgard 184 appears to be interrupted by the addition of the allyl amine. This was further

confirmed when later experiments adding allyl amine to poly (methyl siloxane) with hexachloroplatinic acid resulted in no product. The amine likely complexes with the catalyst, halting its activity. The addition of other functional groups with vinyl end groups was not attempted at this time, but it is possible that other allyl compounds may work better for direct addition to Sylgard 184.

2.3.2 Polysiloxane synthesis from monomers

With commercial polymers not performing as desired, the decision was made to synthesize the polymers from monomers. With this approach, more even incorporation of functional groups along the polysiloxane chain would be anticipated. Superior control of the composition and properties of the resulting polymer would also be expected.

PDMS oligomers can be made through a two step process using dichloro dimethyl silane. The first step involves a reaction with water, where the substitution of the chlorine with an –OH group takes place. The resulting silanol is then free to condense with another silanol, or to react with a chlorine end group, in either case producing a siloxane linkage (see figure 2.2).

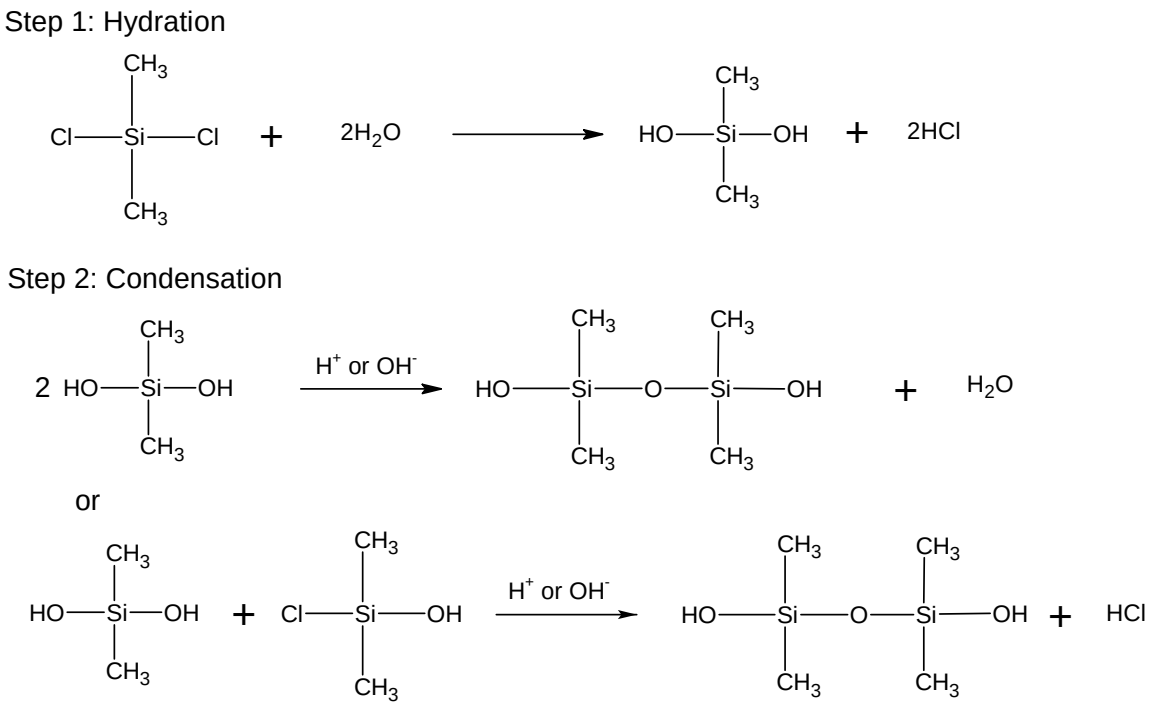

Figure 2.2 Reaction scheme for the condensation of silane monomers

The molecular weight and form of the pre-polymer that is produced during this reaction depends largely on the conditions of the reaction. Since the desired product for the sensor system is a rubbery elastomer, high molecular weight, linear polymer that can be later crosslinked is desirable. Cyclic material, where the head and tail of a polymer chain condense together, is undesirable, as the material will not crosslink into the polymer network. Concentrated reaction solutions reduce the amount of cyclic material as the forming polymer is more likely to encounter and condense with another monomer or oligomer than with itself[12].

The reactions were done with either base or acid catalysis. In the base catalyzed procedure concentrated sodium hydroxide was used. The use of other basic catalysts such as amines, potassium hydroxide, or less concentrated sodium hydroxide was explored. Amines did not produce a product, concentrated potassium hydroxide gave an equivalent product to that of the sodium hydroxide, and the less concentrated sodium hydroxide resulted in lower molecular weight material. Though the use of concentrated sodium hydroxide is not ideal, and requires tedious washing steps to remove salts generated in the reaction, it remained the best of the basic options. Some cyclic material was present in the base catalyzed products as determined by MALDI-TOF-MS. Cyclic material can be identified from the mass spectrum since the molecular weight does not include a contribution from the end groups.

Acid catalysis tends to give a product which is lower in molecular weight than the base catalyzed reaction, unless conditions are carefully controlled[12]. Zimmermann *et al*.[11] demonstrated that the use of glacial acetic acid in methanol gave a high molecular weight product with limited cyclic material. The method is attractive as all of the reagents and byproducts are volatile and can be removed through heating or purging with nitrogen. This avoids the type of washing step used in the base procedure and increases the yield of the reaction.

Using the acid catalyzed procedure resulted in excellent products for PDMS and PDPS. From MALDI-TOF-MS analysis, the PDMS had a similar molecular weight distribution to that obtained from the base catalyzed method, but was free of cyclic material. Acid catalysis failed to produce polymers of

sufficiently high molecular weight for both the PFMS and PMOS polymers. For the PMOS polymers, acid catalysis gave a polymer with between 4 and 11 repeat units, whereas base catalysis resulted in a polymer with 7 to 25 repeat units. The lower molecular weight means that a larger amount of titanium crosslinker is needed for the polymer to form a solid elastomer. Low molecular weights obtained by polymerizing the fluorinated materials with acid could be explained through interference by electronegative substituents. It is unknown why PMOS did not polymerize well in acid as, electronically, it is similar to the PDMS, which polymerized well in acid. The steric inhibition by the octyl group may play a role.

The PCMS pre-polymer required a modified procedure as the extreme conditions of either acid or base catalyzed procedures caused the cyanide group to react. Formic acid in methanol was used. The formic acid, though a stronger acid than acetic acid, is considerably more volatile allowing for fast removal. Compared to the original acetic acid synthesis, the reaction was done at 0 ^{o}C with a lower mole ratio of the formic acid, and the reaction time was shortened. In this way it was possible to preserve the cyanide group and form a polymer of reasonable molecular weight (8-17 repeat units as determined by MALDI-TOF-MS).

Generally, all of the pre-polymers formed by either catalysis method resulted in a somewhat viscous mixture of straight chain polymers. The chains were all silanol terminated, though the acid catalyzed procedure gave some methoxy terminated product, as determined by MALDI-TOF-MS. This did not affect curing steps further on. Some cyclic material was present as well, with

less in the acid catalyzed product, though the small amount did not seem to affect further crosslinking steps or the quality of the polymer.

Crosslinking of this pre-polymer mixture to create the final elastomer was originally carried out by adding small amounts of trichloromethyl silane to the straight chain pre-polymer. This method was variable in its success so a more reliable method was developed. In the final method, crosslinking was accomplished through the addition of titanium(IV) tetraisopropoxide (see figure 2.3). The titanium is tetrafunctional, and forms a tightly crosslinked polymer. It also carries the added advantage of increasing the refractive index of the film. Generally, the titanium compound was not used in concentrations above 2 mole percent. Above this level, the film became brittle. In addition, drift in refractive index over time occured, likely a result of having more Ti-OH groups than polymer end groups after crosslinking. These left over Ti-OH groups were reactive and, over time, they may have reacted with one another, or with the glass surface, changing the morphology of the polymer.

The functional groups used were chosen to create a variety of polymers that would target different analyte classes. PDMS is known to absorb non polar compounds. The diphenyl group presumably would preferably absorb aromatic compounds, the fluorinated group, halogenated compounds, and the cyano group would have a higher affinity for more polar compounds. A 3-aminopropyl substituted silane was also prepared to target more polar analytes, however polymers incorporating this functional group were found to be highly unstable over time.

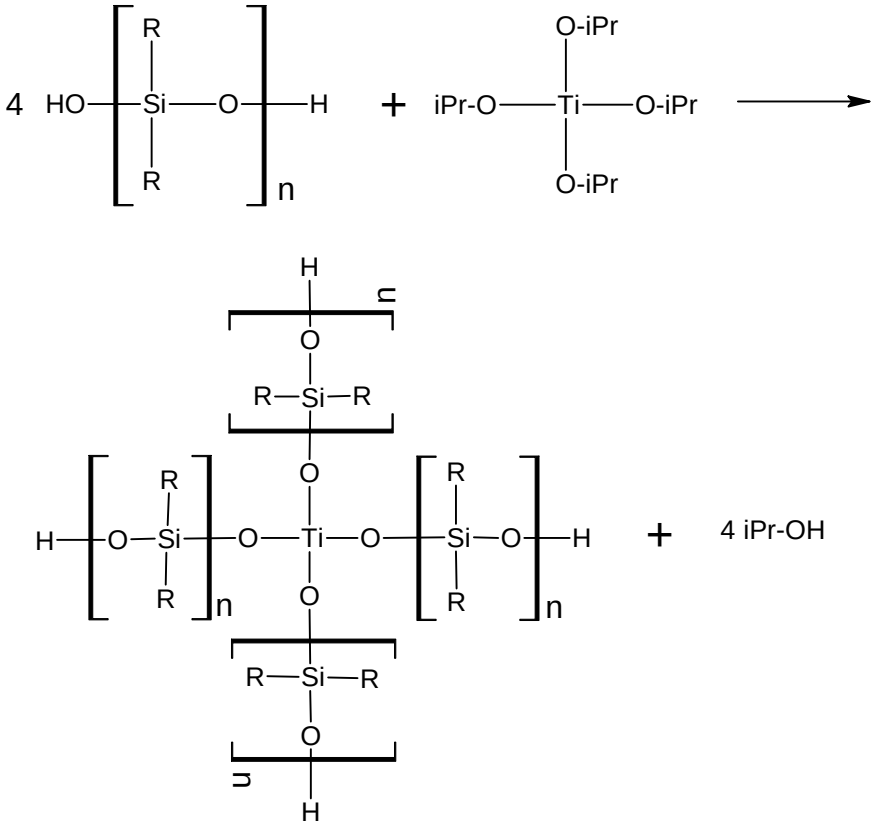

Figure 2.3 Reaction scheme for crosslinking the polymer materials with Titanium(IV) tetraisopropoxide

Although the chemical sensitivity for poly (methyloctyl siloxane) would be expected to be similar to PDMS, this polymer was very important for controlling refractive index. PDMS has a starting refractive index of about 1.39. To raise it to the optimal refractive index of 1.425 (at 1550 nm) required a huge amount of titanium crosslinker, resulting in a brittle film. Incorporation of other high refractive index functional groups can increase the polymer refractive index, but

generally would also change the selectivity of the polymer. Poly (methyloctyl siloxane) has a starting refractive index of approximately 1.44 at 1550 nm, and would be expected to be chemically similar to PDMS in terms of non-polarity. As a result, it is more useful for the non polar compounds.

While disubstituted dichloro silanes were successfully used in several polymers with a variety of polarities and chemical affinities, the number of commercially available monomers of this type is limited. As a result, another synthetic scheme that opened up more possibilities was explored. Using a platinum catalyst, vinyl terminated compounds were coupled onto a polymer backbone with hydrosiloxane groups in it (see figure 2.4). Though this procedure did contain an extra synthetic step, as the polymer backbone must first be constructed and then functionalized, it did have many attractions. Firstly, one large batch of the polymer backbone could be made and used for multiple functional groups. This reduced variability between batches in terms of molecular weight and level of impurities. In addition, more sensitive functional

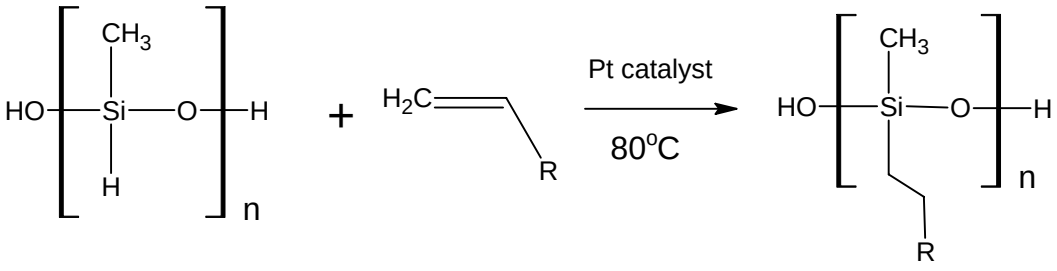

Figure 2.4 Reaction scheme for hydrosilylation with a platinum catalyst

groups that can potentially react in the acidic or basic conditions of the initial polymerization method are spared that step. Instead they must survive the high temperature (about 80 ^{o}C), but pH neutral, hydrosilylation reaction. Multiple functional groups could also be incorporated evenly into the same polymer backbone, enhancing the homogeneity of co-polymers. Finally, as already mentioned, this procedure opens up a large number of functional groups that would be otherwise inaccessible. Conceivably, any compound with a vinyl group-terminated tether attached to it could be incorporated. This could include molecules such as PAHs, pesticides, or other contaminants of interest, potentially even metal chelating agents. In actuality, the choice of vinyl terminated compound is somewhat limited by the reactivity of the catalyst with the desired functional group and by steric considerations.

The platinum coupling reaction was first explored using allyl cyclohexane and hexachloroplatinic acid. While less useful from the perspective of developing another polymer with potentially different chemical selectivity than the others, the allyl cyclohexane provided us with a compound free of reactive groups or electron withdrawing substituents to test the procedure and refine the reaction conditions. The addition of allyl cyclohexane to the poly methyl siloxane backbone was accomplished with a conversion of nearly 100%. The reaction was monitored by ^{1}H NMR, where the disappearance of the Si-H peak indicated completion of the reaction (see figure 2.5).

A similar reaction with 3,4-dichlorobutene was also attempted, however a useful product was never formed. After the reaction, the polymer became

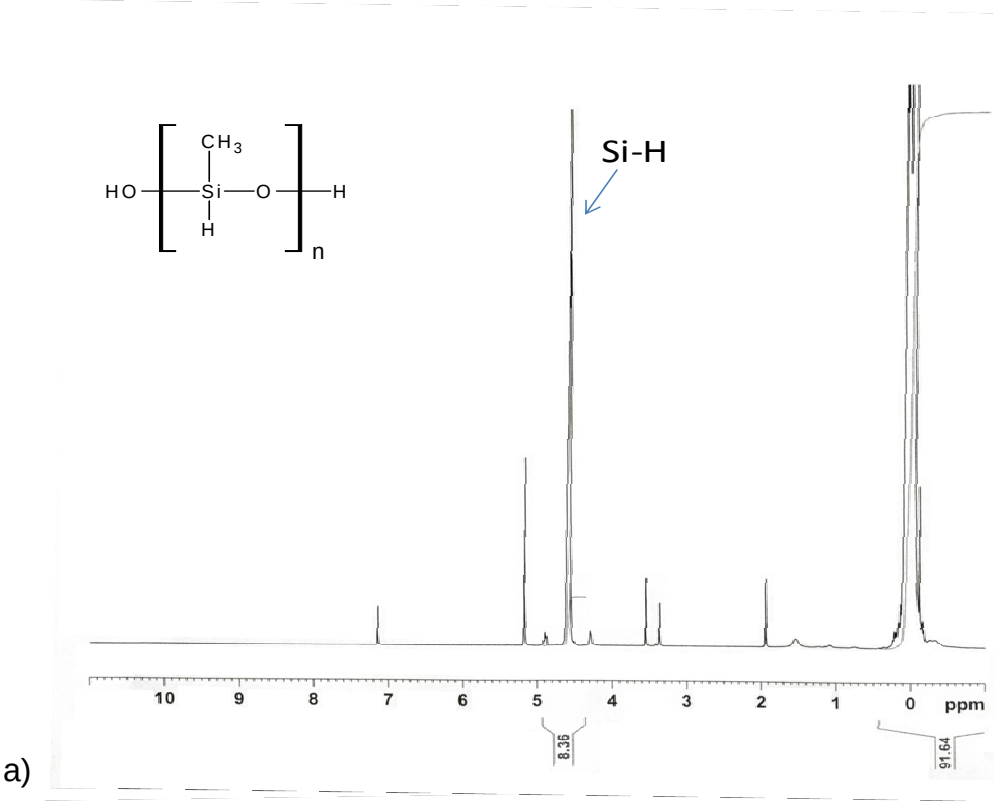

a)

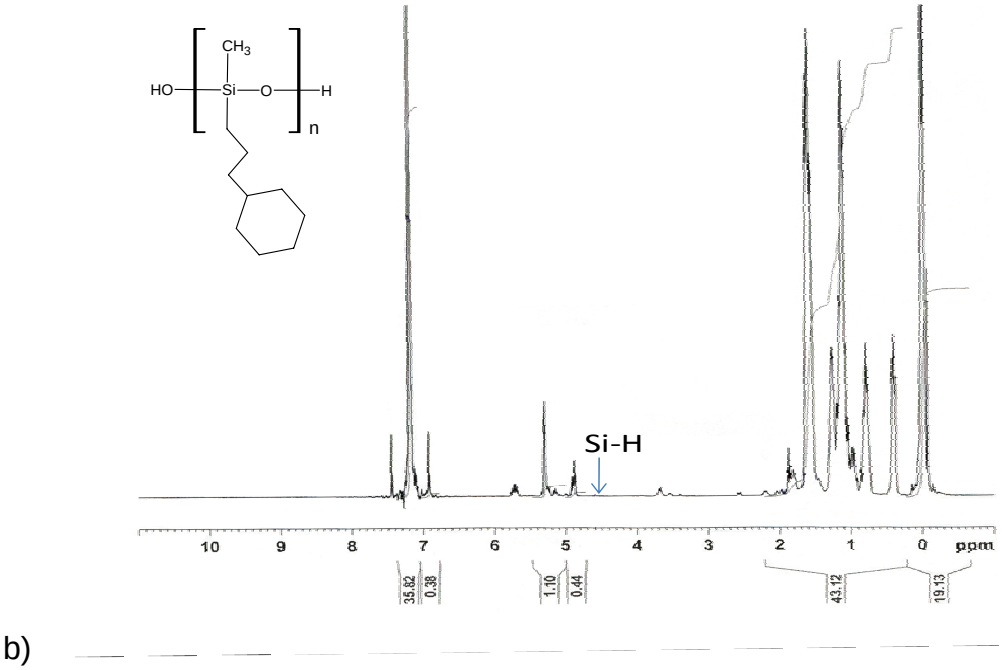

b)

Figure 2.5 Reaction progress in hydrosilylation is monitored by ^{1}H NMR through the disappearance of the Si-H peak at 4.6 ppm. a) Original starting material, 50 mole percent poly (methyl siloxane) with 50 mole percent PDMS (*0.05 ppm (Si-C$\underline{H}_3$); 4.6 ppm (Si-$\underline{H}$)).* b) Final product after allyl cyclohexane has been added *0.05 ppm (Si-C$\underline{H}_3$); 0.4 ppm (Si-C$\underline{H}_2$CH$_2$-); 0.8 ppm (Si-CH$_2$C$\underline{H}_2$CH$_2$-); 1.25 ppm (Si-CH$_2$CH$_2$C$\underline{H}_2$C$_6$H$_{11}$); 1.1 and 1.6 ppm (Si-CH$_2$CH$_2$CH$_2$C$_6$H$_{11}$; 7.1 ppm solvent)*.

crosslinked into a glassy solid. Competing side reactions with the chlorine were most likely the cause. It has been shown that hydrogen substitution by the chlorine competes strongly with hydrosilylation in these types of reactions and that numerous alternate products can be formed[16].

Allyl amine was also used as a test compound. It failed to react at all, leaving the starting materials unchanged. The amine group may react to bind the catalyst.

Hexachloroplatinic acid generally does not work well with allyl compounds containing functional groups such as esters or amides. For these compounds, alternative catalysts, such as *bis*-diethylsulfide platinum(II) salts, have been shown to be more effective.[17]

2.3.3 Polymer Analysis

Pre-polymer materials can be analyzed by standard NMR methods. ^{1}H NMR can be used to determine impurity levels, and the ratio of functional groups in co-polymers. Figure 2.6 shows a typical spectrum for a PDPS pre-polymer material, made of 20 mole percent diphenyl siloxane and 80 mole percent dimethyl siloxane. The ratios of the integration for the aromatic hydrogen peaks (26.14 divided by ten protons per diphenyl siloxane group) and the methyl hydrogen peaks (68.85 divided by six protons per dimethyl siloxane group) demonstrate that the polymer produced contained 18.6 mole percent PDPS, very close to the target 20 mole percent.

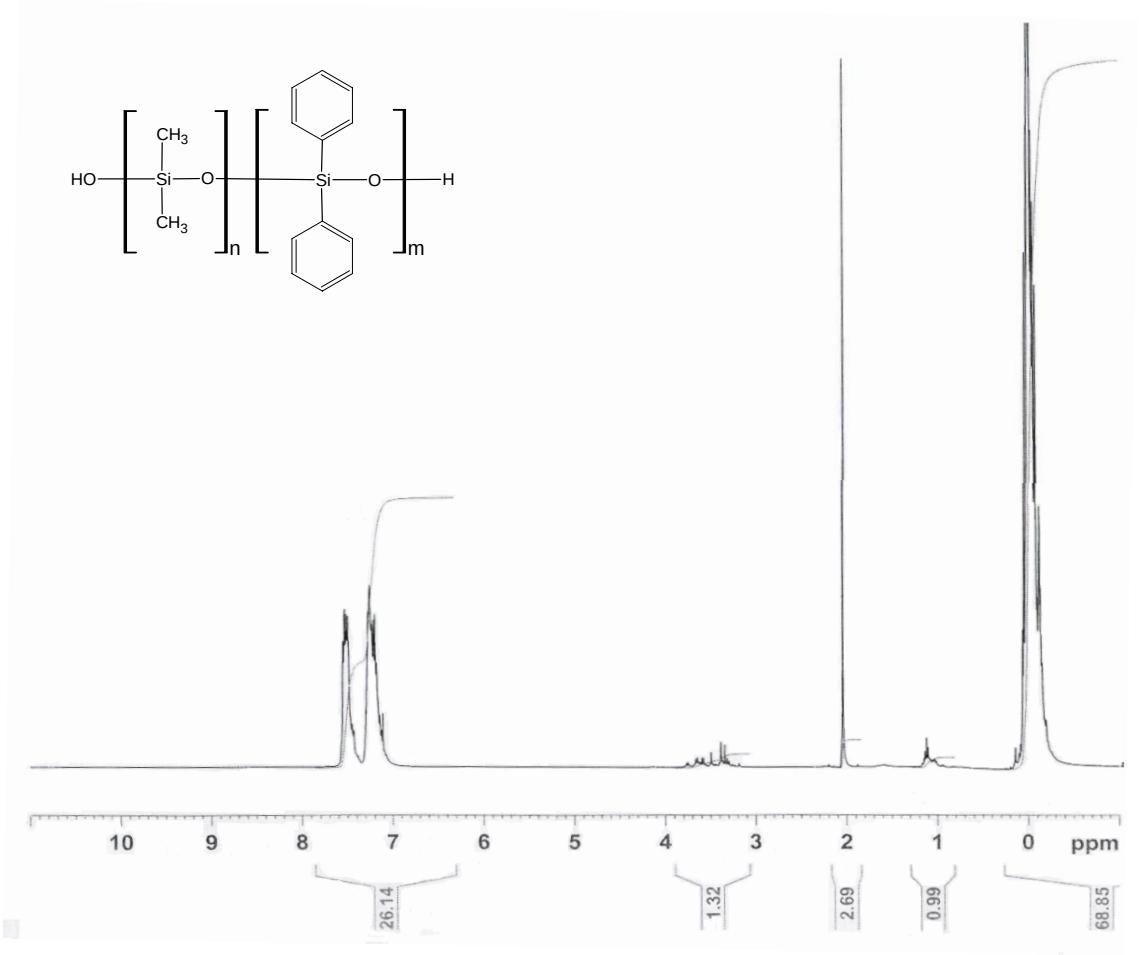

Figure 2.6 ^{1}H NMR spectrum of 20 mole percent PDPS with 80 mole percent PDMS. The actual mole percent of PDPS is 18.6% based on the peak integration. *(7.1 ppm and 7.6 ppm (Si-$C_6\underline{H_5}$); 0 ppm (Si-$C\underline{H_3}$))*

MALDI-TOF-MS can be used to determine the approximate molecular weight of the polymer and its polydispersity. Figure 2.7 gives a typical spectrum for PDMS. Spectra for other pre-polymer materials can be found in Appendix A. Each peak in the spectrum is separated by 74 m/z, the mass of one repeat unit in PDMS. The amount of cyclic material can also be determined from the mass spectrum. MALDI-TOF does carry the limitation of only being useful for

pure polymers. Co-polymers generate a spectrum which is simply too complicated to interpret, due to the many possible molecular weights resulting from the various combinations of repeat groups.

a)

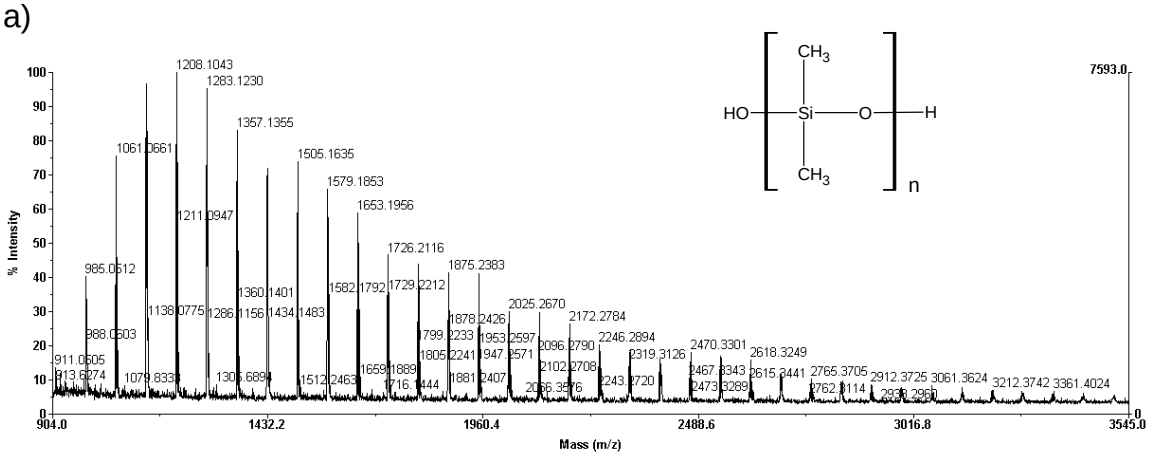

b)

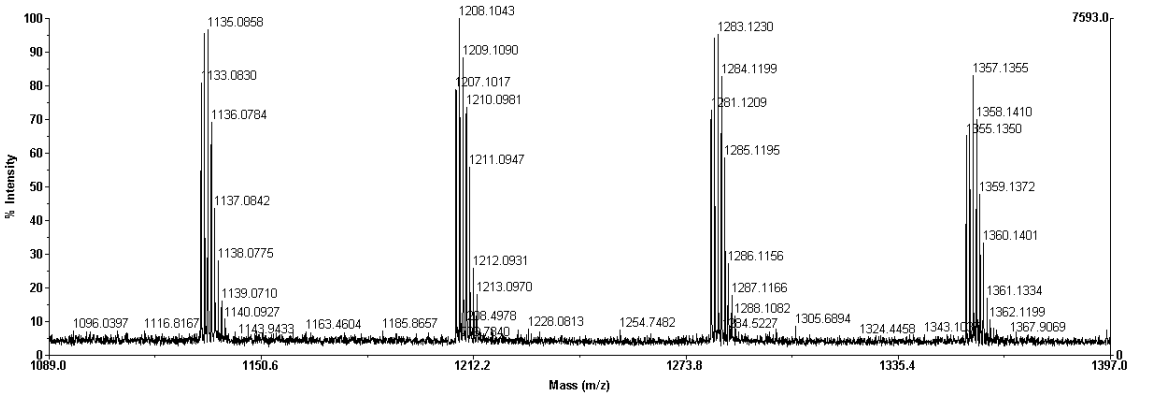

Figure 2.7 MALDI-TOF-MS spectrum (a), with detail (b), of PDMS synthesized with acid catalysis. Peak clusters are separated by 74m/z, the molecular weight of one PDMS repeat unit.

2.3.4 Effect of Composition on Refractive Index

Titanium crosslinked polysiloxane derivatives can be adjusted in composition to fine-tune the refractive index value to a specific level. All of the refractive index values reported are at 1550nm. This is because 1550nm, a common telecommunications wavelength, is expected to be the wavelength used in the finished sensor. The variation in refractive index was accomplished either through the adjustment of the amount of titanium (Figure 2.8) or the proportions of the incorporated functional groups (Figure 2.9). The resulting refractive index is linear with respect to mole percent of the changing component. This result is consistent with other examples in the literature[14,19-21], where the refractive index of a co-polymer changes linearly with mole percent composition.

The slopes of the six graphs in Figure 2.8 might be expected to be quite similar, as in each case the same compound, titanium, is being added. While some of the slopes are similar, some large differences can be seen. To understand this it must be noted that titanium serves a dual purpose of both modifying refractive index and cross-linking the polymer. The process of cross-linking may alter the density, and subsequently the refractive index, of the polymer material. Depending on the molecular weight and properties of each pre-polymer, different cross-linking and density of polymer films may result.

The linear change in refractive index with composition indicates that a Lorenz-Lorentz type of relationship is being followed. This allows us to approximately predict the refractive index of a new co-polymer based on the refractive index of its various components. Linear plots like those found in

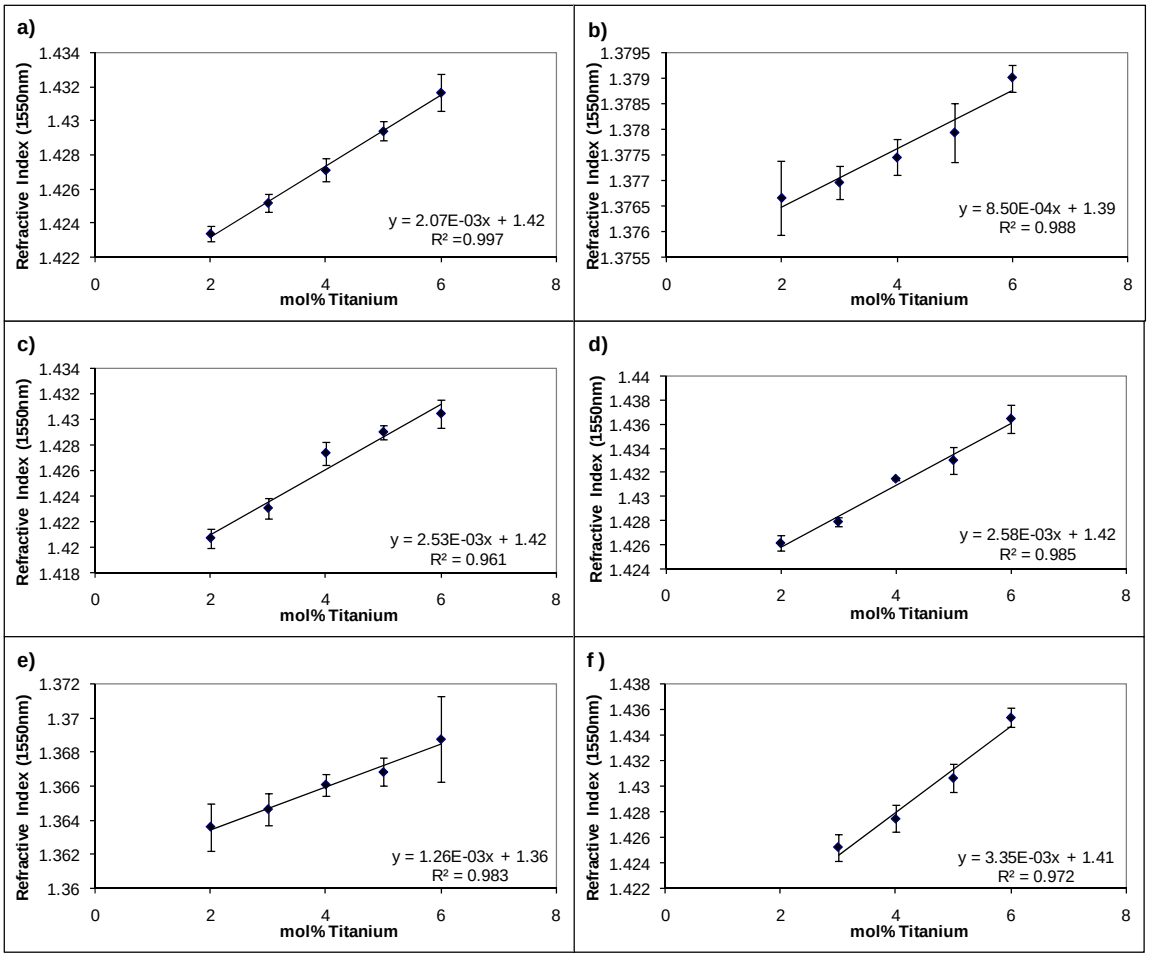

Figure 2.8 Variation in the refractive index as the mol% of titanium is varied between 2 and 6% for a) PDMS with 5 mol% PDPS, b) PDMS, c) PMOS with 15 mol% PFMS, d) PDMS with 60 mol% PMOS, e) PFMS, f) PDMS with 35mol% PCMS and 30 mole% PMOS. Error bars give the standard deviation in the refractive index between samples, with three replicates per data point.

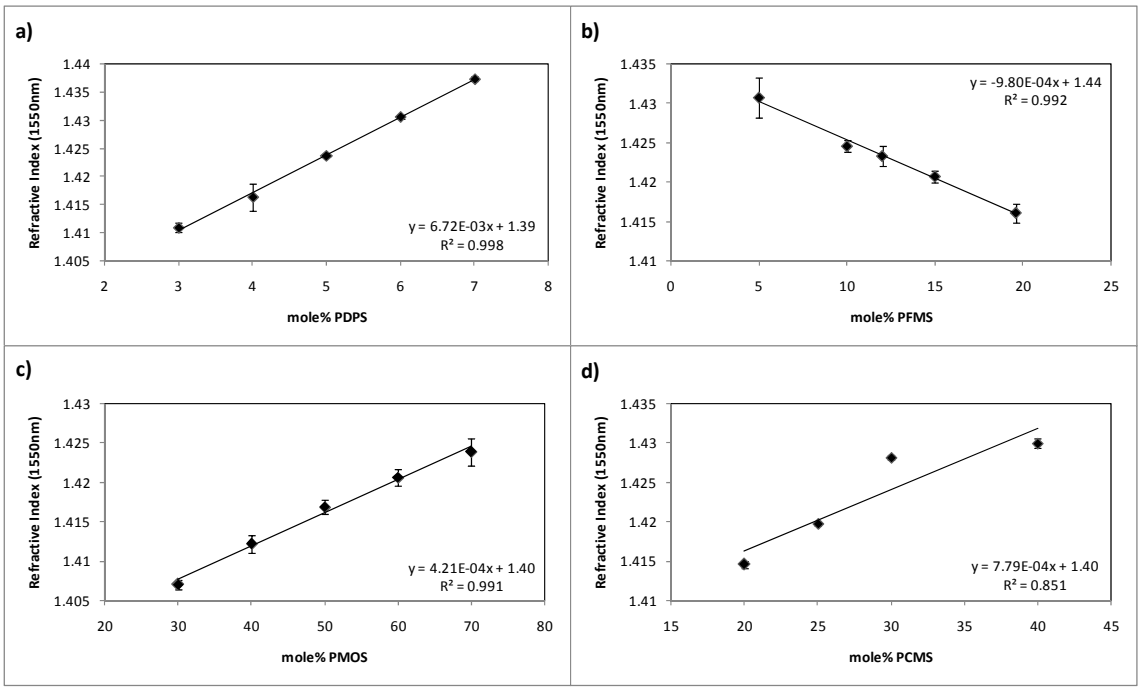

Figure 2.9 Variation in the refractive index of polymers, all having 2mol% Titanium, where the composition is altered. a) PDMS with variable PDPS, b) PMOS with variable PFMS, c) PDMS with variable PMOS and d) PDMS with variable PCMS, 30% PMOS. Error bars give the standard deviation in the refractive index between samples, with three replicates per data point.

figures 2.8 and 2.9 can also serve as "calibration" curves, to determine the necessary composition of a polymer to achieve a desired refractive index.

Fluorinated materials tend to have refractive indices that are lower than analogous non fluorinated materials[22]. For some applications, it is desirous to have a very low refractive index material that still has the mechanical properties and benefits of a compound like PDMS. Pure poly((3,3,3-trifluoropropyl)methyl siloxane) was synthesized and crosslinked with small amounts of titanium. Refractive index values in the range of 1.36 were obtained.

Similarly, for many applications, high refractive index materials are required. Phenyl substituted siloxanes tend to have much higher refractive indices than their aliphatic counterparts. Addition of only 3 mole % diphenyl siloxane into PDMS increased the refractive index from 1.39 to 1.41.

2.3.5 Refractive Index Matched Films for Sensor Application

For the overall sensor project, polymers having a refractive index of approximately 1.425 (at 1550nm) were desired. At this refractive index, just slightly lower than that of the fiber cladding, the sensitivity of the long-period grating to refractive index change is maximized. Using the refractive index data generated, appropriate functional group and titanium levels can be easily adjusted so that a polymer of the desired refractive index can be obtained. In total, four chemically distinct polymer films with refractive indices in the correct range were made (see Table 2.1).

The PDPS film contained only 8.5 mole percent of the diphenyl siloxane because of the high refractive index of the diphenyl material. Lower refractive index PDMS was mixed with it, and only 0.5% titanium was used to keep the refractive index low and allow for as much diphenyl siloxane to be added as possible. One alternative to increase the loading levels of diphenyl within the polymer was to combine it with the fluorinated siloxane, as the low refractive index of the fluorinated materials counteracts the high refractive index of the diphenyl. In this way, loading levels of 25-30 mole percent diphenyl were

Polymer	Composition (mole %)	Refractive Index (1550nm)
PDPS	8.5% diphenyl 91% dimethyl 0.5% titanium	1.4235 +/- 0.0002
PMOS	75% methyl octyl 24% dimethyl 1% titanium	1.4245 +/- 0.0002
PFMS	10% trifluoropropyl methyl 88% methyl octyl 2% titanium	1.4260 +/- 0.0002
PCMS	35% cyanopropyl methyl 30% methyl octyl 33% dimethyl 2% titanium	1.4250 +/- 0.0002

Table 2.1 Composition and refractive indices of the four polymers used for sensor applications. Error represents the instrumental error from the refractometer.

obtained. This kind of film was not used in subsequent testing however, as the combination of the two functional groups would make it difficult to determine if effects seen were due to the diphenyl or fluorinated portion of the polymer, or both.

The refractive index data for PDMS combined with titanium showed that it would be inappropriate for use on an LPG as its refractive index is too low.

Approximately 40 mole percent titanium would be required to bring it up into the right range. Instead, PMOS was used. PMOS has a nonpolar, hydrocarbon functionality, similar to the PDMS, but a higher starting refractive index. 75 mole percent PMOS combined with PDMS and 2 mole percent titanium gave an excellent quality film with a refractive index in the 1.43 range for use on the sensor.

Fluorinated materials have lower refractive indices, so only small amounts were added to the PFMS polymer to maintain the desired refractive index. The 2 mole percent titanium is the highest level that can be added while still maintaining the film quality over an extended period of time. Higher levels of titanium tended to result in film instability.

Poly ((3-cyanopropyl)methyl siloxane) had a starting refractive index similar to that of the poly (methyloctyl siloxane). Based on this, it was assumed that it too should be able to be combined with about 25 mole percent PDMS to form a good film in the proper refractive index range. Unfortunately, the quality of the film produced from high loading levels of the cyanopropyl group was poor. At high levels the film tended to be inhomogeneous, making determination of refractive index difficult. When the amount was reduced to 35 mole percent, the film had good homogeneity.

2.4 Conclusions

Acid or base catalysis can be used to create polysiloxanes from monomeric materials. By controlling the reaction conditions, polymers having higher molecular weights and limited cyclic material were synthesized and later crosslinked into elastomers using titanium(IV) tetraisopropoxide. The use of platinum catalysts to add vinyl substituted groups to a siloxane backbone was shown to be useful to extend the number of chemically distinct siloxanes. In total, six polysiloxanes were synthesized and characterized.

Polysiloxane polymers can be combined together to form a variety of chemically distinct films. The resulting refractive index of the film depended on the ratio of the various functional groups included in the film, following a Lorentz-Lorenz relationship. The change in refractive index with change in mole percent of a given functional group was linear. In addition, titanium was added as a crosslinker to the films. It also raised the refractive index in a linear fashion with increasing mole percent titanium. It is possible, using this information, to generate a polysiloxane film having a very specific refractive index. For optical sensor applications, where the sensitivity of a sensing layer is dependent on the refractive index, this is clearly useful. This also could find use in developing optically transparent materials or for using polymers to optically couple two components together.

2.5 References

1. E. G. Rochow, W. F. Gilliam, Polymeric methyl silicone oxides, J. Am. Chem. Soc., 63, (1941) 798-800.
2. C. Dietz, J. Sanz, C. Camara, Recent developments in solid-phase microextraction coatings and related techniques, J. Chromatogr., A, 1103, (2006) 183-192.
3. J. A. Koziel, I. Novak, Sampling and sample preparation strategies based on solid-phase microextraction for analysis of indoor air, Trends in analytical chemistry, 21, (2002) 840-850.
4. P. Mayer, W. H. J. Vaes, J. L. M. Hermens, Absorption of hydrophobic compounds into the poly(dimethylsiloxane) coating of solid-phase microextraction fibers: High partition coefficients and fluorescence microscopy images, Anal. Chem., 72 (2000) 459-464.
5. R. S. Brown, P. Akhtar, J. Akerman, L. Hampel, I. S. Kozin, L. A. Villerius, H. J. C. Klamer, Partition controlled delivery of hydrophobic substances in toxicity tests using poly(dimethylsiloxane) (PDMS) films, Environ. Sci. Technol., 35, (2001) 4097-4102.
6. C. E. Carraher, Polymer Chemistry, 7th Ed., CRC Press Inc. Boca Raton, 2008, p. 83-88, 597.
7. M. Chomat, D. Berkova, V. Matejec, I. Kasik, G. Kuncova, M. Hayer, Optical detection of toluene in water using an IGI optical fiber with a short sensing region, Sens. Actuators, B, 87 (2002) 258-267.

8. V. Matejec, M. Chomat, D. Berkova, J. Mrazek, R. Ardeleanu, V. Harabagiu, M. Pinteala, B. C. Simionescu, Detection of toluene dissolved in water by using PCS fibers excited by an inclined collimated beam, Sens. Actuators, B, 90 (2003) 204-210.
9. P. Tobiska, M. Chomat, V. Matejec, D. Berkova, I. Huttel, Investigation of fiber-optic evanescent-wave sensors for detection of liquid hydrocarbons, Sens. Actuators, B, 51, (1998) 152-158.
10. E. Sensfelder, J. Burck, H.-J. Ache, Determination of hydrocarbons in water by evanescent wave absorption spectroscopy in the near-infrared region, Fresenius J. Anal. Chem., 354, (1996) 848-851.
11. B. Zimmermann, J. Burck, H.-J. Ache, Studies on siloxane polymers for NIR-evanescent wave absorbance sensors, Sens. Actuators, B, 41 (1997) 45-54.
12. W. Noll, Chemistry and Technology of Silicones, 2nd Ed., Academic Press Inc. Orlando, 1968, p. 191-198.
13. S. Dire, F. Babonneau, G. Carturan, J. Livage, Synthesis and characterization of siloxane-titania materials, J. Non-Cryst. Solids, 147&148, (1992) 62-66.
14. M. Nakade, K. Kameyama, M. Ogawa, Synthesis and Properties of titanium dioxide/polydimethylsiloxane hybrid particles, J. Mater. Sci., 39 (2004) 4131-4137.

15. J. L. Speier, J. A. Webster, G. H. Barnes, The addition of silicon hydrides to olefinic double bonds. Part II. The use of group VIII metal catalysts, J. Am. Chem. Soc., 79, (1957) 974-979.
16. M. Jankowiak, H. Maciejewski, J. Gulinski, Catalytic reactions of hydrosilanes with allyl chloride, J. Organomet. Chem., 690, (2005) 4478-4487.
17. V. von Braunmuhl, R. Stadler, Synthesis of aldonamide siloxanes by hydrosilylation, Polymer, 39, (1998) 1617-1629.
18. M. W. F. Neilen, MALDI Time-of-flight mass spectrometry of synthetic polymers, Mass Spectrometry Reviews, 19, (1999) 309-344.
19. G. Colomines, S. Andre, X. Andrieu, A. Rousseau, B. Boutivin, Synthesis and Characterization of ultraviolet-curable fluorinated polydimethylsiloxanes as ultraviolet-transparent coatings for optical fiber gratings, J. Appl. Polym. Sci., 90 (2003) 2021-2026.
20. Q. G. Gu, Q. L. Zhou, Preparation of high strength and optically transparent silicone rubber, Eur. Polym. J., 34 (1998) 1727-1733.
21. S. Kohjiha, K. Maeda, S. Yamashita, Chemical modification of silicone elastomers for optics, J. Mater. Sci., 25 (1990) 3365-3374.
22. G. Hougham, G. Tesoro, A. Viehbeck, Influence of free volume change on the relative permittivity and refractive index in fluoropolyimides, Macromolecules, 29, (1996) 3453-3456.

Chapter 3

Partitioning between Polymer films and Target Analytes

3.1 Introduction

The refractive index of a polymer film can be related to the overall film composition. In chapter 2, this relationship was used to relate measured refractive index to the composition of polymers made from various mixtures of monomer and cross-linking groups. In this chapter, a similar approach will be used to relate refractive index to the composition of polymers that have absorbed various amounts of analyte molecules.

The use of polymer films as sensitive coatings for LPGs requires that a polymer absorb analytes and experience a detectable change in refractive index upon absorption. Monitoring a polymer film's refractive index response in the presence of analyte allows for determination of the suitability of the film for use in a final sensor platform. Response assessment can be separated into response kinetics and equilibrium response magnitude. Reversibility and repeatability can also be assessed. When response and repeatability is confirmed, then the response magnitude at equilibrium can be used in the calculation of a partition coefficient.

3.1.1 Determination of Partition Coefficients

Determination of a partition coefficient is an important step in evaluating the affinity of a polymer film for one substance over another. There are a variety of methods for discovering the value of the partition coefficient. Brown *et al.*[1] determined the partition coeffiecients of PAHs in PDMS by extracting films with ethanol once they have reached equilibrium in a test solution. The concentration of analyte in the test solution was also independently measured and the ratio of concentration in the film and solution yielded the partition coefficient. This method is less effective for very volatile test compounds as they begin to partition out of the film into the air almost immediately following removal from the sample. Determination of concentration has to be done in-situ.

In this chapter, we use change in polymer refractive index as an indicator of concentration of analyte within the film. This approach is not without precedent. Abdelghani *et al.*[2] determined the change in refractive index resulting from gas phase analyte absorption into a polymer using an SPR sensor. They used this change in refractive index to calculate the partition coefficients.

Spaeth *et al.*[3] further confirmed the link between polymer refractive index and analyte concentration. They show in later work[4] that as PDMS absorbed volatile organic compounds, it swelled, causing its volume to increase linearly with concentration of analyte. This indicated that PDMS can be approximated as a liquid like phase and relationships like the Lorentz-Lorenz equation are valid and can be used to determine concentration.

3.1.2 Measurement of Refractive Index

Methods for determining refractive index are usually based on either the determination of the critical angle[5-6] or on interferometry[7-8]. The common Abbe-type refractometer operates by determining the angle of refraction or total internal reflection when light travels from the sample into a prism of known refractive index. Solid samples such as polymers can also be analyzed on an Abbe refractometer, provided sufficient optical contact can be made between the polymer and the prisms[5]. The refractive index of solid samples can also be determined by ellipsometry, provided that the sample thickness uniform.[9] Ellipsometery was not used in this work because films were not normally uniform in thickness, and an ellipsometer at 1550 nm was not available. In addition, building an analyte exposure system onto an available commercial ellipsometer was not feasible.

In this work, refractive index was measured using an in-house built

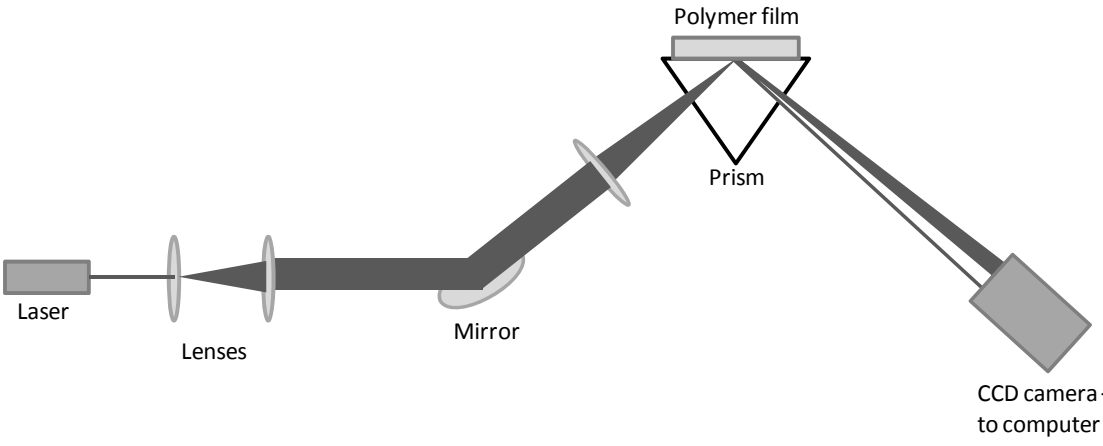

Figure 3.1 Schematic of the refractometer used to determine the refractive index of polymer films

refractometer which determines the critical angle to measure refractive index (Figure 3.1). As described by Zhang[10] a sample is mounted on a prism surface and light from a 1550nm laser is directed into the prism and to the sample at a variety of angles. Those angles that result in total internal reflection travel to a CCD detector, creating a lighted area. Those angles that are refracted travel through the polymer and are lost, resulting in a dark area on the detector (see figure 3.2). The position of the interface between the light and dark regions on the detector indicates the critical angle for that sample. Changes in refractive

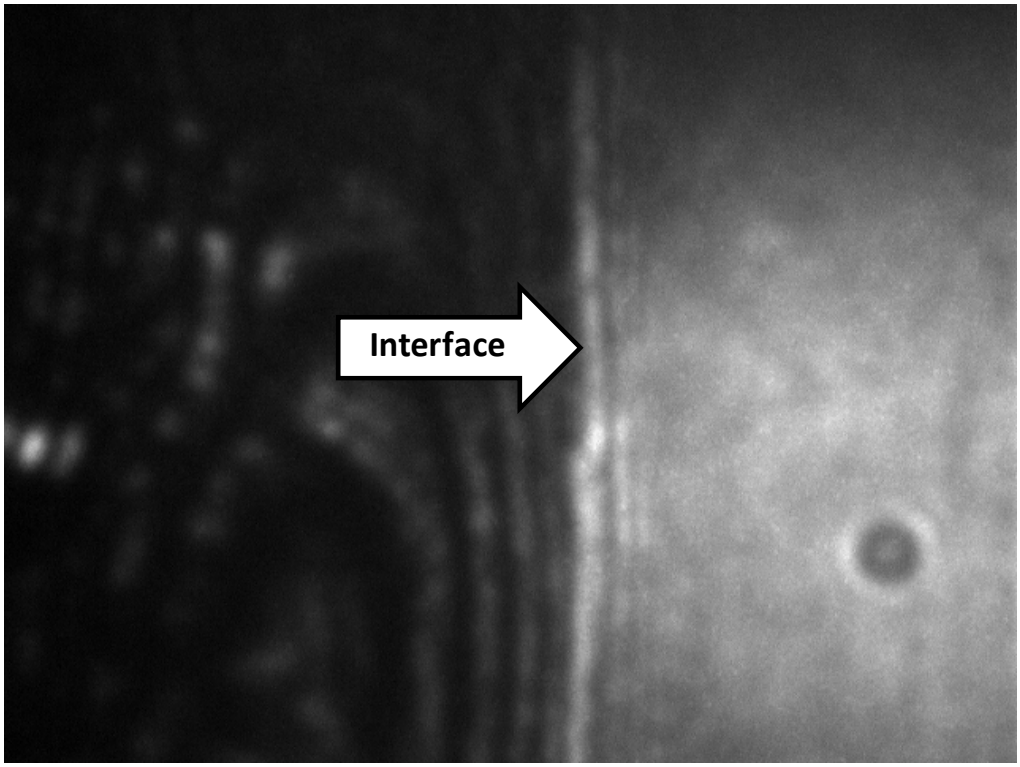

Figure 3.2 CCD camera output from the refractometer showing the interface for a PDMS polymer. Refractive index increases linearly as the interface moves to the right.

index will shift the location of this interface in a linear fashion, which can be calibrated using solutions of known refractive index.

The refractive index of a material is wavelength and temperature dependent. Refractive index is generally reported as the refractive index at 25 ^{o}C and 589 nm, which is the emission of the d-line of sodium. For the instrument described above, refractive index values were measured at 1550 nm.

3.2 Experimental

The compositions of the polymer films used in these experiments are given in Table 2.1. Their synthesis is described in Chapter 2. Refractive indices of the polymer films were measured on a custom built refractometer (figure 3.1) designed for handling solid film samples[10]. All of the refractive index data was recorded at 1550 nm, as opposed to the standard sodium d-line (589 nm), using a LPS-1550-FC laser diode (Thorlabs, Newton, NJ). The refractometer was calibrated using known solutions of DMSO and water, with refractive indices at 1550 nm calculated to be 1.4666 and 1.315, respectively. Measurement of the critical angle interface location and calculation of the refractive index was done using refractometry image analysis software, modified for this application. A sample of the CCD image showing the interface for a PDMS film is given in figure 3.2. The glass slides containing the films were mounted onto the prism of the refractometer, film side up, using 1.7250 refractive index matching fluid.

The polymer films were brought into contact with samples of gaseous solvents of interest, and the change in film refractive index was monitored. A

nitrogen stream was bubbled through pure solvent and then combined with pure nitrogen in a mixing flowmeter to create samples of varying concentration. The gas sample was conducted through a gas cell mounted on the refractometer which contained the polymer coating (see figure 3.3). Gas concentrations in the gas cell were confirmed by gas chromatography (GC), though literature values for saturated solvent vapour were used in calculations. GC experiments were conducted on a Varian CP- 3380 GC (Varian Inc., Palo Alto, CA) with an FID detector. Samples were drawn from the outlet of the mixing flowmeter using a 1 mL gastight syringe and manually injected into the GC. Calibration was done using gas samples of known concentration. All analyses were done isothermally (30 ^{o}C) with a run time of 4 minutes, on a Restek MXT-5 column (0.28 mm ID, 20 m length). Figure 3.4 shows representative GC data for xylenes. The calculated concentration of saturated xylenes was 11670 ppm by GC, which correlates well to the literature value of 11000 ppm. As seen in Figure 3.4, the vapour concentration can be accurately diluted through mixing within the flowmeter. The total flow rate was maintained at about 88 cm^3/min for all experiments.

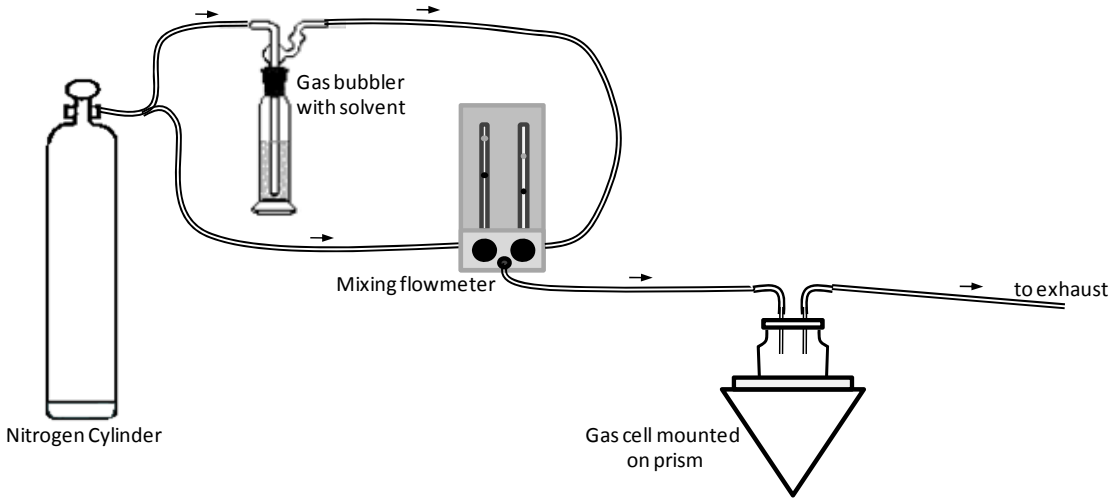

Figure 3.3 Schematic of gas sampling apparatus

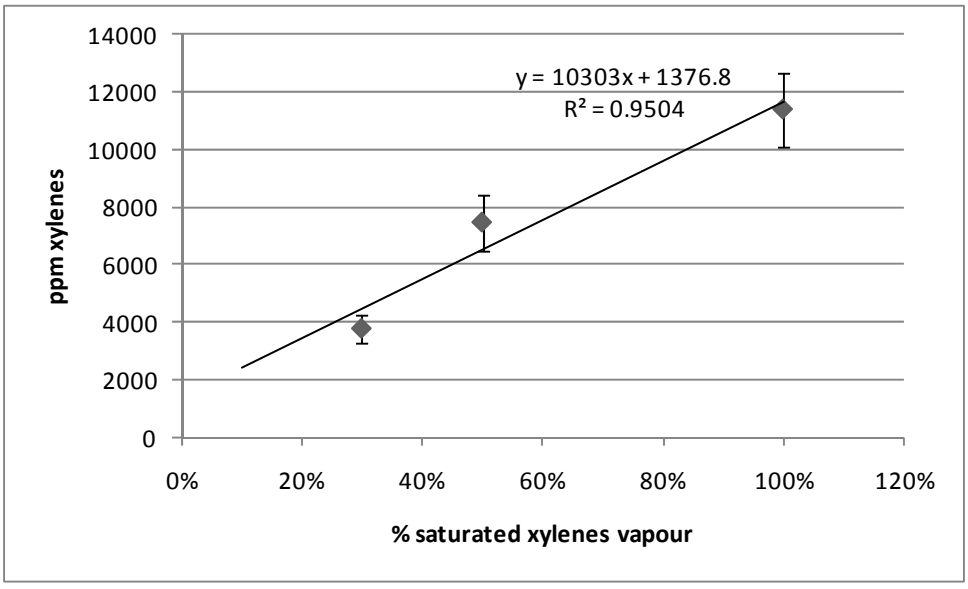

Figure 3.4 Concentration of xylenes, in ppm, as determined by GC analysis, for various percentages of saturated xylenes vapour produced by mixing with nitrogen in a mixing flowmeter. Error bars represent the standard deviation over three experiments.

In order to determine the response kinetics, the polymer film refractive index was recorded at regular intervals until no further change in refractive index occurred. The magnitude of refractive index change at equilibrium was determined and used to calculate partition coefficients. All experiments were done in triplicate, and where multiple vapour concentrations were used, the testing sequence was randomized.

3.3 Results and Discussion

3.3.1 Refractive Index Changes with Absorption of Analytes

For the ultimate sensor application of this project it is desirable to have a set of polymers, all with a specific refractive index and also with different affinities for analytes or classes of analytes. To explore the response and selectivity of the various polysiloxanes, four films were chosen, all having a starting refractive index around 1.425 (Table 2.1). The four films were exposed to vapours from eight different solvents (see Figure 3.5). Various flow ratios of saturated solvent vapour and pure nitrogen were mixed to create different concentrations from 5% to 50% of saturation. The resulting change in film refractive index was monitored.

The response times until equilibrium were typically two to three minutes (see Figure 3.6). Upon removal of the analyte and exposing the film to pure nitrogen the original refractive index was recovered in under five minutes. All of

the responses were completely reversible and reproducible over a period of several months.

The magnitude of the refractive index change at equilibrium is linearly related to the concentration of the analyte in the gas phase. Figure 3.7 shows the linear change in refractive index from a PDPS film exposed to increasing concentrations of xylenes vapour. The slope of the graph gives the change in refractive index per part per million solvent. Greater slopes indicate a greater sensitivity to the solvent.

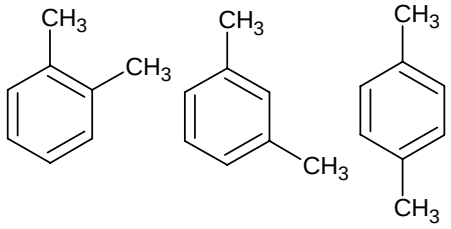

ortho, meta and *para*-xylene

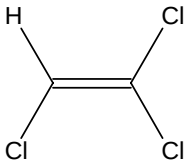

Trichloroethylene (TCE)

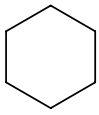

Cyclohexane

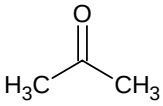

Acetone

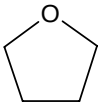

Tetrahydrofuran (THF)

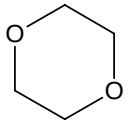

1,4-dioxane

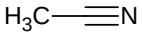

Acetonitrile

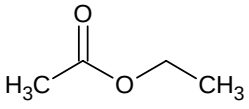

Ethyl Acetate

Figure 3.5 Structures of solvents used in gas phase experiments.

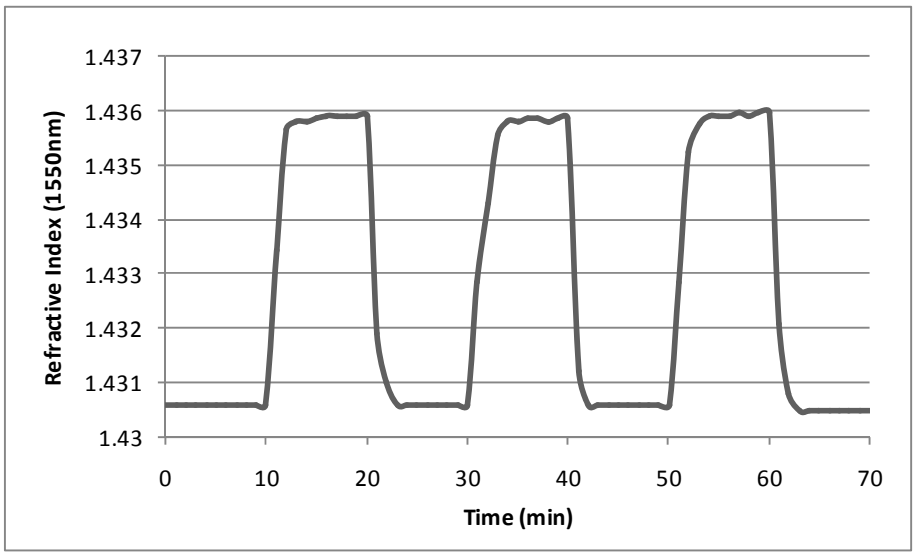

Figure 3.6 Response time profile for PDPS film exposed to 0 and 5000 ppm xylenes repeatedly. Xylenes were introduced at the 10, 30 and 50 min times and removed at the 20, 40 and 60 min times.

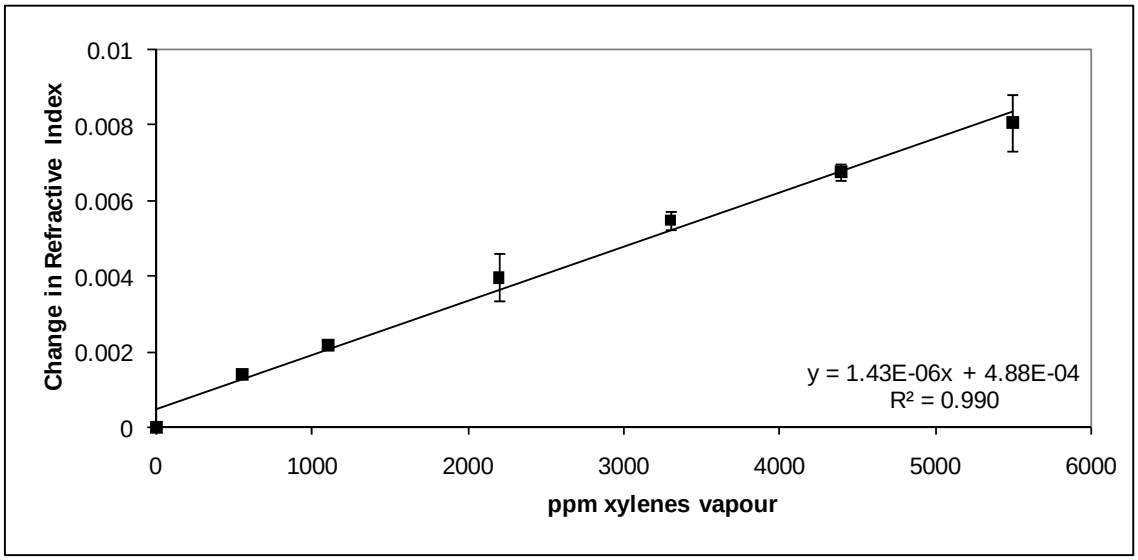

Figure 3.7 Change in refractive index for an 8.5 mol% PDPS film upon exposure to various concentrations of xylenes vapour. Error bars represent the standard deviation over three experiments.

Table 3.1 gives the slopes and R^2 values for each of the solvent-film combinations. Figure 3.8 gives a graphical representation of table 3.1. From the figure, it is apparent that some polymer films had a greater relative preference for one solvent over another. For example, PCMS was the best absorber of polar solvents like acetonitrile, but was comparatively poor at absorbing non polar solvents like cyclohexane. The xylenes response was considerably greater than that of the other solvents. This is because xylenes have a considerably lower volatility as compared to the other solvents, so more readily avoid the air phase and partition well into the polymers.

For xylenes, a change in refractive index of 1.43×10^{-6} per ppm was obtained with the PDPS film. The refractometer can differentiate refractive indices on the order of 2×10^{-4}, so that places the detection limit in the low hundreds of ppm. Ontario air standards place the maximum allowable concentration of xylenes at 0.2 ppm[11], which with the PDPS polymer would require being able to detect a change in refractive index of about 3×10^{-7}. Clearly, the current instrument is unable to detect xylenes at that level. Changes to either the polymer, to make it absorb more xylenes, or to the instrument, to make it sensitive to smaller changes in refractive index would be required. Applications such as spill or leak monitoring are still feasible with the current detection limits, where larger concentrations of the analyte tend to be obtained.

Solvent	PDPS film **Slope ($x10^{-6}$)** and R^2	PMOS film **Slope ($x10^{-6}$)** and R^2	PFMS film **Slope ($x10^{-6}$)** and R^2	PCMS film **Slope ($x10^{-6}$)** and R^2
Xylenes	**1.43**	**1.58**	**1.41**	**1.40**
	0.990	0.996	0.995	0.995
TCE	**0.146**	**0.175**	**0.170**	**0.152**
	0.992	0.999	0.985	0.991
Cyclohexane	**-0.0573**	**-0.0630**	**-0.0568**	**-0.0175**
	0.992	0.970	0.998	0.970
Acetone	**-0.0391**	**-0.0226**	**-0.0294**	**-0.0396**
	0.997	0.997	0.985	0.992
THF	**-0.0435**	**-0.0533**	**-0.0508**	**-0.0314**
	0.967	0.993	0.992	0.995
1,4-dioxane	**-0.0216**	**-0.0890**	**-0.0826**	**-0.0421**
	0.888	0.954	0.988	0.954
Acetonitrile	**-0.0170**	**0.00853**	**-0.0189**	**-0.0717**
	0.970	0.380	0.862	0.991
Ethyl acetate	**-0.147**	**-0.114**	**-0.120**	**-0.0900**
	0.986	0.986	0.993	0.993

Table 3.1 Slope (change in refractive index per ppm solvent) and R^2 values for the graphs of change in refractive index versus solvent concentration.

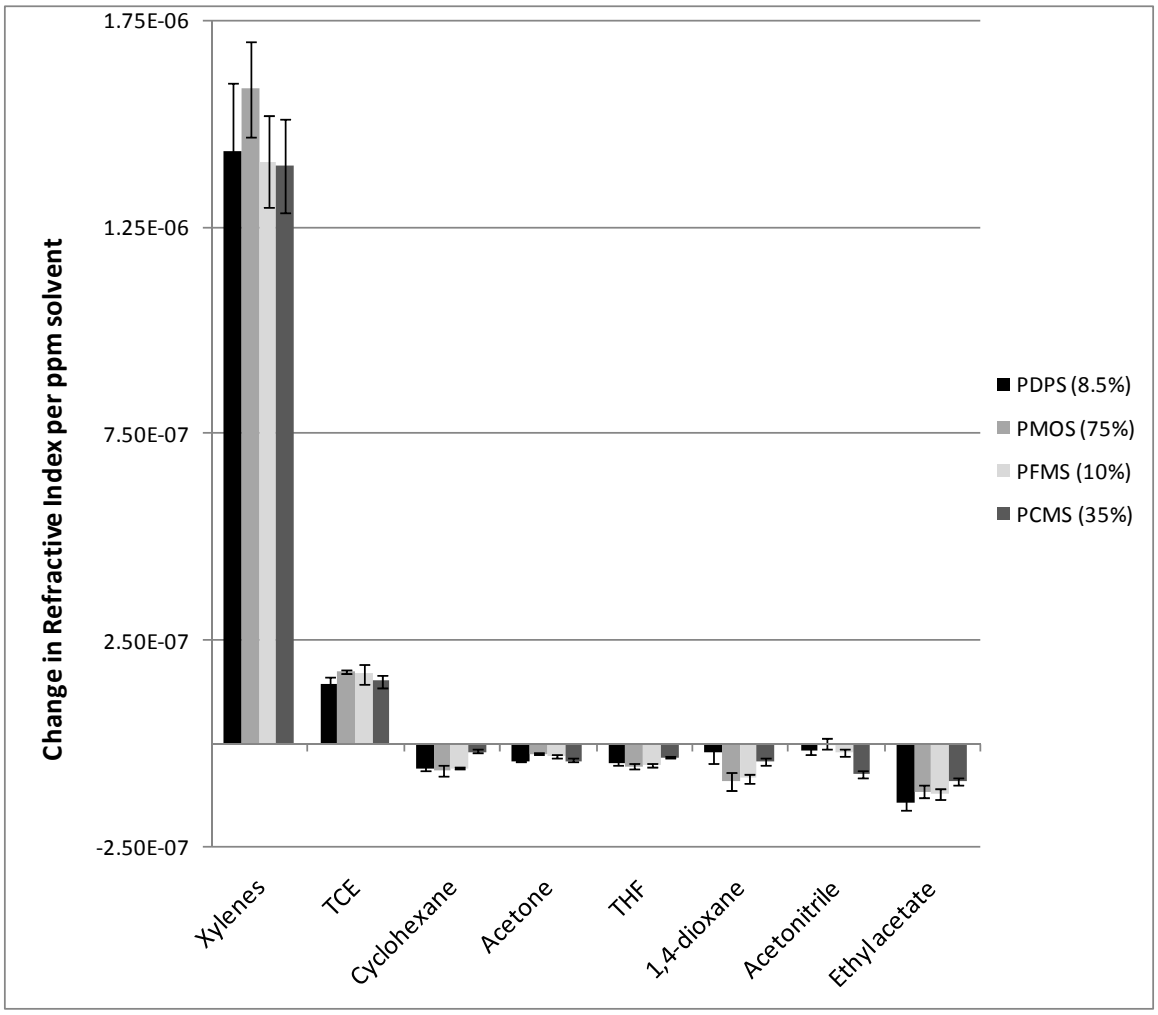

Figure 3.8 Change in refractive index per ppm solvent for the eight test solvents and four films as determined by the refractometer. Error bars represent the 95% confidence limit in the calculated values.

The effectiveness of an array for determining the composition of a mixture was demonstrated with a sample of gasoline. Using a four polymer array, it would be very difficult to determine the exact composition of a complex mixture such as gasoline, but it is possible to elucidate certain characteristics of the mixture. Comparison of the fingerprint response of gasoline to fingerprint

responses of the other test compounds could allow us to infer, for example, whether or not the mixture was polar or non polar. The refractive index change for each polymer film upon being exposed to 50% saturated gasoline vapour was measured. The resulting fingerprint was compared to the fingerprints obtained from the other eight test solvents. The gasoline fingerprint response with the four films is most similar to that of cyclohexane (see figure 3.9). From this, even though it is a mixture, we can infer that the gasoline is mostly composed of hydrocarbon-like compounds, as expected.

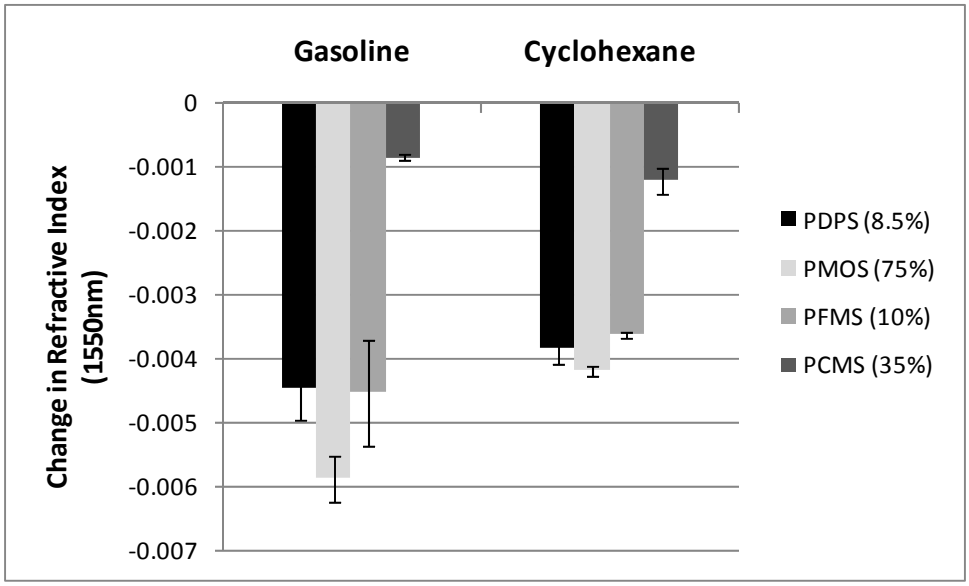

Figure 3.9 Fingerprint response of gasoline compared to cyclohexane for the four polymer films. Exposures are done with 50% saturated vapour in nitrogen. Error bars give the standard deviation over three trials.

3.3.2 Calculation of Partition Coefficients

Considering change in refractive index alone does not completely indicate a polymer's affinity for a given compound. If the starting refractive index of polymer and analyte are far apart, absorption of even a small amount of analyte will cause a greater response than if a polymer and analyte have similar starting refractive indices. To understand the selectivity of a polymer for one analyte over another, the partition coefficient must be considered. The partition coefficient, K_{fa}, is defined, at equilibrium, as:

$$K_{fa} = \frac{[analyte]_{film}}{[analyte]_{air}} \quad (1)$$

To calculate a partition coefficient, the Lorentz-Lorenz equation was used to determine the amount of analyte in the film. The Lorentz-Lorenz equation describes the relationship between the composition of a mixture and its resulting refractive index. Generalized to m components it is:

$$\frac{n_{1\to m}^2 - 1}{n_{1\to m}^2 + 2} = \sum_{i=1}^{m} \Phi_i \frac{n_i^2 - 1}{n_i^2 + 2} \quad (2)$$

Where Φ_i is the volume fraction, n_i is the refractive index of pure component i and $n_{1\to m}$ is the refractive index of the mixture of components 1 through m.

This equation was developed for liquid mixtures, so the polysiloxane films are approximated as a liquid phase. Previous studies have shown that PDMS swells its volume linearly with analyte absorption[4], and a linear change in refractive index with concentration was observed, suggesting that it is reasonable to assume a Lorentz-Lorenz relationship. Based on this, the quantity of analyte present in the polymer can be estimated from the measured change in refractive index.

Equation 2 was used to determine the volume fraction of solvent within the polymer, $\Phi_{solvent}$, using the measured values of the refractive indices of the solvent and film and the experimentally determined change in refractive index with their mixing. The concentration of the solvent in the film was determined as follows:

$$C_{film} = \Phi_{solvent} \times d \qquad (3)$$

Where C is the concentration in mg/L and d is the density of the solvent in mg/L. This approach makes the assumption that the density of the solvent within the polymer is similar to the density of the liquid solvent. Alternatively, this could be expressed as the assumption that the molar volume of the liquid is conserved. The partition coefficient can be determined using equation 1, using the film concentration from equation 3 and the gas phase concentration of the solvent (also in mg/L).

The K_{fa} values calculated from the experimental data are shown graphically in Figure 3.10 and tabulated in Table 3.2. The trends seen in the refractive index data are also shown in the K_{fa} data, confirming the chemical behavior independent of the refractive index differences of each solvent. The more polar PCMS film has a greater K_{fa} value for more polar solvents, such as acetonitrile and acetone, while having lower values for nonpolar solvents such as cyclohexane. THF, 1,4-dioxane and, to a lesser extent ethyl acetate, are

Solvents	**K_{fa}**				**K_{oa}**
	PDPS	**PMOS**	**PFMS**	**PCMS**	
Xylenes	4974	5968	5362	5085	5023
TCE	674	850	873	886	627
Cyclohexane	800	740	651	335	409
Acetone	164	90	124	200	355
THF	353	398	434	263	1007
1,4-dioxane	533	1185	1323	836	2736
Acetonitrile	121	0	80	350	300
Ethyl acetate	470	396	487	309	1010

Table 3.2: Summary of experimentally determined partition coefficients (K_{fa}) for each film/solvent combination. Octanol-air partition coefficients (K_{oa}) values are included for comparison.

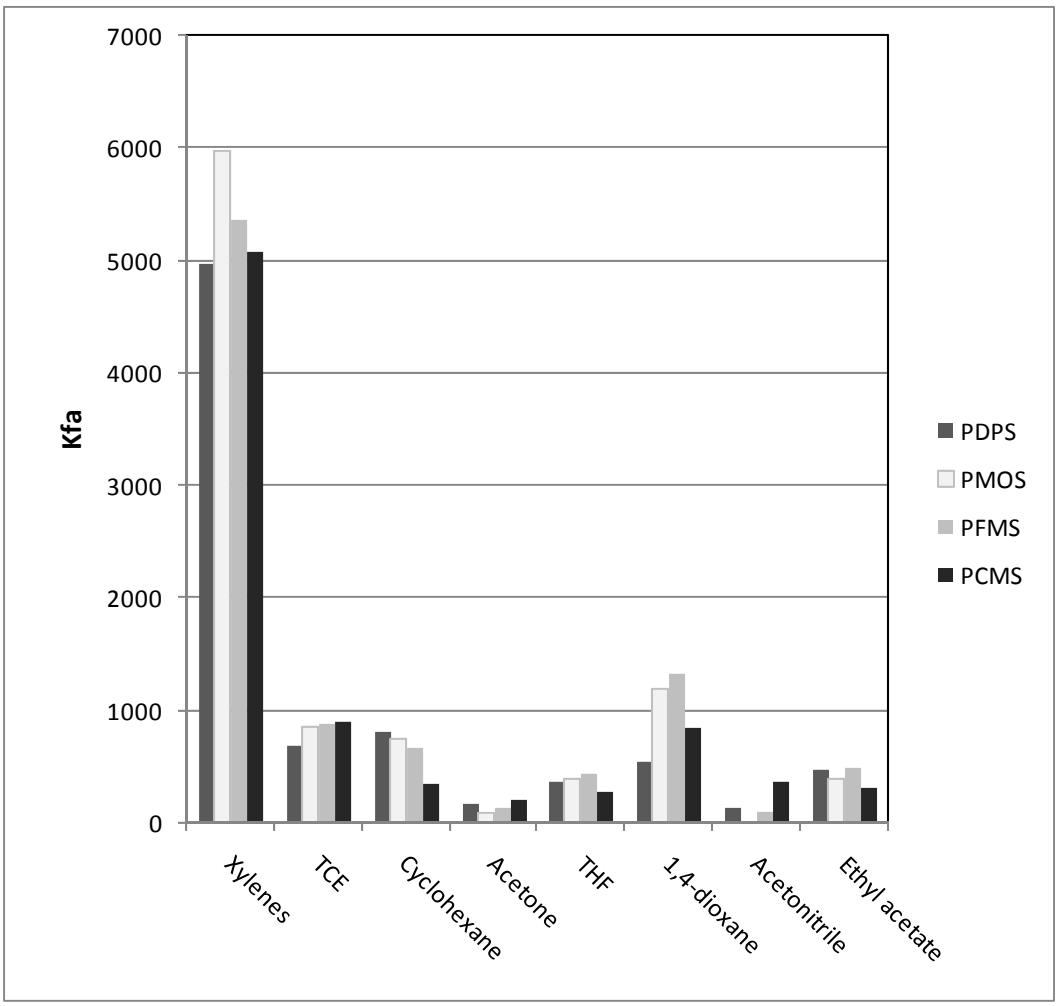

Figure 3.10 Summary of K_{fa} values for the four films.

preferred by the PFMS polymer. The electrophilic nature of the trifluoropropyl group makes it a good absorber of compounds with lone pair electrons, such as the ethers.

For comparison, the octanol-air partition coefficient (K_{oa}) can be calculated for each of the sample solvents. Values for K_{oa} can be accurately calculated from the octanol-water partition coefficient (K_{ow}) and the Henry's Law constant (H) following the approach of Meylan[12] using the equation:

$$K_{oa} = K_{ow}\frac{RT}{H} \quad (4)$$

Where R is the ideal gas constant and T is the temperature in degrees Kelvin.

Data obtained for each of the solvents is summarized in Table 3.3.

Solvent	Refractive Index (1550nm)[a]	Concentration in saturated N_2 (atm)[b]	log K_{ow}[b]	H (m^3 atm mol^{-1})[b]	log K_{oa}[e]
Xylenes	1.4776	0.011-0.012	3.1-3.2	0.0066-0.0072	3.67-3.73
TCE	1.4821	0.091	2.4	0.0098	2.80
Cyclohexane	1.4075	0.13	3.4	0.15	2.61
Acetone	1.3459	0.31	-0.24[c]	0.00004	2.55
THF	1.3882	0.21	0.46	0.00007	3.00
1,4-dioxane	1.4047	0.05	-0.27[d]	0.0000048	3.44
Acetonitrile	1.3333	0.12	-0.38[c]	0.000034	2.48
Ethyl acetate	1.3553	0.12	0.73	0.00013	3.00

Table 3.3: Properties of test solvents at 25 ^{o}C. [a]experimentally determined on refractometer; [b]from the database at http://glad.syrres.com unless otherwise indicated; [c] Nalecz-Jawecki *et al.*[13]; [d] Dietz *et al.*[14]; [e]calculated using equation 4.

The film-air partition coefficient (K_{fa}) for p-xylene and o-xylene in pure PDMS is reported to be 2731 and 3388 respectively[15]. This can be compared to both the literature K_{oa} value for xylenes, 5023 (Table 3.2), and the calculated K_{fs} value for xylenes with the PMOS film of 5968. Values for K_{ow} are typically somewhat larger than the partition coefficients seen for pure PDMS[1]. It would be expected that PMOS, with the longer octyl chain, would have more hydrophobic character than PDMS, so it is not surprising that the K_{fa} for PMOS is higher and closer in line with the octanol data.

Similarly, the film-solution partition coefficient for TCE in pure PDMS is reported to be 260[16]. This can be compared to the value for K_{ow}, which is about 250 (Table 3.3). From the K_{ow}, the K_{oa} is calculated to be 627, compared to the K_{fa} for PMOS of 850. Once again, the PMOS film is more selective than the pure PDMS film for the compound of interest.

Figure 3.11 compares the calculated K_{oa} values with the K_{fa} values for the PMOS polymer film across all of the solvents tested. PDMS has been shown to absorb compounds from water in good correlation to K_{ow}[1,17]. We would expect a similar correlation for PMOS in absorbing compounds from the gas phase, as it is also hydrophobic in nature. The correlation between K_{oa} values and the K_{fa} values for PMOS does show a trend, though there is some variability. This further indicates that the estimated K_{fa} values are reasonable.

a)

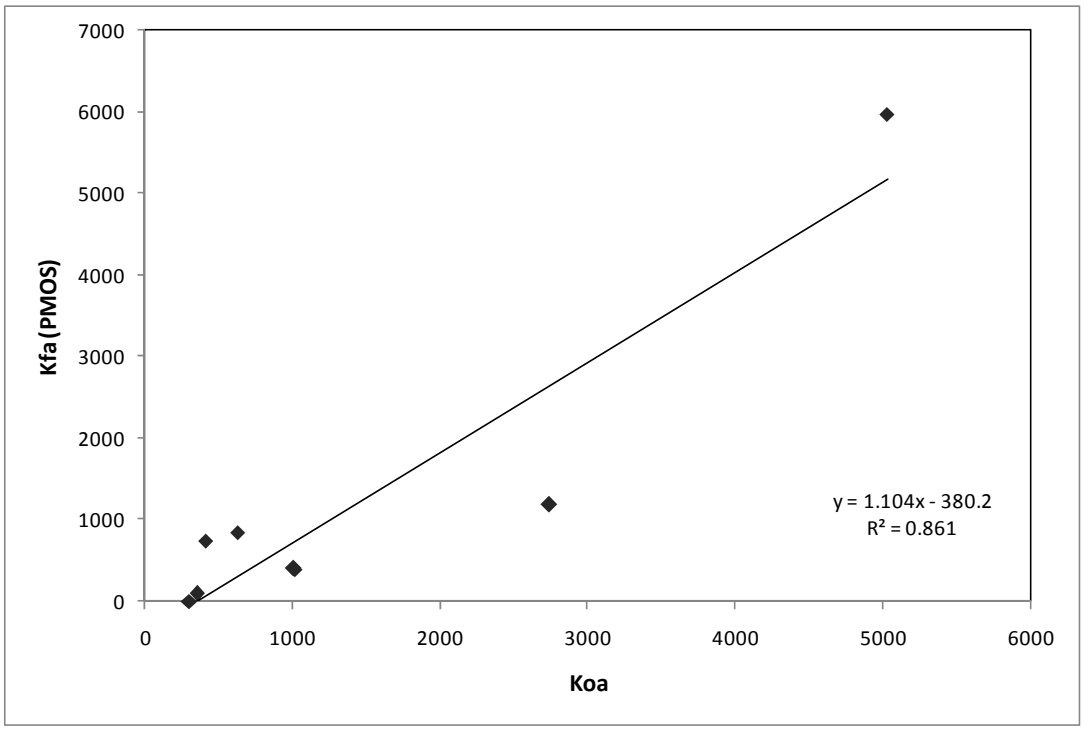

b)

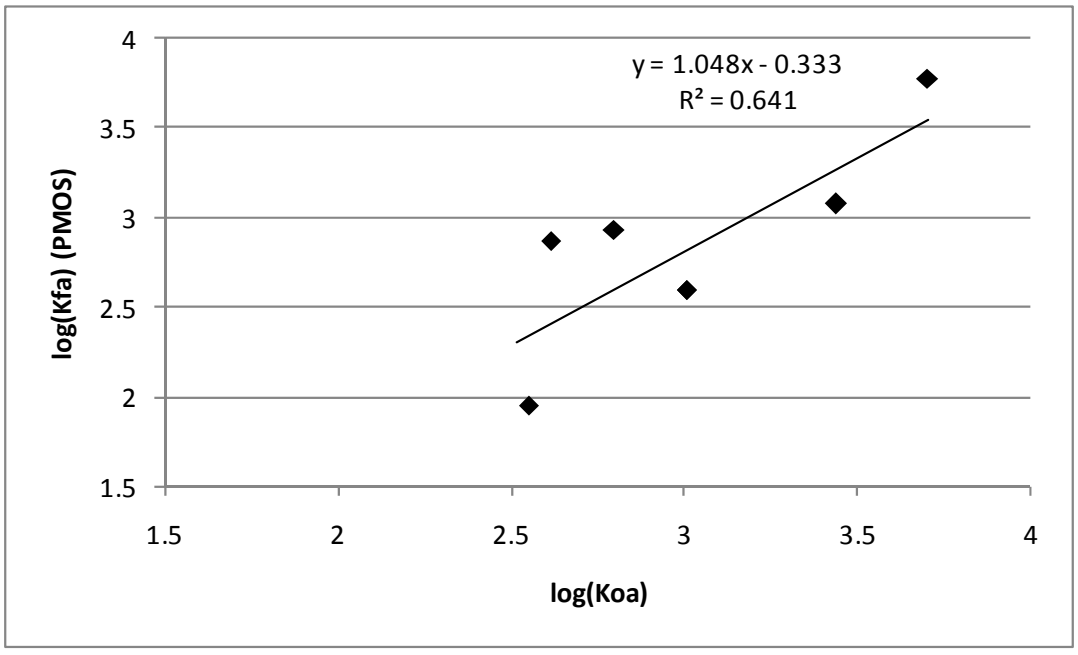

Figure 3.11 Comparison of calculated values of K_{oa} with experimental values of K_{fa} for PMOS for eight different solvents in numeric (a) and in logarithmic (b) form

3.4 Conclusions

Four distinct polysiloxane films were tested for their affinity for a set of eight test solvents. Change in film refractive index upon exposure to the gas phase solvents was monitored. All of the films absorbed analytes reversibly and reproducibly, with equilibrium being established in about five minutes. The degree of change in refractive index with vapour phase concentration was linear. Refractive index changes upon exposure to saturated vapours typically occurred in the second or third decimal place. For a compound such as xylenes, this corresponds to a detection limit in the range of hundreds of ppm. This detection limit is limited by the error in the current refractometer and could be improved by using a more sensitive instrument. Using the magnitude of refractive index change at equilibrium, partitioning coefficients were calculated for the four polymer films with each of the test solvents. The four films showedsome variable selectivity for the solvents, demonstrating that it is possible to usea set of polymers like these in the development of a chemical sensor array for rudimentary compound identification. Gasoline, when tested on the array, showed a similar fingerprint to cyclohexane, indicating the hydrocarbon makeup of the gasoline. Finally, the partition coefficients for the non-polar PMOS film were compared to the octanol-air coefficients, K_{oa}, for the solvents and found to follow a similar trend.

3.5 References

1. R. S. Brown, P. Akhtar, J. Akerman, L. Hampel, I. S. Kozin, L. A. Villerius, H. J. C. Klamer, Partition controlled delivery of hydrophobic substances in toxicity tests using poly(dimethylsiloxane) (PDMS) films, Environ. Sci. Technol., 35, (2001) 4097-4102.
2. A. Abdelghani, N. Jaffrezic-Renault, SPR fiber sensor sensitised by fluorosiloxane polymers, Sens. Actuators, B, 74, (2001) 117-123.
3. K. Spaeth, G. Kraus, G, Gauglitz, In-situ characterization of thin polymer films for applications in chemical sensing of volatile organic compounds by spectroscopic ellipsometry, Fresenius J. Anal. Chem., 357, (1997) 292-296.
4. K. Spaeth, G. Gauglitz, Characterization of the optical properties of thin polymer films for their application in detection of volatile organic compounds, Mater. Sci. Eng., C, 5 (1998) 187-191.
5. K. Kuhler, E. L. Dereniak, M. Buchanan, Measurement of the index of refraction of the plastic Phenoxy PKFE, Appl. Opt., 30, (1991) 1711-1714.
6. S. Sainov, N. Dushkina, Simple laser microrefractometer, Appl. Opt., 29, (1990) 1406-1408.
7. H. Moosmuller, W. P. Arnott, Folded Jamin interferometer: a stable instrument for refractive-index measurements, Opt. Lett., 21, (1996) 438-440.
8. T. Li, X. Tan, Stepwise interferometric method of measuring the refractive index of liquid samples, Appl. Opt., 32, (1993) 2274-2277.

9. A. Sharma, M. Katiyar, Deepak, Optical constants and degradation studies of diphenyl and methylphenyl polysilane copolymer using ellipsometry, Synthetic Metals, 174, (2004) 139-142.
10. J. Zhang, Development of a coated long period grating sensor for monitoring contaminants in ground water, M.Sc. thesis, Queen's University, March 2007.
11. Ontario Ministry of the Environment, (2005) <http://www.ene.gov.on.ca/envision/env_reg/er/documents/2005/airstandards/PA04E0035.pdf>, accessed Sept. 2008.
12. W. M. Meylan, P. H. Howard, Estimating octanol-water partition coefficients with octanol-water partition coefficients and Henry's Law constants, Chemosphere, 61, (2005) 640-644.
13. G. Nalecz-Jawecki, J. Sawicki, Spirotox - a new tool for testing the toxity of volatile compounds, Chemosphere, 38, (1999) 3211-3218.
14. A. C. Dietz, J. L. Schnoor, Advances in phytoremediation, Environ. Health Perspect., 109, (2001) 163-168.
15. P. A. Martos, J. Pawliszyn, Calibration of solid phase microextraction for air analyses based on physical chemical properties of the coating, Anal. Chem., 69, (1997) 206-215.
16. B. Zimmermann, J. Burck, H.-J. Ache, Studies on siloxane polymers for NIR-evanescent wave absorbance sensors, Sens. Actuators, B, 41 (1997) 45-54.

17. P. Mayer, W. H. J. Vaes, J. L. M. Hermens, Absorption of hydrophobic compounds into the poly(dimethylsiloxane) coating of solid-phase microextraction fibers: High partition coefficients and fluorescence microscopy images, Anal. Chem., 72, (2000) 459-464.

Chapter 4

Application of Polymer Films to Long-Period Grating Sensors

4.1 Introduction

4.1.1 Long-Period Grating Chemical Sensors

Long-period gratings (LPGs) are sensitive to changes in the refractive index of their immediate environment[1-3]. Application of a polymer coating to the LPG surface allows for monitoring of the polymer refractive index as analytes of interest partition into the polymer. Changes in polymer refractive index cause a shift in the attenuation maximum for a given mode of the LPG. This change is non-linear, with the greatest change occurring at refractive indices just below that of the polymer cladding (see Figure 1.3).

The shift in the wavelength of the attenuation maximum can be monitored in two ways. One method is to record the entire LPG spectrum over the area of interest. This has the advantage of conveying the most information as peak position, shape and intensity are all registered. It has the disadvantage of requiring more advanced equipment, including either a broadband light source with an optical spectrum analyzer or a laser capable of scanning over a range of wavelengths with a broadband detector.

Alternatively the attenuation at one given wavelength can be monitored. As the peak moves, this will either increase or decrease depending on the

wavelength monitored, the peak shift direction and magnitude of the change. This arrangement conveys less information, but requires a simpler light source and detector. Initial testing of the sensor is being conducted with information from the entire spectrum, however, the long term goal of the project will be to just monitor transmission intensity at a single wavelength.

4.1.2 Long Period Gratings in Single Mode Fibers

Long period gratings act to couple light from the core propagating mode into cladding modes. This occurs when there is a phase match between the core and cladding modes. Depending on the refractive index of the core, cladding and external environment, this phase match will only occur at one wavelength, giving the discreet attenuation maximum seen in the LPG spectrum. In a single mode fiber there is only one core mode, but several cladding modes, thus an LPG spectrum has several attenuation peaks, each corresponding to coupling with another cladding mode. Higher order modes result in maxima at progressively higher wavelengths[3]. Figure 4.1 shows both core and cladding modes travelling through a long period grating. The sensitivity of the grating to external refractive index is due to the portion of the cladding waveform travelling exterior to the fiber. Note that higher order cladding modes extend further out in the area exterior to the fiber. Higher order cladding modes tend to show greater sensitivity to changes in external refractive index for this reason.

The sensitivity of an LPG to external change in refractive index is also dependent on the periodicity of the grating, with a lower periodicity resulting in

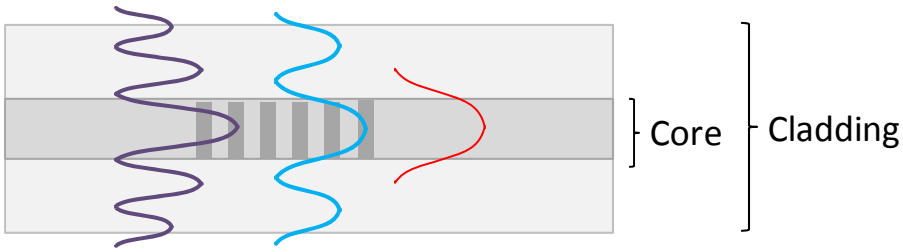

Figure 4.1 Core (red) and cladding (blue and purple) modes travelling through a single mode optical fiber with a long period grating. The higher order cladding mode (purple) has a greater sensitivity to changes in external refractive index. The curves for each mode represent the variation in light intensity across the fiber.

greater sensitivity, and on the cladding diameter. The LPGs used in our experiments had a period of 320 μm, which was chosen as it has good sensitivity and produces an appropriate mode near the necessary wavelength window.

The change in wavelength of the attenuation maximum with change in refractive index is inversely proportional to the cube of the cladding radius[4].

$$\frac{\partial \lambda_{res}}{\partial n_{sur}} \propto \frac{1}{r_{cl}^3} \qquad (1)$$

Here, λ_{res} is the resonant wavelength, n_{sur} is the refractive index of the surroundings and r_{cl} is the cladding radius. To increase the sensitivity of the LPG to refractive index, the diameter of the cladding was reduced through chemical etching. Chemical etching is also used to move the desired mode within the range of the laser used, as reduction in the cladding diameter shifts the modes to longer wavelengths[5].

4.1.3 Fiber-Loop Ring-Down Spectroscopy

Fiber-loop ring-down spectroscopy (FLRDS) is a sensitive method to measure optical loss[6]. Laser light is injected into the loop and the decrease in intensity of the light as it makes successive laps around the loop is recorded. The technique measures "ring – down" time, the time required for the intensity of an input light pulse to decay to 1/e of its original intensity. Loss can also be determined by measuring the relative phase-shift in sinusoidally modulated light[7]. Using this technique, the phase of the input sinusoidally modulated light (modulation frequency was 300 kHz) is compared to that of the output light from the fiber-loop. Transmission losses within the loop cause a phase-shift between the two, with greater loss in the loop resulting in a greater phase shift. FLRDS is not dependent on the light source intensity, which eliminates one major source of noise, and is more sensitive to situations where only small optical losses are observed. These characteristics made it an attractive method to use in the final sensor application.

4.1.4 Challenges of the LPG model

The introduction of a long-period grating should allow for more sensitive measurements of refractive index change as compared to the refractometry experiments detailed in the previous chapter. Detectable shifts in the attenuation maximum of an LPG can be caused by changes in refractive index in the fifth decimal place[8]. The system is also more amendable to an independent remote sensor platform than the refractometer, as it is much smaller. Also, one laser

source can theoretically be used on multiple LPG containing fibers, allowing for continuous monitoring of multiple films and the system contains no moveable parts, operating safely without human intervention. New challenges do arise from the use of the LPG however.

Perhaps most significantly, the LPG is sensitive to factors other than refractive index, namely temperature and strain. Efforts to keep the system at a constant temperature and at the same level of tension minimize these effects. A solid polymer layer applied to the grating may also induce strain depending on the degree of crosslinking and attachment to the fiber surface. .

4.1.5 Experimental Approach

The following chapter details two sets of experiments used to evaluate the use of a coated LPG as a chemical sensor. In the first set, an optical spectrum analyzer (OSA) was used to monitor the transmission spectrum of coated LPGs over a wide wavelength window (about 100 nm). The coated LPGs were exposed to a variety of gas phase analytes. Changes in the attenuation maximum as analytes partitioned into the polymer coating could be accurately determined.

In the second experiment, the coated LPG was inserted into a fiber-loop and monitored using phase-shift fiber-loop ring-down spectroscopy. The phase shift at a single wavelength was monitored, as opposed to a wider spectrum. As analytes partitioned into the polymer coating and caused a change in the

attenuation spectrum of the LPG, the attenuation at that one wavelength, and consequently the phase shift, changed.

4.2 Experimental

Long-Period gratings written into Corning SMF-28 single mode optical fibers were provided by Avensys Inc. (Montreal, QC). The diameter of the fiber core and cladding was 8.2 μm and 125 μm respectively. The cladding had a refractive index of 1.4682 at 1550 nm and the refractive index of the core was 0.36% higher. The gratings had a period of 320 μm. The diameter of the fiber cladding was reduced though etching with a saturated aqueous solution of ammonium bifluoride ($NH_4(HF_2)$). The initial diameter of the fiber prior to etching was 125 μm. After etching, it was estimated to be approximately 100μm, as determined by optical microscopy. The etching process took between 10 and 20 minutes with the extent of etching being monitored by observing the shift of the grating transmission spectrum on an optical spectrum analyzer (OSA). Etching was considered complete when the LPG attenuation peak had shifted into the appropriate wavelength window (see figure 4.2).

Three polymer coatings were tested, all with varied functional groups added into a PDMS base, as described in Chapter 2. The polymer compositions and refractive indices are given in table 4.1. After etching with ammonium bifluoride, the fibers were immersed in 1 M KOH for ten minutes and then rinsed with deionized water. Polymer films were applied to the LPG by dragging

droplets of the polymer diluted in hexanes (5 times dilution by volume) across the fiber several times until no further change in the LPG transmission spectrum occurred. The coatings were estimated to be about 20-30 μm thick. During the coating process, the attenuation maximum shifted to lower wavelengths, in agreement with the higher refractive index of the polymer as compared to air. Polymer coatings were annealed in an oven at 84 ^{o}C until no further peak shift occurred.

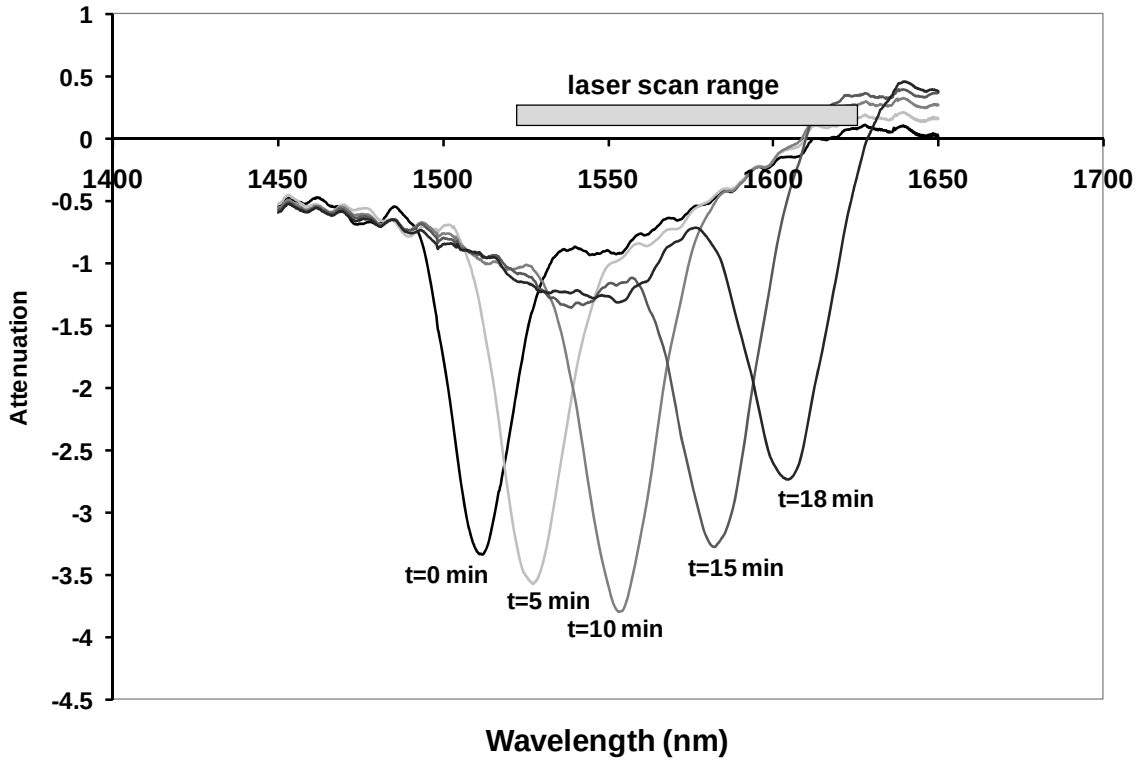

Figure 4.2 Wavelength shift caused by reduction in the LPG cladding diameter from chemical etching. Time points represent the duration of immersion in etching solution.

LPG spectral measurements were acquired using an Agilent 8614 Optical Spectrum Analyzer (OSA) (Agilent Technologies, Santa Clara, CA) with an EXFO

FOS-120A Fiberoptic light source (EXFO, Quebec, QC), operating at 1550 nm. The LPG portion of the fiber was suspended in a gas cell. Various concentrations of saturated solvent vapours in nitrogen were obtained by bubbling nitrogen though a gas bubbler and mixing with pure nitrogen in a flowmeter. This is analogous to the refractometer gas exposure apparatus used in Chapter 3.

Polymer	Composition (mole percent)	Refractive index (1550nm)
LPG-PDPS	8.5% diphenyl siloxane 91.0% dimethyl siloxane 0.5% $Ti(O\text{-}iPr)_4$	1.4236 +/- 0.0002
LPG-PMOS	70% methyl octyl siloxane 29.5% dimethyl siloxane 0.5% $Ti(O\text{-}iPr)_4$	1.4254 +/- 0.0002
LPG-PFMS	7.0% trifluoropropylmethyl siloxane 11.67% diphenyl siloxane 80.83% dimethyl siloxane 0.5% $Ti(O\text{-}iPr)_4$	1.4265 +/- 0.0002

Table 4.1 Composition and refractive index of the three polymers coatings used in the optical spectrum analyzer experiments.

a)

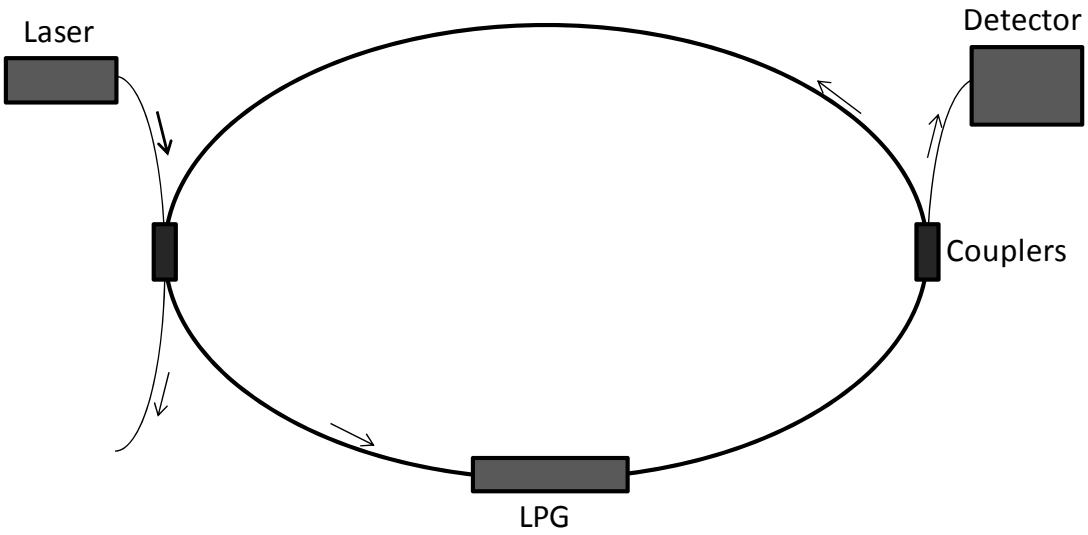

b)

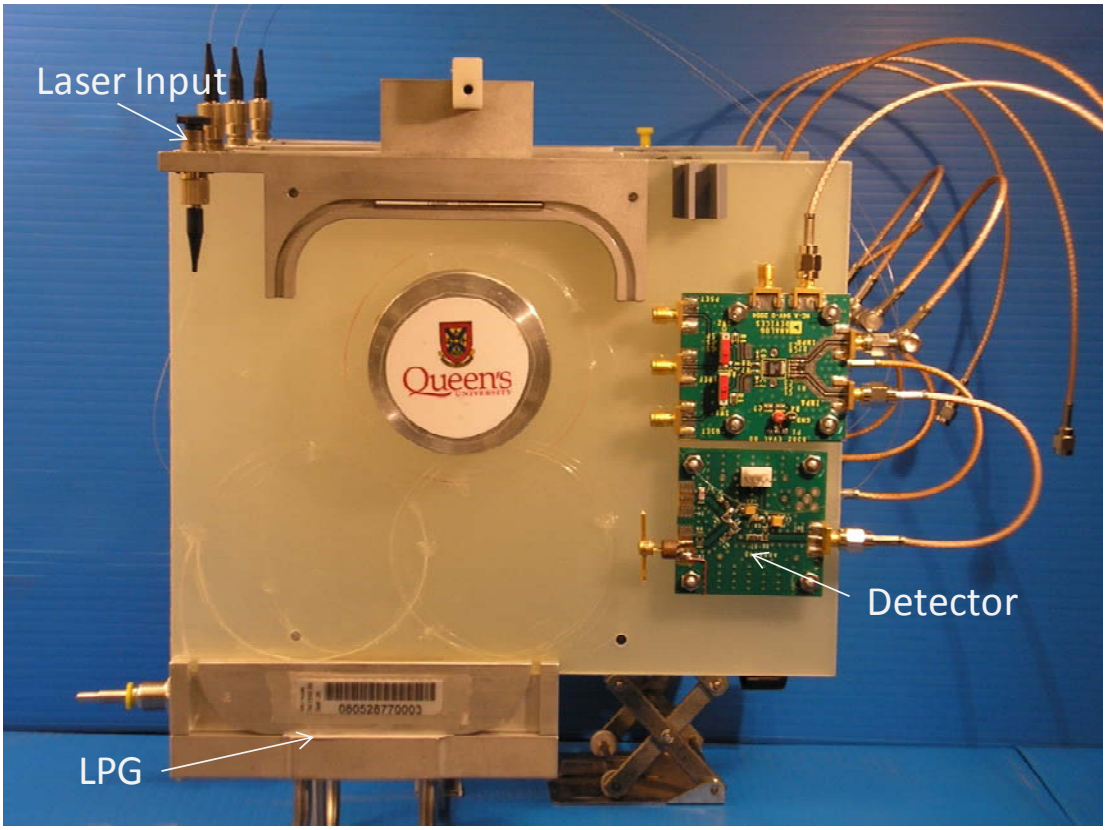

Figure 4.3 Schematic (a) and photograph (b) of Fiber-Loop Ring down spectroscopy apparatus with an LPG

Fiber-loop experiments were conducted using a tunable Ando AQ4320D laser as a source (Yokogawa Electric Corporation, Tokyo, Japan). The apparatus is pictured in Figure 4.3[4].

4.3 Results and Discussion

4.3.1 Optical Spectrum Analyzer experiments

Solutions with different ratios of DMSO and water, having known refractive indices were used to characterize the response of the etched long-period grating. Typical calibration data for a 320 μm LPG, etched with ammonium bifluoride to a diameter of 100μm, is given in Table 4.2. The data from the table is plotted in Figure 4.4.

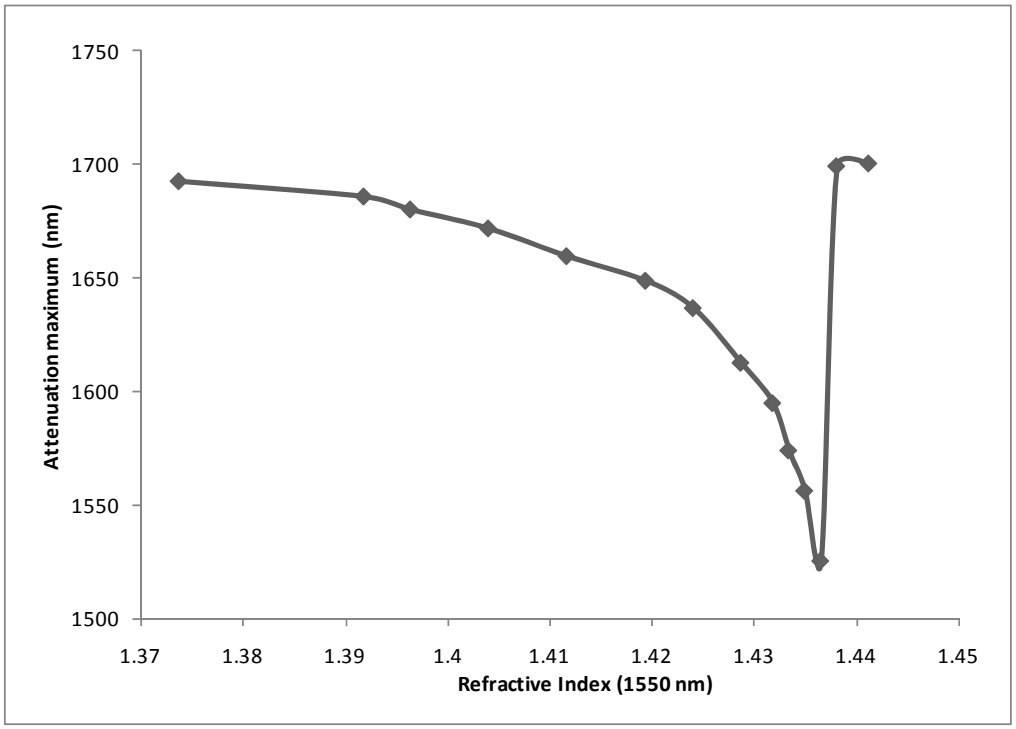

Figure 4.4 Plot of LPG calibration data from Table 4.2

% DMSO (v/v)	Refractive Index (1550 nm)	Wavelength of LPG Attenuation Maximum (nm)
40	1.3737	1692.2
52	1.3918	1685.5
55	1.3964	1679.8
60	1.4040	1671.5
65	1.4117	1659.3
70	1.4194	1648.5
73	1.4241	1636.5
76	1.4287	1612.5
78	1.4318	1594.8
79	1.4334	1574.0
80	1.4350	1556.3
81	1.4365	1525.5
82	1.4381	1698.8
84	1.4412	1700.0

Table 4.2 Calibration of a 320 μm etched LPG using DMSO/water solutions of known refractive index

Three polymer films were prepared and applied to an LPG for the OSA based experiments (see table 4.1). The refractive index of each film was independently determined by casting some of the polymer solution on a glass slide and measuring on a refractometer (as described in chapter 3). Using the DMSO/water calibration data, the peak shift expected upon application of the polymer can be determined, given its refractive index. Application of each polymer to the grating shifted the attenuation peak to the wavelength range expected. Slight variations in the refractive index of the polymer were observed over time, so the polymer coating was annealed to drive off volatile impurities and stabilize the coating.

The spectrum of the LPG shifted as gas phase analytes partitioned into the polymer coating. Figure 4.5 shows the spectra of an LPG-PDPS coated grating as the concentration of xylenes is increased in the gas phase. Concentrations of xylenes are reported as percentages of saturated xylenes, with saturated xylenes being equal to 11000 ppm.

As more xylenes partition into the film, we would expect the refractive index of the film to increase, since xylenes have a refractive index which is higher than the film. Increasing refractive indices should cause a shift in the LPG spectrum to lower wavelengths, as observed. Overall, exposure to 50 percent saturated xylenes vapour resulted in a shift of approximately 15 nm. Five percent saturated vapour, which corresponds to 550ppm, did produce a detectable level of response. Based on the fact that a 1 nm peak shift can be

readily detected, the limit of detection for this instrument is about 300 ppm for xylenes.

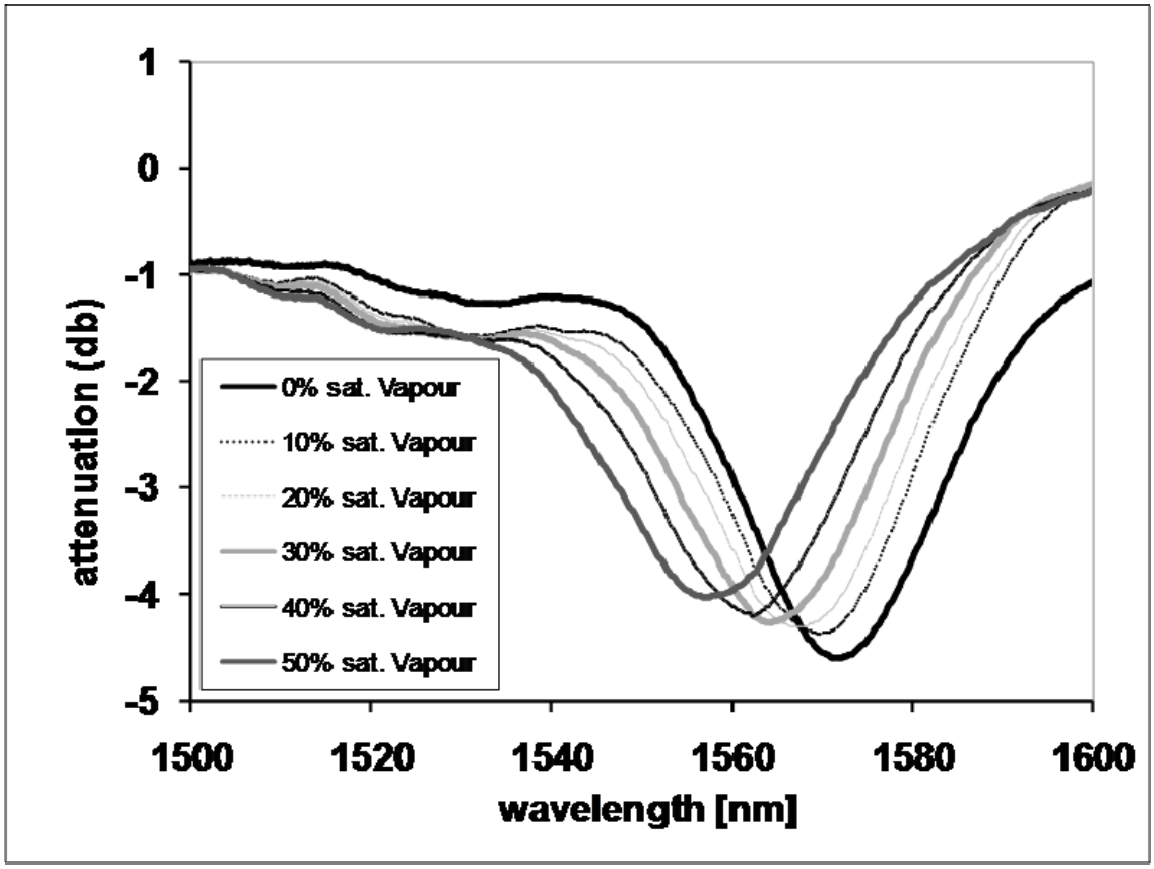

Figure 4.5 Shift in the spectrum of an LPG-PDPS coated LPG with exposure to increasing concentrations of xylenes vapour in nitrogen. Saturated xylenes vapour corresponds to 11000 ppm.

Each of the three films was tested with the same eight solvents used in the refractometer experiments. The peak shift, in nanometers per ppm gas phase solvent, is given in Figure 4.6. While some of the responses seem very small, at 50% vapour saturation, all of the films could detect all of the test solvents, except for the PFMS film, which only responded to xylenes, TCE, acetone and ethyl acetate. The peak shifts given can be roughly translated into a

refractive index change from calibration curves like the one in figure 4.4. For a PDPS coated LPG exposed to xylenes, the estimated refractive index change was 8.9×10^{-7} per ppm of xylenes. This can be compared to the refractometer result where a PDPS film exposed to xylenes resulted in a refractive index shift of 1.43×10^{-6} per ppm of xylenes. Similarly, for the same film, exposure to TCE resulted in an estimated change in refractive index of 1.7×10^{-7} per ppm TCE with the LPG and 1.4×10^{-7} per ppm with the refractometer. This demonstrates that the magnitude of peak shift observed in the LPG based experiments was within an expected range.

The variation in the polymer fingerprint for the test solvents was not as obvious for the LPG experiments as with the refractometer. The LPG-PDPS film gave the greatest peak shift for all analytes except xylenes. The LPG-PFMS film gave the poorest response across the entire range of analytes. The fluorinated polymer used here contained diphenyl groups as well, so its selectivity was not be expected to be the same as the purely fluorine substituted polymer used with the refractometer.

Factors unique to the LPG platform, such as strain induced by polymer swelling, may contribute to the results and differences from those seen on the refractometer.

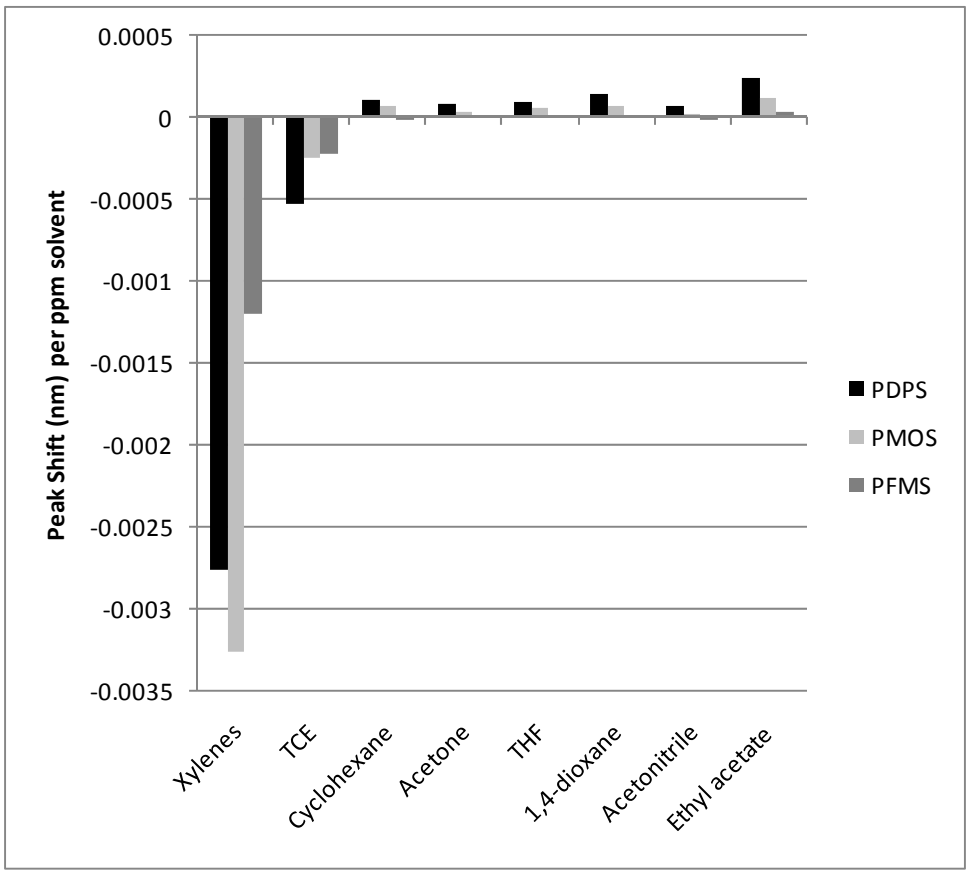

Figure 4.6 Peak shift of a polymer coated LPG per ppm vapour phase solvent.

4.3.2 Fiber-loop ring-down experiments

Fiber-loop ring-down experiments were conducted by inserting the LPG into a loop in the instrument described in Barnes *et al*.[9]. Ring-down experiments were done with the LPG-PDPS film only. Its response to xylenes vapour was considered. Shifts in the attenuation maximum were detected with the laser fixed at one wavelength instead of monitoring the entire spectrum. Loss was determined through measurement of phase shift within the loop.

The wavelength at which measurements are taken affects the sensitivity of the measurement as seen in Figure 4.7. Measurements taken at 1530 nm (figure

4.7a) are more sensitive than those at 1540 nm (figure 4.7b), as the same changes in concentration yield greater phase shifts at 1530 nm. From 0-40% of saturated xylenes vapour, the attenuation maximum is moving towards 1540 nm, however past 40%, it is moving away from 1540 nm (Figure 4.7c). This explains the sudden reduction in phase shift seen at 50% saturated xylenes when recorded at 1540 nm. The attenuation maximum does not reach 1530 nm which is why a similar reduction is not seen there.

As illustrated by figure 4.7, response times for the system are quite fast and reversible, with the phase shift returning to the original baseline value with the reapplication of nitrogen.

These results demonstrate that though less information is conveyed through monitoring only one wavelength instead of an entire spectrum, valuable information can still be obtained and anaytes can be quantitatively detected.

The sensitivity of a FLRDS experiment is comparable to that of the experiments using the OSA. A detection limit of approximately 300 ppm for xylenes can be achieved in both cases. Careful selection of which wavelength to monitor can have a great impact on the sensitivity of the FLRDS experiment.

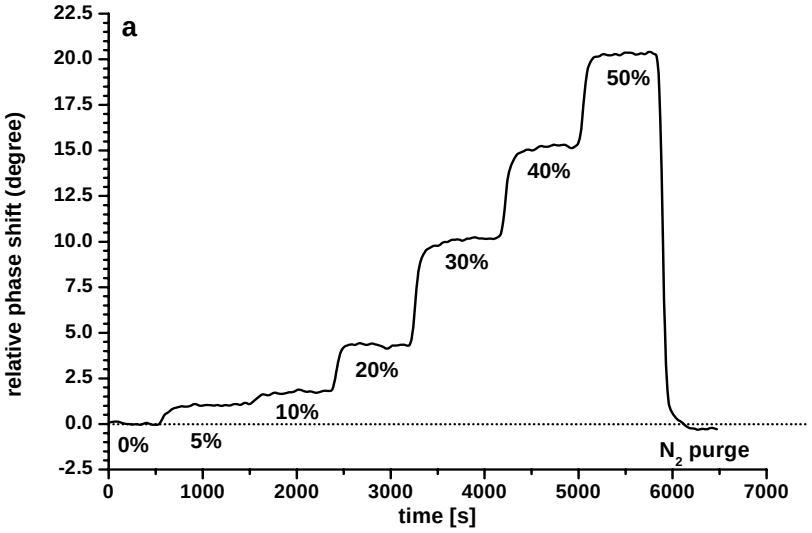
a
relative phase shift (degree)
time [s]
0%
5%
10%
20%
30%
40%
50%
N2 purge

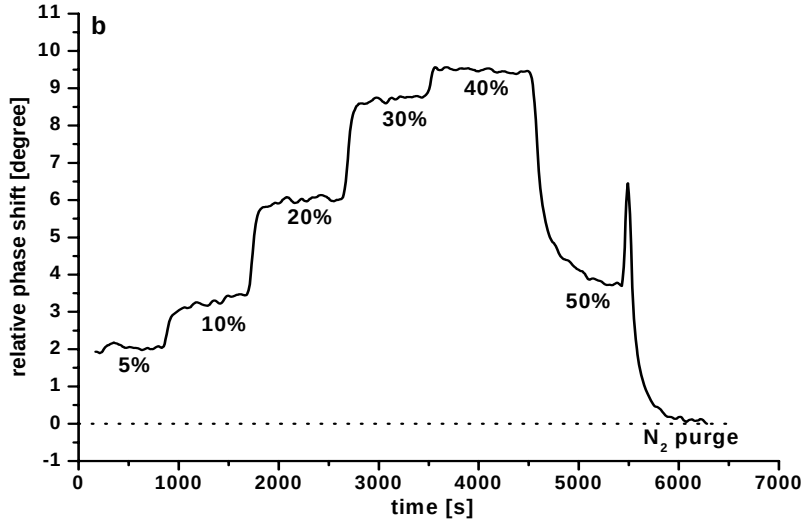
b
relative phase shift [degree]
time [s]
5%
10%
20%
30%
40%
50%
N2 purge

c)

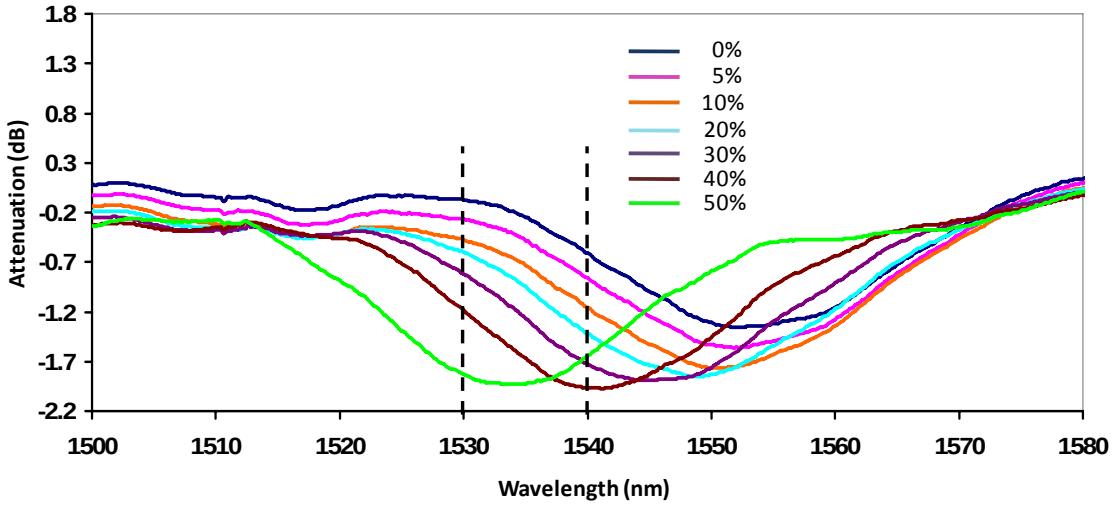

Figure 4.7 Phase shift caused when an LPG-PDPS coated LPG is exposed to xylenes vapour of increasing concentration. The percentages represent percent of saturated xylenes vapour, which is 11000ppm. The phase shift was monitored at 1530nm (a) and 1540nm (b). The entire spectrum was also monitored (c).

4.3.4 Challenges with the Long-period grating platform

Several challenges were encountered with the long-period grating sensor platform over the course of experimentation. One difficulty is the inability to achieve the desired level of sensitivity. Detection limits for compounds like xylenes, which exhibit strong responses, still lie in the 300 ppm range. The sensitivity to analytes obtained with the LPG based system is not better than that from the refractometer set up. This issue can be addressed with a variety of approaches. Changes to the actual LPG, such as using a grating with a lower periodicity, can improve the amount of wavelength shift observed with change in refractive index. Different modes within the same LPG also exhibit differential responses to change in refractive index. Generally higher order modes are more

sensitive. Selecting a mode with greater sensitivity would improve the instrument, though it may also introduce other difficulties if it does not fall within a convenient wavelength window. In FLRDS experiments, careful choice of the wavelength selected for monitoring and its position relative to the attenuation peak can improve sensitivity. Background noise and other sources of loss in the fiber-loop also contribute to the lower sensitivity. Finally, changes to the polymers to further optimize refractive index and also to increase uptake of the analyte would improve the detection limits.

In order to achieve more sensitive measurements with a coated LPG, the starting refractive index of the polymer must fall within a narrow range where the change in attenuation maximum with refractive index is the greatest. With the refractometer model, the starting refractive index of the polymer also affects sensitivity, but only in that a polymer with a refractive index very different from that of the analyte will have a greater change with absorption.

While fine tuning of the refractive index of a polymer has been demonstrated, this places limitations on the type of functional groups that can be used, or the level to which they can be incorporated. For example, higher loading levels of the diphenyl siloxane would be desirable for selectivity, but would cause the refractive index of the polymer to become too high. One possible alternative would be to use a high refractive index coating ($n_{exterior}>n_{clad}$). This would allow for higher levels of diphenyl siloxane within the polymer, but the thickness and uniformity of the polymer coating itself would have to be carefully controlled[10].

Also, polymer films applied to an LPG have a shorter “shelf life” than those applied to glass slides and used on the refractometer. On the glass slides, films were capable of absorbing analytes reproducibly over several months with no change to response or the starting refractive index of the film. On an LPG, over a period of days or weeks the refractive index of the film tended to drift, and the response to analytes was reduced until it became entirely insensitive. The annealing of polymers was introduced and partially addressed this issue. It is unknown why this polymer aging effect occurs. Since an LPG is only sensitive to refractive index within a short distance from the cladding, it may be a surface effect, where the bonding of the polymer to the quartz cladding material is different from the bonding to the borosilicate glass of the slides. Rearrangement over time may also occur.

Finally, challenges arise in the coating of an LPG with a polymer. The response of a bare LPG to solutions of various refractive indices can be characterized using solutions of DMSO and water. When applying a polymer of known refractive index, it is possible to predict what the peak shift should be, based on the DMSO/water calibration. In many cases, however, the peak shift observed was a fraction of that which was be expected, and the coated grating showed little-to-no shift upon analyte absorption. Coating a grating with a polymer made without crosslinking material did produce the expected peak shift. As a result, it is thought that the problem may be associated with the crosslinking by titanium(IV) tetraisopropoxide.

These factors require considerable investigation and improvement before an LPG based sensor platform could be a viable technology.

4.4 Conclusions

Preliminary investigation has shown that it is possible to detect gas phase analytes using a polymer coated long period grating. The sensitivity of the coated LPG to gas phase analytes is comparable to the refractometer system described in Chapter 3. The response of polymer coated LPGs to test solvents was determined and compared to the results obtained in Chapter 3. The selectivity of the polymer films was not as distinct as that found on the refractometer. Differences in starting refractive indices or composition of the polymers may account for some of these differences.

The use of FLRDS as a detection scheme was shown to be effective for detecting xylenes vapour. Challenges in the areas of sensitivity, long term reproducibility, and coating the LPG are currently limiting factors and must be addressed before this technology can succeed in real life sensor applications.

4.5 References

1. V. Bhatia, Application of long-period gratings to single and multi-parameter sensing, Opt. Express, 4, (1999) 457-466.
2. S. W. James, R. P. Tatam, Optical fiber long-period grating sensors: characteristics and application, Meas. Sci. Technol., 14, (2003), R49-R61.
3. H. J. Patrick, A. D. Kersey, F. Bucholtz, Analysis of the response of long period fiber gratings to external index of refraction, J. Lightwave Technol., 16, (1998) 1606-1612.
4. J. Barnes, M. Dreher, K. Plett, R. S. Brown, C. M. Crudden, H.-P. Loock, Chemical sensor based on a long-period fiber grating modified by a functionalized polydimethylsiloxane coating, The Analyst, accepted July 2008.
5. K. Zhou, H. Liu, X. Hu, Tuning the resonant wavelength of long period fiber gratings by etching the fiber's cladding, Optics Commun., 197, (2001) 295-299.
6. R. S. Brown, I. Kozin, Z. Tong, R. D. Oleschuk, H.-P. Loock, Fiber-Loop ring-down spectroscopy, J. Chem. Phys., 117, (2002) 10444-10447.
7. Z. Tong, A. Wright, T. McCormick, R. Li, R. D. Oleschuk, H.-P. Loock, Phase-shift fiber-loop ring-down spectroscopy, Anal. Chem., 76, (2004) 6594-6599.
8. T. Allsop, L. Zhang, I. Bennion, Detection of organic aromatic compounds in paraffin by a long-period fiber grating optical sensor with optimized sensitivity, Opt. Commun., 191, (2001) 181-190.

9. J. A. Barnes, R. S. Brown, J. Cipot-Wechsler, C. M. Crudden, J. Du, H.-P. Loock, K. Plett, Long-period gratings in chemical sensing, Proc. of SPIE, 7099, (2008) 70992C1-8.
10. R. Hou, Z. Ghassemlooy, A. Hassan, C. Lu, K. P. Dowker, Modelling of long-period fibre grating response to refractive index higher than that of cladding, Meas. Sci. Technol., 12, (2001) 1709-1713.

Chapter 5

Conclusions and Future Work

5.1 Overview

The goal of this study was to develop polysiloxane coatings for the proposed LPG based sensor that demonstrate selectivity for analytes of interest, have a refractive index just below that of the fiber cladding and absorb compounds reversibly and reproducibly. Commercially available polysiloxane materials fulfilled some of these requirements, however, difficulty in modifying the materials made the adjustment of both the refractive index and chemical selectivity difficult. The synthesis of polysiloxane pre-polymers from monomers, using either an acid or base catalyzed procedure, allowed for maximum control of the final product. Titanium(IV) tetraisopropoxide was used to crosslink these pre-polymers in elastomeric films. Adjustment of the proportions of functional groups or amount of titanium within the polymer caused a linear change in the refractive index, allowing the refractive index to be tuned to a specific value. This refractive index adjustment has application not only in optical based sensors, but in many other optics applications where a specific refractive index is needed, such as in optical coupling.

Four films were made for further testing, each having refractive indices tuned to the ideal range of approximately 1.425 (at 1550nm). These films

incorporated octyl (PMOS), phenyl (PDPS), trifluoropropyl (PFMS) and cyanopropyl (PCMS) groups. The various functional groups were used to incorporate selectivity into the films for non-polar, aromatic, halogenated or polar compounds, respectively. These four films were tested for their uptake of eight gas phase compounds using a custom built refractometer and their change in refractive index was monitored. All of the responses of the films used on the refractometer were reproducible over a period of months and their refractive indices remained stable. A partition coefficient was calculated for each film/solvent combination. It was discovered that some selectivity was evident between the films, though, differences in the response of the films to analytes were not as significant as desired. This could be due to the fact that loading levels of the various functional groups were restricted, either by film quality demands, as in the case of PCMS, or by refractive index demands, as for PDPS or PFMS. For the PDPS and PFMS films, the functional group is restricted to 10 mole percent or less within the film in order to obtain the correct refractive index, so they could not be expected to exhibit dramatically different response patterns. Continued investigation of other siloxane functional groups, the use of polymers outside of the siloxane family, or moving to a sensor platform that does not require refractive index tuning are all possible solutions to the issue of selectivity.

In principle, it is possible to generate an array of polymer coated sensors, each with their differing response to an analyte, which would produce a fingerprint response to that analyte, allowing for species determination. We do see variation in response with the four test polymers in this study. While the

variation may not be sufficient to determine the composition of a mixture, it is sufficient for single compound identification, and could have application as a basic screening tool. For instance, compounds like acetonitrile and cyclohexane can be easily differentiated based on their fingerprints. The general chemical class of a mixture can also be differentiated, as was illustrated using gasoline, by comparing the mixture fingerprint to that of compounds from known chemical classes.

The viability of the LPG sensor project was tested with the application of some of the polymer coatings to an LPG. It was found that the LPG platform is able to sense the presence of analytes, both through analyzing the entire LPG spectrum with an OSA, and through monitoring loss at a single wavelength using fiber-loop ring-down spectroscopy. Several difficulties with the LPG sensor platform arose which would need to be addressed for further work to proceed. One of the most significant problems was that of coating stability. Experiments on the refractometer demonstrated consistency, both in film refractive index and in film response over time. This was not reflected in the LPG experiments, where film response degraded over a period of days to weeks, and refractive index tended to drift. Films applied to LPGs also tended to have a starting refractive index that was different as compared to the values given by the refractometer. These issues may have to do with problems pertaining to the cylindrical geometry of the LPG, effects such as strain unique to the LPG, or an effect at the film/LPG interface.

Using coated LPGs, detection limits for xylenes were in the hundreds of ppm range. This was good as a preliminary proof of concept test, however, for real applications, detection limits in the ppm or sub-ppm range are necessary. For fiber-loop ring-down experiments, careful choice of which wavelength to monitor can have a great effect on sensitivity. As well, optimization of the physical specifications of the LPG, such as periodicity, can improve sensitivity. Finally, the use of a polymer that has a refractive index precisely in the range of greatest shift with change in refractive index would greatly improve sensitivity.

5.2 Conclusions and Summary

a) Both an acid and a base catalyzed synthetic route to obtain siloxane oligomers were developed. Acid catalysis was preferred as it produced a cleaner product in higher yield, however for electron withdrawing or sterically hindered functional groups, base catalysis is necessary to produce high molecular weight product. The synthesis protocol was used with six silane monomers to obtain various prepolymer materials for later experiments. The structures of all of the siloxane prepolymers obtained were confirmed by either MALDI-TOF MS or ^{1}H NMR.
b) Preliminary testing of a new method of generating polysiloxane prepolymers using a platinum catalyzed hydrosilylation reaction was completed. Hexachloroplatinic acid was used as the catalyst and shown to be effective for adding vinyl terminated hydrocarbons, such as allyl

cyclohexane. The presence of other functional groups on the vinyl compound, such as amines, inhibited the addition.

c) Titanium(IV) tetraisopropoxide was found to be an effective catalyst and crosslinking agent for the production of elastomeric films from the siloxane oligomers.

d) The dependence of film composition on refractive index was explored. Refractive index increased linearly with increasing mole percent titanium or higher refractive index functional siloxanes. Using this information it was shown that it is possible to make siloxane films having tuned refractive indices for specific applications.

e) Four chemically distinct polysiloxane films were made, all having refractive indices around 1.425, the refractive index necessary for eventual LPG based sensor applications. The films included siloxane substituted with diphenyl (PDPS), methyloctyl (PMOS), (3,3,3-trifluoropropyl)methyl (PFMS) and (3-cyanopropyl)methyl (PCMS) groups.

f) The responses of the four films above to a set of eight environmentally relevant analytes were characterized by monitoring change in refractive index. All of the responses were linear, reversible and repeatable over the concentration range used. Comparison of the responses between films showed that some chemical selectivity was being exhibited.

g) The change in refractive index of the polymer films with analyte absorption was used in conjunction with the Lorentz-Lorenz equation to calculate partition coefficients for each of the solvent/film combinations.

h) The effectiveness of an array of polymers to determine the approximate composition of a mixture was demonstrated using gasoline. The response across the array of four polymers to gasoline was most similar to that of cyclohexane, highlighting that gasoline is a mixture of hydrocarbons.

i) Three polymer films were applied to etched long-period gratings. The shift in peak position with analyte absorption was monitored for eight solvents using an optical spectrum analyzer. This experiment showed that it is possible to detect the solvents using a polymer coated LPG with a sensitivity comparable to the refractometer. The response pattern seen from the three films to the eight solvents showed some similarities to those from the refractometer experiments. The selectivity between films, however, was less apparent.

j) The response of a PDPS coated LPG to xylenes was characterized using fiber-loop ring-down spectroscopy. Loss was monitored at a single wavelength. It was shown that it is possible to detect and quantify various concentrations of xylenes using this technique.

5.3 Future Work

a) Further work should be conducted on the platinum catalyzed hydrosilylation synthetic method. The method should be explored to be able to add in different functional groups to the polysiloxane backbone.

The use of alternate platinum catalysts or reaction conditions could be explored.

b) In order to characterize more complex mixtures using an array format, more polymer coatings with different chemical affinities will need to be synthesized. Some of these can be accessed through the platinum catalyzed hydrosilylation method. If the polysiloxane family is not sufficient to obtain the range of selectivity required, it is possible that other polymer families may need to be explored.

c) Existing and future polymers will have to be further characterized for their response to target analytes, in terms of change in refractive index, partition coefficients and LPG response. The response of an array to mixtures of known analytes should also be characterized.

d) The issues related to coating an LPG with a polymer need to be addressed. Some effect unique to crosslinked materials seems to interfere with the LPG response, making it unable to properly register the refractive index of the polymer and have little to no sensitivity to analytes. Uncrosslinked materials do not have this effect on the LPG and normal peak shifts occur. A systematic approach of modifying factors related to the production of the LPG, the etching process, coating the fiber, and the crosslinking and chemical makeup of the film is required to determine which factor is contributing to this.

e) Polymer aging when applied to an LPG will also have to be considered. For use in a final remote monitoring sensor platform, the polymers will

have to be able to respond reversibly and reproducibly over a period of months. Polymers applied to glass slides and used in refractometer experiments do have lifetimes on the order of months, however, polymers on LPGs typically degrade within a week or two. It is possible that the resolution of the coating issue above will also help this issue.

f) The detection limits of the proposed sensor need to be improved. Adjustment of the LPG parameters, such as periodicity, can improve the sensitivity of the sensor. Additionally, fine tuning of the polymer coatings to achieve a refractive index precisely in the area of greatest sensitivity to refractive index change would improve sensitivity.

g) All of the analyte uptake experiments have been done from the gas phase. Ultimately, a sensor that can monitor contaminants in water would be desirable. Working with aqueous samples is therefore an area that will have to be explored. Some work was done earlier in the project with aqueous samples, however, the results were difficult to interpret due to the fact that the water affected the quality of the interface seen on the refractometer. Polymer coatings will have to have no response, or a constant response, to water. While PDMS does not absorb water, some of the more polar variants may.

Appendix A

Additional Mass Spectra

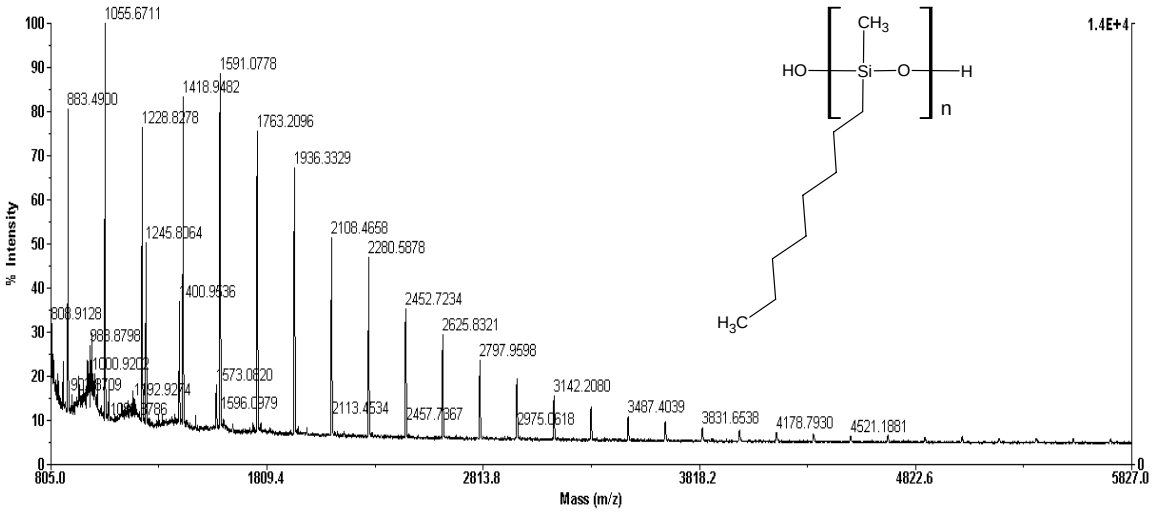

Figure A.1 MALDI-TOF-MS of polymethyloctyl siloxane (PMOS) pre-polymer, with some cyclic impurity. Peaks are separated by 172 m/z, the molecular weight of one PMOS repeat unit.

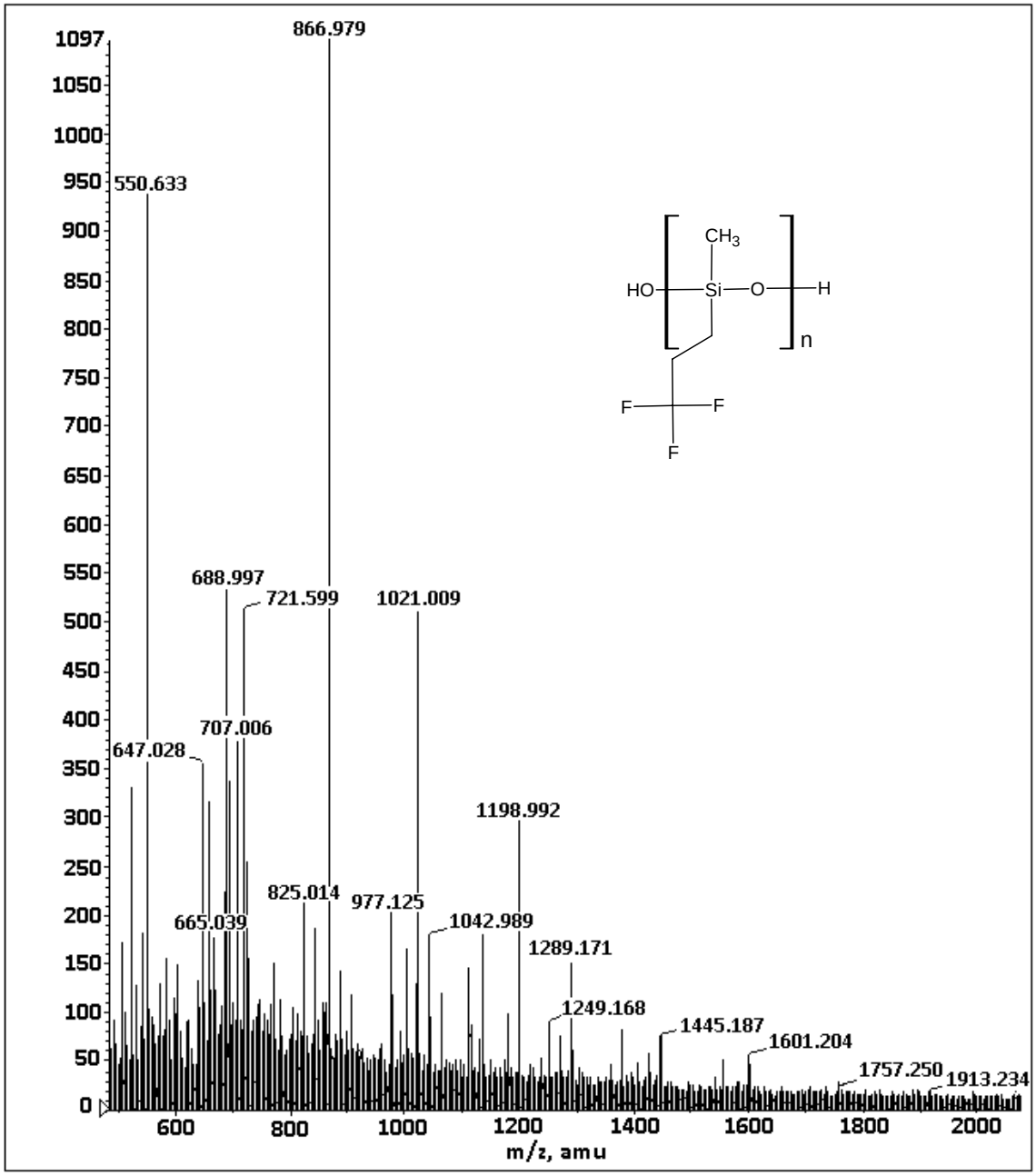

Figure A.2 MALDI-TOF-MS of poly(3,3,3-trifluoropropyl)methyl siloxane (PFMS) pre-polymer, showing peaks separated by 156 m/z, the molecular weight of one PFMS repeat unit.

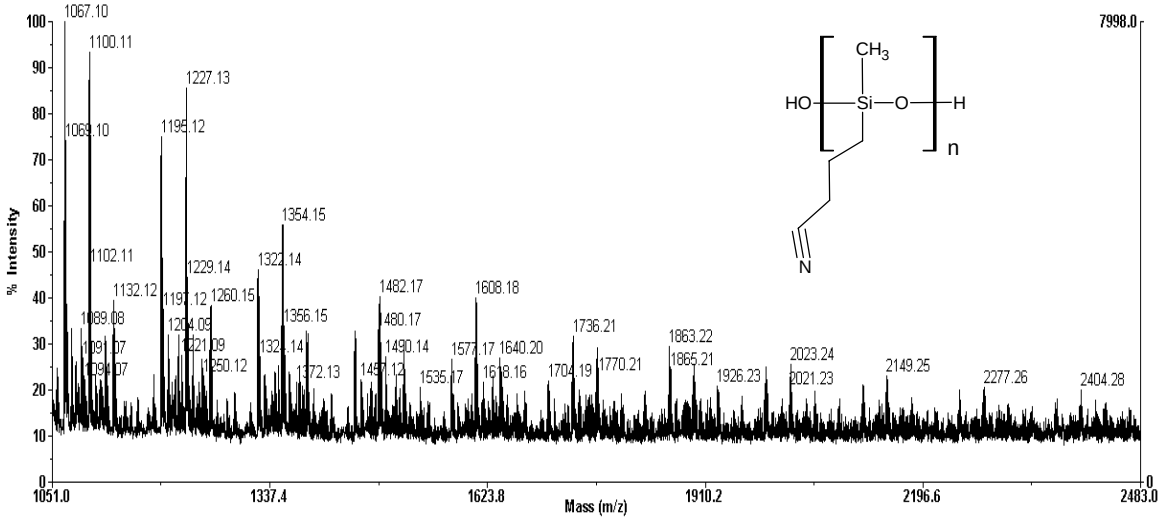

Figure A.3 MALDI-TOF-MS of poly(3-cyanopropyl)methyl siloxane (PCMS) pre-polymer, showing peak clusters separated by 127 m/z, the molecular weight of one PCMS repeat unit.

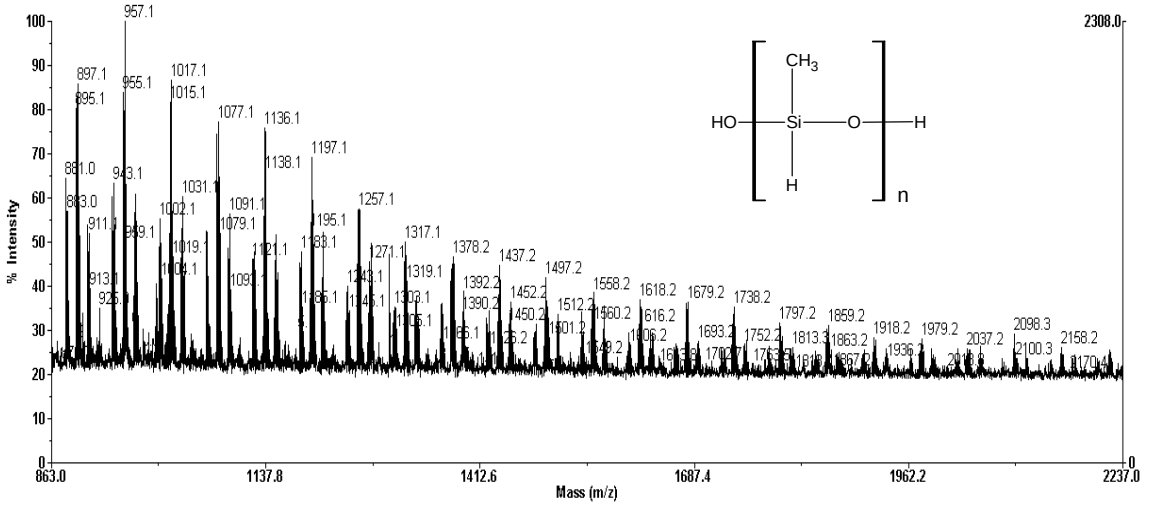

Figure A.4 MALDI-TOF-MS of polymethyl siloxane (PMS) pre-polymer showing peak clusters separated by 60 m/z, the molecular weight of one PMS repeat unit.